Automatic Phonocardiogram Segmentation Using the Sliding Window Autocorrelation Algorithm

by

Sankua Chao, B. Eng.

A Thesis submitted to the Faculty of Graduate Studies and Research

in partial fulfillment of the requirements for the degree of

Master of Applied Science

in

Biomedical Engineering

Ottawa-Carleton Institute for Biomedical Engineering

Department of Systems and Computer Engineering

Carleton University

Ottawa, Ontario, Canada

April 2009

Your file Votre référence
ISBN: 978-0-494-51983-7
Our file Notre référence
ISBN: 978-0-494-51983-7

Abstract

This thesis investigated the automated synchronous segmentation of cardiac cycles in phonocardiograms (PCGs) containing noise of varying degrees and types. Segmentation was performed using the Sliding Window Autocorrelation (SWA) algorithm. The SWA involved correlations between a heartbeat template and PCG, and relied on an estimate of heartbeat period. The objective of this thesis was to improve the accuracy and robustness of the SWA by addressing PCG variability in heart rate, heart sound intensity, and non-cardiac noise presence. Methods examined to enhance the SWA included an average heartbeat period estimate, an average heartbeat template estimate, a shifted heartbeat template competition, and data de-noising. An objective scoring method was introduced to evaluate segmentation accuracy. The results of this thesis indicated the SWA achieved correct segmentation, synchronous to within 50 ms of actual cardiac cycle boundaries, for 93.5% of the 2453 cardiac cycles in a dataset of 195 PCGs. Therefore, an improvement of 3.4% was achieved for the overall accuracy of the SWA.

To all my grandmothers and grandfathers

Acknowledgements

I would like to thank my supervisor, Prof. Adrian Chan, for his guidance, support, and patience. I am grateful to Prof. Chan, the Department of Systems and Computer Engineering, and the Faculty of Graduate Studies and Research, for their financial support. I would like to acknowledge Pat Beirne, whose original work is the basis of this thesis.

To all of my colleagues over the past few years: Your company and conversations were memorable, and will be appreciated in the years to come.

To the numerous individuals who have provided invaluable advice throughout my studies: Your time and thoughtfulness will continue to be greatly appreciated.

I would like to express my deepest gratitude to my mother, who has continually encouraged and supported my creative development.

Thank you.

Table of Contents

List of Tables

List of Figures

List of Abbreviations

		Introduced in
AV	Atrioventricular	1.1.1
CHEO	Children's Hospital of Eastern Ontario	4.1
ECG	Electrocardiogram	2.2.1
GSB	Gold Standard Heartbeat Boundary	4.2
HBP	Heartbeat Boundary Prediction	3.4
HRE	Heart Rate Estimation	3.2
HTL	Heartbeat Template Location	3.3
LA	Left Atrium	1.1.1
LV	Left Ventricle	1.1.1
PCG	Phonocardiogram	1
PED	Peak Energy Detector	3.5
PGD	Prediction-Gold Standard Difference	4.4
RA	Right Atrium	1.1.1
RV	Right Ventricle	1.1.1
S1	First Heart Sound	1.2.1
S2	Second Heart Sound	1.2.1
S3	Third Heart Sound	1.2.1
S4	Fourth Heart Sound	1.2.1
SWA	Sliding Window Autocorrelation	1

List of Symbols

		Introduced in
X	number of scales	8.2.1
δ	Deviation	4.4
γ	set of sample locations of Gold Standard Heartbeat Boundaries	4.2
η	set of Correctly Segmented Heartbeats	4.4
$\overline{\eta}$	set of Incorrectly Segmented Heartbeats	4.4.1
K	number of Heartbeat Boundary Predictions	4.4.1
λ	Possible Heartbeat Template identifier	6.2.1
μ	Mean Peak Similarity Correlation Coefficient	6.2.2
v	Vicinity	4.4
ρ	set of sample locations of Heartbeat Boundary Predictions	3.4
τ	time offset, in units of samples	3.1
τ_{max}	Peak Offset, or time offset of highest peak	3.2
τ_{null}	Nulling time offset	3.2
Z	number of Gold Standard Heartbeat Boundaries	4.2
a, b	Step identifiers	3.3
C	taper time constant	3.2
$d(k,z)$	Prediction-Gold Standard Difference	4.4

		Introduced in
$D[a,b]$	Range of Variability for portion of Peak Offset Sequence	3.3
E	total energy	3.1
f	frequency	8.2.1
g	sample location of Gold Standard Heartbeat Boundary	4.2
$G(\tau)$	Similarity Correlation	3.1
$G_T(\tau)$	tapered Similarity Correlation	3.3
h	Heartbeat identifier	4.4
HPE_A	Automatic Average Heartbeat Period Estimate	7.1
$HPE_{A,\lambda}$	Possible Automatic Average Heartbeat Period Estimate	7.2.2
$HPE_{A,m}$	Running Automatic Average Heartbeat Period Estimate	7.2.1
HPE_{AS}	Shifted Automatic Average Heartbeat Period Estimate	7.1
HPE_M	Manual Average Heartbeat Period Estimate	5.1
HPE_O	Original Heartbeat Period Estimate	3.2
$HTL_A(t)$	Automatic Average Heartbeat Template	7.1
$HTL_{A,\lambda}(t)$	Possible Automatic Average Heartbeat Template	7.2.2
$HTL_{A,m}(t)$	Running Automatic Average Heartbeat Template	7.2.1
$HTL_{AS}(t)$	Shifted Automatic Average Heartbeat Template	7.1
$HTL_M(t)$	Manual Average Heartbeat Template	5.1
$HTL_O(t)$	Original Heartbeat Template	3.3

		Introduced in
$HTL_{O,\lambda}(t)$	Possible Heartbeat Templates based on Original	6.2.1
$HTL_{OS}(t)$	Shifted Original Heartbeat Template	6.1
i	Step identifier	3.3
I	number of Steps	3.3
j	Span identifier	3.3
k	Heartbeat Boundary Prediction identifier	3.4
ℓ	Longest Span identifier	3.3
$L(t)$	rectangular window	3.1
m	Iteration identifier	7.2.1
$M(\tau)$	windowed energy	3.1
n	time, in units of samples	7.2.1
N	sample length of $s(t)$	3.1
N_1	sample length of $w_1(t)$	3.1
N_2	sample length of $w_2(t)$	3.1
N_{HTL}	sample length of Heartbeat Template	3.3
$N_{HTL,m}$	sample length of Running Automatic Average Heartbeat Template	7.2.1
N_{inc}	sample length of Shift Increment	6.2.1
N_{offset}	sample length of Maximum Shift Offset	6.2.1
N_s	sample length of $w_s(t)$	7.2.1

		Introduced in
N_{span}	sample length of Span	3.3
N_{step}	sample length of Step	3.3
p	sample location of Heartbeat Boundary Prediction	3.4
$P_o[i]$	Peak Offset Sequence	3.3
$P_o[a,b]$	portion of Peak Offset Sequence	3.3
q	Estimated Heartbeat Period	7.2.1
q_0	Start of Initial Running Average Heartbeat Template	7.2.1
Q	Mode PGD	4.4
r	scale	8.2.1
$R(\tau)$	cross-correlation	3.1
$R_{xx}(\tau)$	auto-correlation of $x(t)$	3.2
$R_{xx,T}(\tau)$	tapered auto-correlation of $x(t)$	3.2
$s(t)$	original waveform of digitized PCG	3.1
$\overline{s(t)}$	DC component of $s(t)$	3.1
$s_{AC}(t)$	AC component of $s(t)$	3.1
$s_{BP}(t)$	bandpass filtered $s_{norm}(t)$	8.2.1
$s_{norm}(t)$	RMS-normalized waveform of digitized PCG	3.1
$s_P(t)$	preprocessed time-aggregate waveform	8.2.1
t	time, in units of samples	3.1

		Introduced in
$T_G(\tau)$	taper window for Similarity Correlation	3.3
$T_R(\tau)$	taper window for cross-correlation	3.2
u	sample location	3.3
$w(t)$	RMS-normalized signal magnitude of digitized PCG	3.1
$w_1(t)$	Template Window	3.1
$w_2(t)$	Search Window	3.1
$w_\lambda(t)$	shortened $w(t)$	7.2.2
$w_{BP}(t)$	signal magnitude of $s_{BP}(t)$	8.1
$w_m(t)$	Portion of $w(t)$ corresponding to Estimated Heartbeat Template	7.2.1
$w_P(t)$	normalized signal magnitude of $s_P(t)$	8.2.1
$w_s(t)$	shortened $w(t)$	7.2.1
$w_z(t)$	portion of $w(t)$ corresponding to cardiac cycle marked by Gold Standard Heartbeat Boundary z	5.2.1
$W(r,t)$	time-scale matrix	8.2.1
$x(t)$	square magnitude of $w(t)$	3.2
z	Gold Standard Heartbeat Boundary identifier	4.2

Subscripts and Superscripts

λ	of Possible Heartbeat Template λ	6.2.1

		Introduced in
A	Automatic Average	7.1
AS	Automatic Average with Shift Competition	7.1
correct	that are correct	4.4.1
h	of Heartbeat h	4.4
h,vic	within vicinity of Heartbeat h	4.4.1
i	of Step i	3.3
incorrect	that are incorrect	4.4.1
j	of Span j	3.3
k	of Heartbeat Boundary Prediction k	3.4
ℓ	of Longest Span ℓ	3.3
m	of Iteration m	7.2.1
M	Manual Average	5.1
O	Original	3.2
OS	Original with Shift Competition	6.1
unused	that are unused	4.4.1
z	of Gold Standard Heartbeat Boundary z	4.2

1 INTRODUCTION

The phonocardiogram (PCG) is a biological signal associated with cardiac sounds, or sounds originating from structures within the heart. The PCG is a fundamental clinical tool for obtaining information regarding the health of the heart, since heart valve malfunctions can be diagnosed using cardiac sounds heard during a heartbeat or cardiac cycle. Segmentation of a PCG into individual cardiac cycles is an essential step prior to murmur analysis and diagnosis, since the timing of a murmur within a cardiac cycle is an important feature for diagnosis. In addition, segmentation enables the analysis of multiple cardiac cycles by an automated PCG analysis system, to increase the system's accuracy and robustness. The aim of this thesis was to achieve automated synchronous segmentation of PCGs exhibiting varying degrees and types of noise. This work focuses on the Sliding Window Autocorrelation (SWA) segmentation algorithm. This work hypothesized that the segmentation accuracy of the SWA could be improved by: (i) enhancements to the SWA segmentation algorithm to increase robustness (specifically in the heartbeat period estimate and the heartbeat template), and (ii) de-noising PCGs prior to segmentation.

1.1 The Heart

1.1.1 Anatomical Structure of the Heart and Valves

The structure of the heart consists of chambers, valves, veins and arteries, as seen in Figure 1.1. Upper chambers are called atria, and lower chambers are called ventricles. Atria are connected to ventricles via atrioventricular (AV) valves, and ventricles are

connected to major arteries via semilunar valves. On the left side of the heart, the AV valve connecting the left atrium (LA) and the left ventricle (LV) is called the mitral valve. The semilunar valve connecting the LV and aorta is called the aortic valve. On the right side of the heart, the AV valve connecting the right atrium (RA) and the right ventricle (RV) is called the tricuspid valve. The semilunar valve connecting the RV and pulmonary artery is called the pulmonary valve.

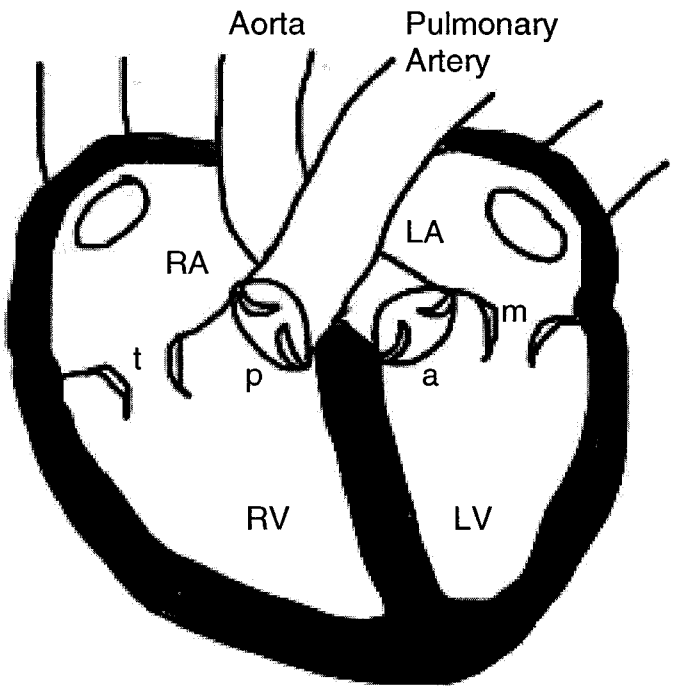

Figure 1.1: Anatomical structure of the heart: LA = left atrium, m = mitral valve, LV = left ventricle, a = aortic valve, RA = right atrium, t = tricuspid valve, RV = right ventricle, p = pulmonary valve.

The contraction of muscle tissue allows blood to be pumped through the heart [71]. Typically, as seen in Figure 1.2, oxygenated blood from the lungs is received by the LA, pumped by the LA through the mitral valve to the LV, pumped by the LV through the aortic valve to the aorta, and circulated to the body where the oxygen will be used. Likewise, de-oxygenated blood from the body is received by the RA, pumped by the RA through the tricuspid valve to the RV, pumped by the RV through the pulmonary valve to the pulmonary artery, and circulated to the lungs where the blood will be re-oxygenated.

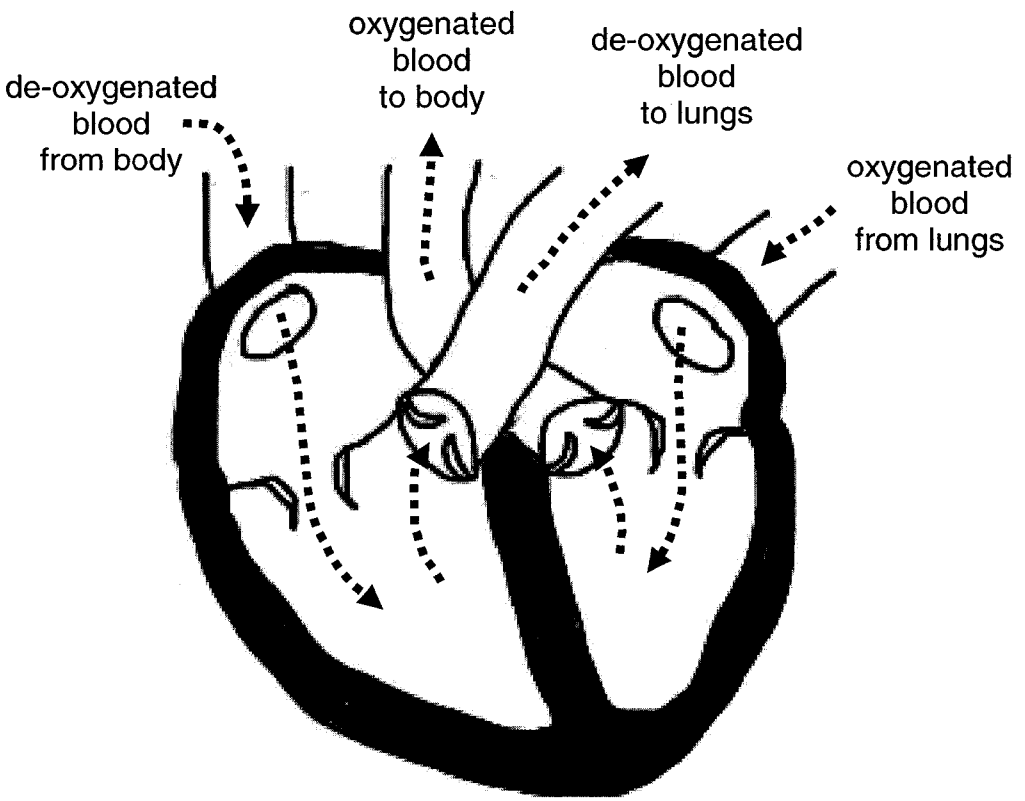

Figure 1.2: Direction of blood flow through the heart.

1.1.2 Physiological Basis of the Cardiac Cycle

Heartbeats are cyclic, with a period of 300-1500 ms [60]. A single heartbeat, or cardiac cycle, consists of two phases: systole and diastole. In a sequence of heartbeats, systole typically has shorter duration and less variation of duration than diastole. A cardiac cycle can be considered a cyclostationary process, which is a process whose statistical characteristics vary periodically with time [19].

Systole is characterized by ventricular contraction, when the ventricles contract to pump blood into the major arteries via the semilunar valves. At the beginning of systole, the ventricles are filled with blood, resulting in increased ventricular pressure which causes: (i) the AV valves to close, so that blood does not flow backward from the ventricles into the atria; and (ii) the semilunar valves to open, so blood can flow forward from the ventricles into the major arteries.

Diastole is characterized by ventricular relaxation, when the atria contract to pump blood into the ventricles via the AV valves, and the ventricles relax and fill with blood. At the beginning of diastole, the ventricles are not filled with blood, resulting in decreased ventricular pressure which causes: (i) the semilunar valves to return to a closed position, so blood does not flow forward from the ventricles into the major arteries; and (ii) the AV valves to return to an open position, so that blood can flow forward from the atria to the ventricles.

The status of heart chambers and valves during systole and diastole can be seen in Table 1.1 and Table 1.2, respectively, as well as in Figure 1.3. According to [50], blood flow changes and valve vibrations are associated with cardiac sounds heard during the

cardiac cycle. According to [71], audible sounds are produced from the opening and closing of heart valves, the flow of blood in the heart, and the vibration of heart muscles. Cardiac sounds heard during the cardiac cycle are described in the next section.

Table 1.1: Status of heart chambers and valves at various times within systole.

TIMING / STRUCTURE	At Beginning	During	At End
Atria	Empty	Filling	Full
AV Valves	Closed	Closed	Closed
Ventricles	Full	Emptying	Empty
Semilunar Valves	Closed	Opened	Opened
Blood Flow		(i) From ventricles to major arteries; (ii) From major veins to atria	

Table 1.2: Status of heart chambers and valves at various times within diastole.

TIMING / STRUCTURE	At Beginning	During	At End
Atria	Full	Emptying	Empty
AV Valves	Closed	Opened	Opened
Ventricles	Empty	Filling	Full
Semilunar Valves	Closed	Closed	Closed
Blood Flow		From atria to ventricles	

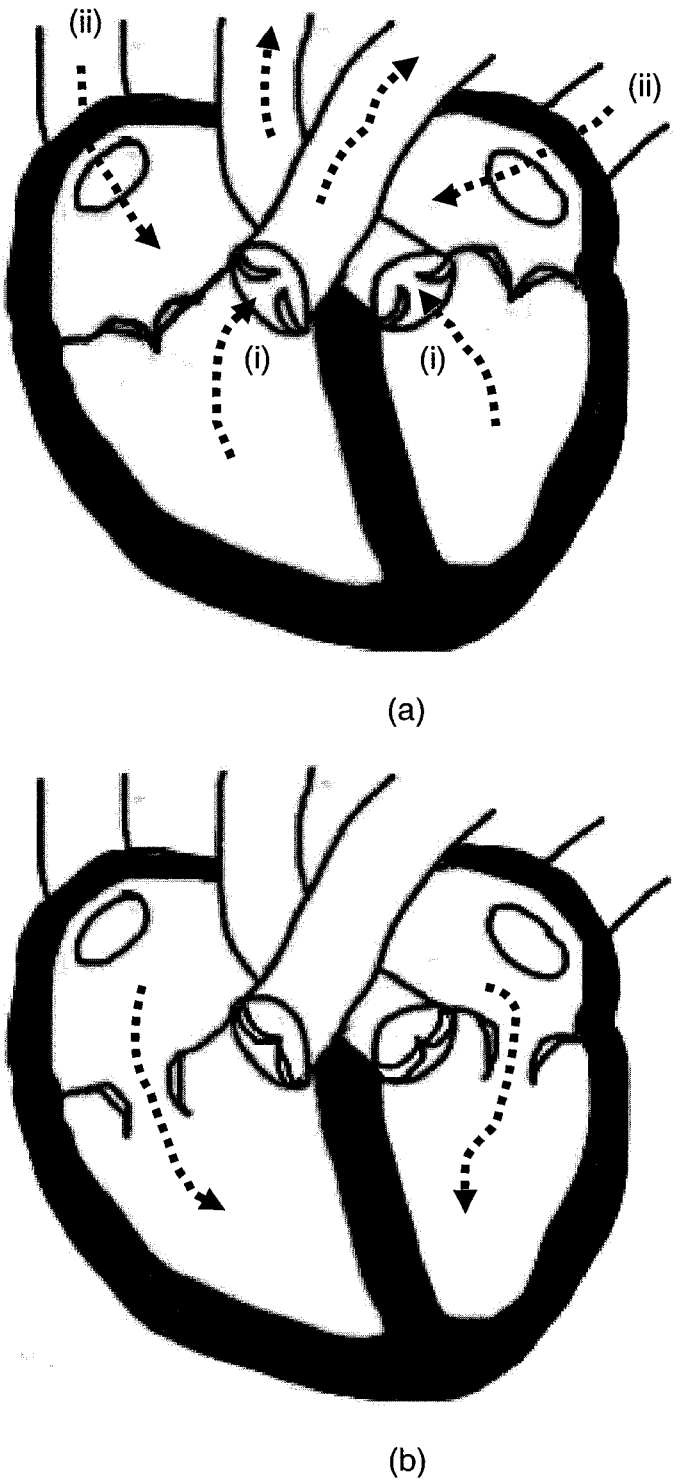

Figure 1.3: Heart chambers and valves during: (a) systole, (b) diastole.

1.2 Cardiac Sounds

1.2.1 Normal Sounds

Normal cardiac sounds heard during the cardiac cycle are the first heart sound (S1) and the second heart sound (S2), which in sequence form the typical "lub-dub" heard during a heartbeat [8]. S1 occurs at the beginning of systole, and is associated with the closing of the AV valves [8]. S2 occurs at the beginning of diastole, and is associated with the closing of the semilunar valves [8]. Graphically, cardiac sounds can be represented as sound intensity along the time domain. An example of S1 and S2 from two heartbeats can be seen in Figure 1.4.

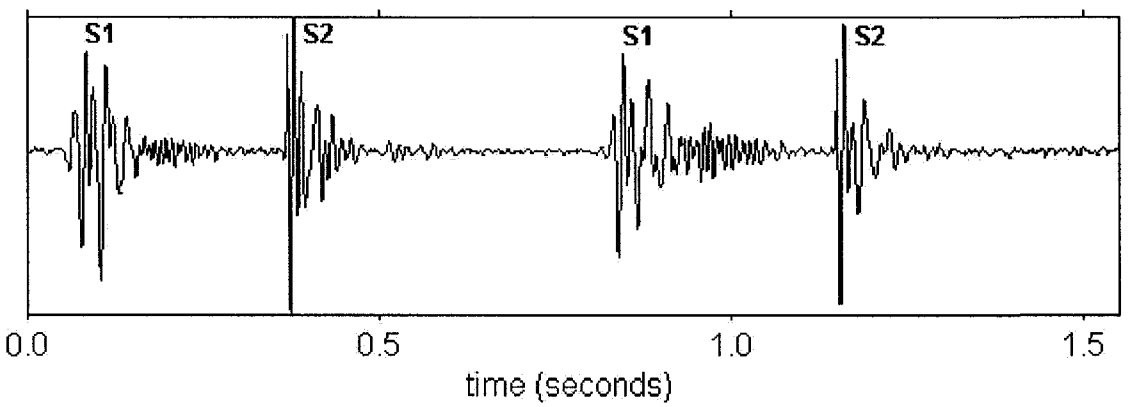

Figure 1.4: Example of normal cardiac sounds in two heartbeats.

1.2.2 Murmurs

Murmurs are another type of cardiac sound. A murmur is caused by blood flow turbulence, and is perceived as vibratory and more prolonged than S1 and S2 [8][50][67]. A murmur can be characterized by: timing in the cardiac cycle (systolic, diastolic, continuous), intensity (or loudness), frequency (or pitch), configuration (or shape),

duration (long, short), radiation (to other auscultatory areas), and variation with patient manoeuvres (such as breathing, position change, Valsalva) [67]. Example PCGs containing different timing of murmurs in the cardiac cycle can be seen in Figure 1.5.

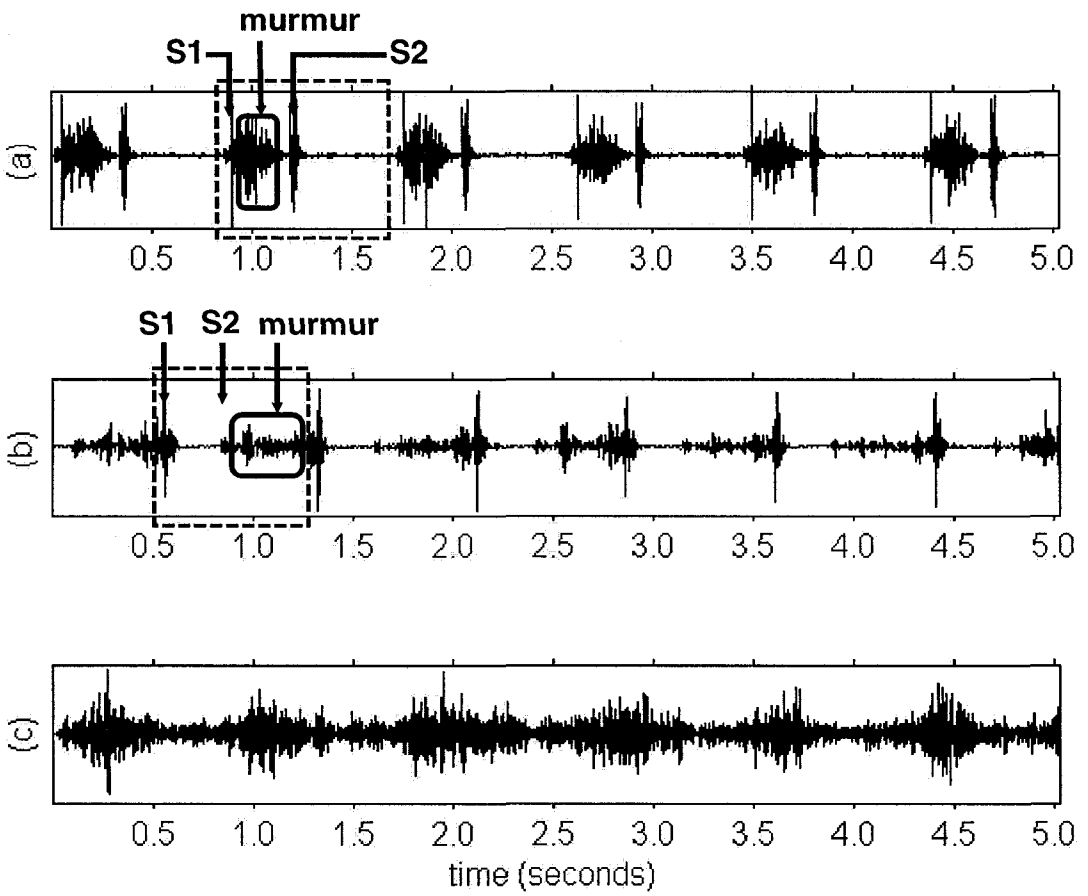

Figure 1.5: Examples of PCGs containing: (a) systolic murmur, (b) diastolic murmur, (c) continuous murmur. In (a) and (b), the dashed rectangle encloses a complete cardiac cycle.

The timing of a murmur within the cardiac cycle can indicate potential pathology of the heart and/or heart valves [8][71]. Systolic murmurs may or may not be abnormal, whereas diastolic murmurs and continuous murmurs (which occur throughout the cardiac cycle) tend to be abnormal [8].

Murmurs are typically associated with heart valve pathology, such as stenosis and insufficiency [50][71]. Heart valve stenosis (or narrowing) refers to when a heart valve does not open fully (e.g. due to stiffening), obstructing forward blood flow. Heart valve insufficiency (or leaking) refers to when a heart valve does not close fully, causing regurgitation or backward blood flow. Systolic murmurs are typically associated with semilunar valve stenosis or AV valve insufficiency, whereas diastolic murmurs are typically associated with AV valve stenosis or semilunar valve insufficiency. A grid showing the relationship between murmur timing in the cardiac cycle and possible heart valve pathology can be seen in Table 1.3.

Table 1.3: Timing of common heart valve pathologies.

PATHOLOGY / VALVE	Stenosis	Insufficiency
AV	Diastolic murmur	Systolic murmur
Semilunar	Systolic murmur	Diastolic murmur

1.2.3 Other Sounds

Depending on the health of the heart, other cardiac sounds may be heard during the cardiac cycle, such as: click, third heart sound (S3), fourth heart sound (S4), knock, and opening snap. A click can occur during systole, and is perceived as higher pitch and briefer duration than S1 and S2 [8]. The occurrence of clicks could be related to blood flow changes, abnormal tension in the ventricular wall or a heart valve, or pathological weakening of a heart valve [8].

Diastolic sounds (such as S3, S4, knock, and opening snap) generally have lower pitch, softer intensity, and longer duration than systolic sounds [8]. The occurrence of

diastolic sounds (with the exception of S2) is always abnormal in adults [8]. S3 can occur in early diastole, and indicates serious ventricular dysfunction in adults [8]. S4 can occur in late diastole, and indicates ventricular dysfunction to a lesser degree than S3 [8]. The occurrence of S4 is associated with augmented ventricular filling caused by atrial contraction [8]. A knock can occur in early diastole, and is perceived as a louder thudding sound than S3 and S4 [8]. The occurrence of a knock indicates abrupt arrest of ventricular filling caused by a non-compliant constricting pericardium (or membrane surrounding the heart) [8]. An opening snap can occur in early diastole, and is perceived as high pitch with brief duration [8]. The intensity of an opening snap is related to heart valve stiffness [8].

1.2.4 Diagnosis of Pathology

Through auscultation (i.e. by listening to the internal sounds of the body) using a stethoscope, an experienced health-care practitioner can hear cardiac sounds. The diagnosis of heart valve pathology through auscultation depends greatly on the timing of murmurs in the phases of the cardiac cycle; therefore, systole and diastole must first be discerned, relying on the perception of intervals between normal cardiac sounds (i.e. S1 and S2) by a health-care practitioner. Although a skilled practitioner can usually yield a conclusive diagnosis of heart valve pathology through auscultation, the correctness of diagnosis is usually dependent on the skill and experience of individual health-care practitioners. Since different heart pathologies may manifest with similar perceptible murmur characteristics, it would be useful to objectively analyze the characteristics of

cardiac sounds that may not be immediately apparent to human listeners, such as frequency and timing.

In order to aid the diagnosis of heart valve pathology, the phonocardiogram (PCG) can be analyzed to detect and classify murmurs. The PCG is a recording of sounds heard at the surface of the chest in the vicinity of the heart.

1.3 Automatic Phonocardiogram Analysis

With the advent of high-speed computing, the PCG can be efficiently analyzed in an automatic, objective, and repeatable manner using digital signal processing techniques. An automatic PCG analysis system could supplement traditional auscultation, as a differential diagnostic aid or screening device in clinical situations.

In general, an automatic PCG analysis system which seeks to detect and identify murmurs could be decomposed into multiple stages (as seen in Figure 1.6): preprocessing, segmentation, sound analysis, and murmur analysis. The preprocessing component prepares the data, to make the PCG suitable for analysis. Preprocessing operations could include amplification, filtering, normalization, and digitization. The segmentation component locates the boundaries of all the individual cardiac cycles in a PCG. The sound analysis component discerns systole and diastole within individual cardiac cycles, by detecting and classifying S1 and S2. (In another configuration of an automatic PCG analysis system, the sound analysis component can precede the segmentation component. In such a configuration, the segmentation component locates the boundaries of cardiac cycles as the locations of S1.) The murmur analysis component

locates any murmurs, determines features of the murmurs (such as the timing of a murmur in the phases of individual cardiac cycles), and classifies the murmur.

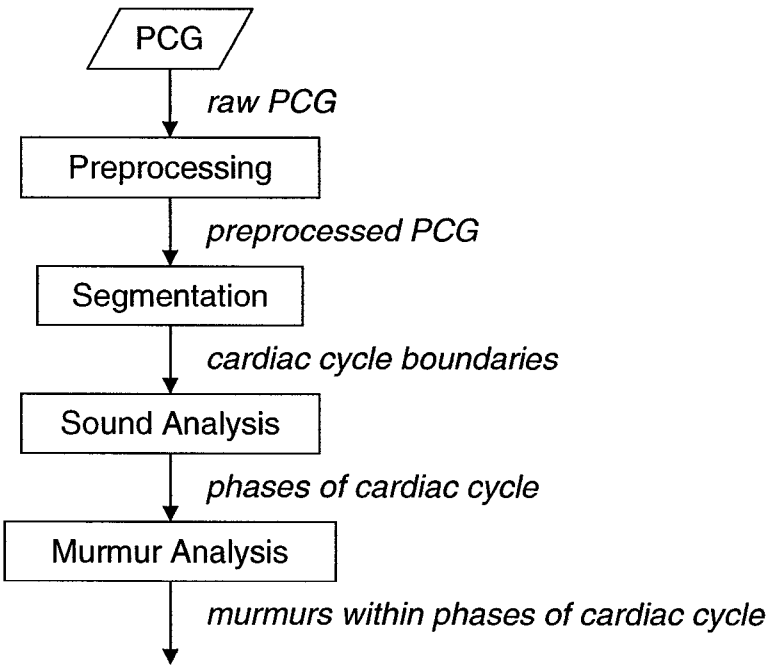

Figure 1.6: Components of an automatic PCG analysis system.

Achieving accurate segmentation of PCGs is necessary in an automatic PCG analysis system. Since an automatic murmur analysis component should be capable of examining many different types of heart pathologies, the segmentation component should be robust enough to handle PCGs containing varying degrees and types of noise.

1.3.1 Phonocardiogram Noise

A PCG is expected to contain normal cardiac sounds, as well as murmurs depending on the health of the heart. Depending on the PCG acquisition environment, PCGs may also contain non-cardiac noise, such as: biological noise from the patient (e.g. respiration, coughing), and non-biological noise from the environment (e.g. vibrations,

motion). Such aberrant noise can confound segmentation, especially if the noise resembles cardiac sounds.

Since non-cardiac noise typically does not contribute to the cyclostationary behaviour of the cardiac cycle, it may be possible to distinguish non-cardiac noise from cardiac sounds. It would be beneficial to de-noise, or suppress non-cardiac noise contributions from, PCGs prior to segmentation in an automatic murmur analysis tool.

After PCG segmentation and prior to determining the timing of patient-specific murmurs in the cardiac cycle, it would be useful to improve the signal-to-noise ratio of the cardiac cycle. Cardiac sounds which contribute to the cyclostationary behaviour of the cardiac cycle can be reinforced, while suppressing noise, by aligning and superimposing the cardiac sounds from multiple cardiac cycles. In order to properly align cardiac sounds, the automatic murmur analysis tool would need to achieve synchronous segmentation. In the context of this research, synchronous segmentation requires that every cardiac cycle in a PCG have the same time offset between S1 of the cardiac cycle and the boundary representing the beginning of the cardiac cycle.

1.4 Thesis Objectives

This thesis examines accurate and robust automated synchronous segmentation of heartbeats in PCGs exhibiting varying degrees and types of noise. In the context of an automatic murmur analysis tool, a PCG segmentation method ideally should be able to handle realistic PCGs with heartbeat-to-heartbeat variability in: heart sound intensity and duration, heart rate, murmur intensity and duration, and non-cardiac noise intensity and

duration. An existing PCG segmentation algorithm called the Sliding Window Autocorrelation (SWA) [9] accommodated variability in murmur presence, and attempted to address variability in heart sound intensity and heart rate.

The objective of this thesis was to improve the robustness of the SWA by further addressing variability in heart rate, variability in heart sound intensity, and the presence of non-cardiac noise. It was hypothesized that improvements can be achieved by: (i) increasing the accuracy of a heart rate estimate which is used to set parameters in the SWA, (ii) improving the selection of a heartbeat template which is used to segment heartbeats through a correlation methodology, and (iii) preprocessing PCGs to remove noise prior to applying the SWA.

1.4.1 Thesis Contributions

The major contributions are as follows:

I. **Proposed a heartbeat template shift competition, for automatically selecting a heartbeat template that exhibits the highest similarity to the cardiac cycles in a PCG.**

   By judging multiple possible heartbeat templates based on highest overall similarity to other cardiac cycles in a PCG, the chances of finding a suitable heartbeat template are greater than if only a single heartbeat template is considered. When unaffected by incorrect heartbeat period estimate, the heartbeat template shift competition was able to increase the overall segmentation accuracy of the SWA by up to 5.1%.

II. **Proposed an automated average heartbeat template method, for generating an averaged heartbeat template in an automated manner from all the cardiac cycles in a PCG.**

An averaged heartbeat template containing contributions from all cardiac cycles in a PCG more closely represents and correlates with the majority of the cardiac cycles. This addresses variability of heart sound intensity and heart rate among the cardiac cycles in a PCG. When unaffected by incorrect heartbeat period estimate and incorrect template location, the automated average heartbeat template method was able to increase the overall segmentation accuracy of the SWA by up to 2.4%.

III. **Proposed a preliminary de-noising method, for reducing or removing aberrant noises from PCG prior to segmentation.**

Reducing aberrant noise prior to segmentation decreases the dissimilarity between cardiac cycles in a PCG, and improves the effectiveness of correlations between cardiac cycles. The preliminary de-noising methods were able to increase the overall segmentation accuracy of the SWA by up to 2.3%.

IV. **Proposed a synchronous scoring method, for objectively evaluating the synchronous segmentation performance of PCG segmentation algorithms.**

By evaluating segmentation results in a repeatable and reproducible manner, and with explicit quantifiable criteria and metrics, the segmentation accuracy of different segmentation algorithms can be judged and compared based on

the same benchmark. This reduces the subjective influence of human investigators in the accurate reporting of results.

The minor contributions are as follows:

V. **Established a large PCG dataset, including manually located cardiac cycle boundaries and characterization of complexity, for evaluating the synchronous segmentation performance of PCG segmentation algorithms on the dataset.**

By manually locating cardiac cycle boundaries for the PCG dataset, other cardiac information (such as the electrocardiogram) is not required for evaluating the segmentation results. In conjunction with the automatic scoring method, the segmentation accuracy of different segmentation algorithms can be judged and compared based on the same dataset.

Contributions in this thesis have also been disseminated in the following publications:

- Chao S. and Chan A. D. C., "Sliding window autocorrelation for the synchronous unsupervised segmentation of the phonocardiogram," in *31st Conference of the Canadian Medical & Biological Engineering Society*, Montreal, PQ, Canada, A3-1, 2008.
- Chao S. and Chan A. D. C., "Selective heartbeat template location in the sliding window autocorrelation phonocardiogram segmentation algorithm,"

accepted to *32nd Conference of the Canadian Medical & Biological Engineering Society*, Calgary, AB, Canada, 2009.

1.5 Overview of Thesis Dissertation

In this thesis dissertation, existing PCG segmentation methods will be reviewed in ch. 2. The existing PCG segmentation algorithm called the Sliding Window Autocorrelation (SWA) will be described in ch. 3. The dataset and Automatic Scoring Method used to evaluate the SWA will be described in ch. 4. The effect of heart rate estimation and heartbeat template location in the SWA will be described in ch. 5. An extension to heartbeat template location, based on a shift competition, will be described in ch. 6. Enhancements to heart rate estimation and heartbeat template, based on averaging, will be described in ch. 7. Preliminary attempts to improve the PCG data by de-noising prior to segmentation will be described in ch. 8. Finally, conclusions and potential future work will be presented in ch. 9.

The existing SWA algorithm described in ch. 3, and the collection of the dataset described in ch. 4.1, were the work of a previous graduate student. The rest of this thesis dissertation, including the characterization and classification of the dataset described in ch. 4.1, are original work.

2 LITERATURE REVIEW

In this chapter, previous phonocardiogram (PCG) segmentation research is reviewed (section 2.1). The benefits and drawbacks of common segmentation techniques are discussed (section 2.2). The requirements and characteristics of a robust PCG segmentation algorithm for this research are then described (section 2.3).

2.1 Review of Previous Phonocardiogram Segmentation Research

Much of the previous PCG literature has focused on automatic sound analysis and murmur analysis assuming accurate PCG segmentation, such as in [1], [2], [6], [14], [15], [16], [17], [18], [22], [24], [25], [27], [29], [31], [36], [37], [46], [47], [48], [54], [62], [65], [66], [69], [70]. Many of such previous works rely on accurate PCG segmentation. However, research in the area of automatic PCG segmentation has not been pursued to as great an extent as automatic sound and murmur analysis. Table 2.1 provides an overview of previous works in the area of automatic PCG segmentation.

Table 2.1: Review of previous PCG segmentation research. Number of cardiac cycles, type of heart condition, type of murmur, and type of noise, are specified if available.

	YEAR	PCG SEGMENTATION METHODOLOGY	DATASET				RESULTS
			# PCGs *(# cycles)*	Includes Heart Conditions *(type)*	Includes Murmur *(type)*	Includes Noise *(type)*	
[20]	1962	Locate normal cardiac sounds using average power of contiguous windows, and amplitude thresholds. Classify S1 & S2 using timing relationships of cardiac cycle phases.	(i) 112 (ii) 134	(i) No (ii) Unknown	(i) No (ii) Yes : *split*	(i) No (ii) Yes : *respiratory, recording artifact*	Correct S1 & S2 detection: (i) 92% (ii) 88%
[26]	1980	Locate normal cardiac sounds using magnitude tracking of frequency band spectra. Classify S1 & S2 using linear prediction analysis.	187 *(881)*	Yes : *mitral insufficiency, aortic insufficiency, atrial septal defect, ventricular septal defect*	Yes	Unspecified	Correct S1 & S2 detection: 98% & 89%
[32]	1987	Locate S1 using R wave of ECG. Locate S2 using dicrotic notch in carotid pulse.	47	Yes	Yes : *systolic, diastolic*	Unspecified	Not reported
[7]	1989	Segment cardiac cycles using R wave of ECG. Locate A2 (of S2) using low pass filter or Hilbert transform envelope.	30	Yes : *implanted bioprostheses*	Yes	Unspecified	Correct S1 & S2 detection: 86.7% & 100%

	YEAR	PCG SEGMENTATION METHODOLOGY	DATASET				RESULTS
			# PCGs *(# cycles)*	Includes Heart Conditions *(type)*	Includes Murmur *(type)*	Includes Noise *(type)*	
[23]	1995	Segment cardiac cycles using ECG. Locate S1 & S2 using energy in frequency band of contiguous windows, and thresholds.	30 *(960)*	Yes	Unspecified	Unspecified	Not reported
[33]	1997	Locate normal cardiac sounds using Shannon energy of contiguous windows, and thresholds. Classify S1 & S2 using timing relationships of cardiac cycle phases.	37 *(515)*	Yes : *pediatric*	Yes	Yes : *speech, crying, stethoscope, ambient*	Correct S1 & S2 detection: 93%
[34]	1997	Preprocess using intensity envelopes of low frequency wavelet-decomposed levels, and frequency band selection for segmentation. Segmentation using method of [33].	(i) 37 *(515)* (ii) 40 *(650)*	Yes : *pediatric*	Yes	Yes : *speech, crying, stethoscope, ambient*	Correct S1 & S2 detection: (i) 97% (ii) 93%
[58]	1997	Segment cardiac cycles using matching pursuit method, i.e. adaptive time-frequency decomposition.	25	Yes : *bioprosthetic valve, stenosis*	Yes	Unspecified	Correct cardiac cycle segmentation: 96%

	YEAR	PCG SEGMENTATION METHODOLOGY	DATASET				RESULTS
			# PCGs *(# cycles)*	**Includes Heart Conditions** *(type)*	**Includes Murmur** *(type)*	**Includes Noise** *(type)*	
[59]	1998	Segment cardiac cycles using method of [58].	100	Yes : *bioprosthetic valve, stenosis, regurgitation*	Yes	Unspecified	Correct cardiac cycle segmentation: 84-96%
[52]	1998	Locate S1 using Morlet wavelet-based bank of correlators, and discriminant network.	Not specified	Yes	Unspecified	Unspecified	Not reported
[43]	2001	Segment cardiac cycles using hysteresis threshold, and timing relationships of cardiac cycle phases.	2	Yes : *aortic stenosis, mitral regurgitation*	Yes : *systolic*	Unspecified	Not reported
[38]	2003	Locate S1 & S2 using instantaneous energy of ECG.	15 *(210)*	Yes : *mitral regurgitation, mitral stenosis, ventricular septal defect*	Unspecified	Unspecified	Not reported
[49]	2004	Locate normal cardiac sounds using Shannon energy of low frequency wavelet-decomposed levels. Classify S1 & S2 using timing relationships of cardiac cycle phases.	Not specified	Yes	Unspecified	Unspecified	Not reported

	YEAR	PCG SEGMENTATION METHODOLOGY	DATASET				RESULTS
			# PCGs *(# cycles)*	**Includes Heart Conditions** *(type)*	**Includes Murmur** *(type)*	**Includes Noise** *(type)*	
[57]	2004	Segment cardiac cycles using estimate of heart rate. Locate S1 & S2 using data-adaptive thresholds, and timing relationships of cardiac cycle phases.	145 *(645)*	Yes	Yes	Unspecified	Correct S1 & S2 detection: 96%
[11]	2005	Locate S1 using ECG. Locate normal cardiac sounds using accentuated changes in variance fractal dimension. Classify S2 based on highest regularity of S1-S2 interval.	3 *(105)*	Yes : *bioprosthetic valve, aortic mechanical valve, mitral mechanical valve*	Unspecified	Unspecified	Correct S1 & S2 detection: 96%
[45]	2005	Locate normal cardiac sounds using simplicity, i.e. eigen-value spectrum.	5	Yes : *mitral stenosis*	Yes : *diastolic, overlapping*	Unspecified	Not reported
[68]	2005	Locate S1 using magnitude tracking of adaptive wavelet-based frequency band spectra, Shannon energy, and timing relationships of cardiac cycle phases.	30 *(207)*	Yes	Yes	Yes	Correct cardiac cycle segmentation: 93.24%

	YEAR	PCG SEGMENTATION METHODOLOGY	DATASET				RESULTS
			# PCGs *(# cycles)*	Includes Heart Conditions *(type)*	Includes Murmur *(type)*	Includes Noise *(type)*	
[55]	2005	Locate and classify S1 & S2 using Shannon energy of contiguous windows, Mel-spaced filterbanks, time-domain regression coefficients, and Hidden Markov Model.	46	Unspecified	Yes : *split*	Unspecified	Correct S1 & S2 detection: 98%
[21]	2005	Locate normal cardiac sounds using homomorphic filtering, and amplitude thresholds. Classify S1 & S2 using timing relationships between cardiac cycle phases and K-means clustering.	Not specified *(340)*	Unspecified	Yes : *systolic, diastolic*	Unspecified	Correct cardiac cycle segmentation: 90.45 %
[53]	2006	Locate normal cardiac sounds using Morlet wavelet-based bank of correlators, data-adaptive threshold, and singular value decomposition. Classify S1 & S2 using timing relationships of cardiac cycle phases.	42 *(534)*	Yes : *bioprosthetic valve*	Yes	Yes	Correct S1 & S2 detection: 90.5%

	YEAR	PCG SEGMENTATION METHODOLOGY	DATASET				RESULTS
			# PCGs *(# cycles)*	**Includes Heart Conditions** *(type)*	**Includes Murmur** *(type)*	**Includes Noise** *(type)*	
[10]	2006	Locate normal cardiac sounds using Morlet wavelet-based bank of correlators, right singular vectors, and K-means clustering. Label S1 & S2 clusters manually.	42 *(612)*	Yes : *bioprosthetic valve*	Yes : *systolic*	Unspecified	Correct S1 & S2 detection: 97.5%
[28]	2006	Locate normal cardiac sounds using wavelet-decomposed levels, Shannon energy of contiguous windows, and adaptive thresholds. Classify S1 & S2 using wavelet-based high frequency markers, and timing relationships of cardiac cycle phases.	55 *(7530)*	Yes : *bioprosthetic valve, mechanical valve*	Unspecified	Unspecified	Sensitivity: 97.95% Specificity: 98.20%
[44]	2007	Locate normal cardiac sounds using wavelet-decomposed levels, Shannon energy of contiguous windows, and data-adaptive threshold. Classify S1 & S2 using timing relationships of cardiac cycle phases.	Not specified	Unspecified	Unspecified	Unspecified	Segmentation results not reported

	YEAR	PCG SEGMENTATION METHODOLOGY	DATASET				RESULTS
			# PCGs *(# cycles)*	**Includes Heart Conditions** *(type)*	**Includes Murmur** *(type)*	**Includes Noise** *(type)*	
[5]	2008	Locate normal cardiac sounds using estimate of cardiac cycle duration, energy, data-adaptive and iterative thresholds. Classify S1 & S2 using timing relationships of cardiac cycle phases.	71 *(357)*	Yes	Yes	Yes	Correct cardiac cycle segmentation: 97%
[64]	2008	Locate normal cardiac sounds using wavelet-decomposed levels, simplicity (i.e. eigen-value spectrum), energy of contiguous windows, and thresholds. Classify S1 & S2 using timing relationships of cardiac cycle phases.	Not specified *(160)*	Yes : *aortic stenosis*	Yes : *systolic*	Unspecified	Correct S1 & S2 detection: 84%

	YEAR	PCG SEGMENTATION METHODOLOGY	DATASET				RESULTS
			# PCGs *(# cycles)*	Includes Heart Conditions *(type)*	Includes Murmur *(type)*	Includes Noise *(type)*	
This work	2009	Preprocess using bandpass filter, Morlet wavelet decomposition, and Hilbert transform. Segment cardiac cycles using heartbeat period estimate, similarity correlations, shifted heartbeat template competition, and heartbeat averaging.	195 *(2453)*	Yes : *aortic stenosis & regurgitation, atrial septal defect, AV block, Blalock Taussig shunt, Ebstein, Eisenmenger, Gallavardin, hypertrophic cardiomyopathy, mitral stenosis & regurgitation, mitral valve prolapse, Noonans, patent ductus arteriosus, pulmonary stenosis & regurgitation, Stills, tetralogy of Fallot, transposition, tricuspid stenosis & regurgitation, ventricular septal defect*	Yes : *systolic, holosystolic, diastolic, holodiastolic, continuous*	Yes : *speech, respiration, crying, coughing, background*	Correct cardiac cycle segmentation (synchronous within 50 ms): 93.5%

2.2 Common Phonocardiogram Segmentation Techniques

Previous PCG literature concerning cardiac cycle segmentation makes use of some common techniques for detecting and classifying normal cardiac sounds. Common segmentation techniques include: (i) use of an auxiliary signal [7][11][23][32][38][57]; (ii) use of energy measures with threshold detectors [5][10][20][21][23][28][33][44][45] [49][53][57][64][68]; (iii) use of timing relationships of cardiac cycle phases [5][20][21] [23][28][33][43][44][45][49][53][57][64][68]; (iv) use of frequency domain [10][23][26] [53][55][58]; and (v) use of wavelet transform [10][28][34][44][49][52][53][64][68]. Many previous works used a limited dataset [11][21][43][44][45][49][52][55][64]. Few of the previous works aimed to provide synchronous segmentation [4][30][35][55]. Some of the previous works did not report quantitative results [23][32][38][43][44][45][49] [52].

2.2.1 Use of Auxiliary Signal

Some PCG segmentation methods have relied on the use of auxiliary signals to locate S1 and S2. The beginning of S1 has been estimated as the onset of the R wave in the electrocardiogram (ECG) [7][11][23][32][38]. The beginning of S2 has been corresponded to the dicrotic notch in the carotid pulse [32]. There are benefits and drawbacks associated with using these auxiliary signals.

The ECG is synchronous with the PCG, since S1 in the PCG typically occurs immediately after the QRS complex in the ECG [42]. The QRS complex is easy to detect, since it manifests as a clear dominant part of the cardiac cycle, typically five times larger

than other aspects of the ECG. However, the timing between the electrical and mechanical activities of the heart varies among individuals, particularly with a number of pathological activities [23].

Furthermore, the use of auxiliary signals for PCG segmentation complicates the implementation of a practical PCG analysis system, especially the patient interface. Specifically, for ECG, at least two electrode sites are required for ECG monitoring. A system that only involves the placement of a stethoscope bell to gather the PCG is better suited for clinical work, telemedicine, or offline analysis. Since the PCG can be non-invasively detected at the surface of the skin, it is a practical diagnostic modality.

2.2.2 Use of Energy Measures with Threshold Detectors

Some PCG segmentation methods have used energy measures with threshold detectors [5][10][20][21][23][28][33][44][45][49][53][57][64][68]. Such methods may detect normal cardiac sounds as the peaks in an energy profile (such as normalized Shannon energy) which surpass a fixed or adaptive threshold.

The use of an energy profile does not necessarily preclude nor encourage robust PCG segmentation; however, general sound intensity relationships which are commonly assumed when using energy measures may not always apply. For example, some methods which use energy measures with threshold detectors to locate normal cardiac sounds generally assume that *the intensity of normal cardiac sounds is greater than the intensity of noise*; however, this may not be true for PCG containing high intensity non-cardiac noise. Some methods may differentiate between S1 and S2 assuming the *loudness of S2 is*

greater than that of S1; however, such simplistic rules are not true for all heart conditions and may not work well in noisy conditions. For example, the loudness of S2 may be less than that of S1 due to decreased intensity of S2 (e.g. aortic stenosis) or increased intensity of S1 (e.g. mitral stenosis). Furthermore, S1 and/or S2 may be rendered indistinct by a holosystolic murmur (e.g. ventricular septal defect) or may be split (e.g. hypertrophic cardiomyopathy, Ebstein's anomaly).

2.2.3 Use of Timing Relationships of Cardiac Cycle Phases

Some PCG segmentation methods have used timing relationships of cardiac cycle phases [5][20][21][23][28][33][43][44][45][49][53][57][64][68]. Such methods may classify or discriminate between S1 and S2 based on the time intervals between previously detected normal cardiac sounds.

General assumptions regarding the timing relationships of the cardiac cycle phases (systole and diastole) may not always apply. Some methods may differentiate between systole and diastole using general rules, such as *the duration of systole is less than the duration of diastole* or *the duration of systole is half the duration of diastole*; however, the duration of systole may be greater than the duration of diastole, due to rapid heart rate (e.g. ventricular tachycardia). Additionally, the duration of diastole may vary, due to irregular heart rate (e.g. sinus arrhythmia).

2.2.4 Use of Frequency Domain

Some PCG segmentation methods have used information from the frequency domain and the time-frequency domain. Such methods may have corresponded the

energy in particular frequency bands to the energy of normal cardiac sounds [23][26][55]. Some methods have also used information from the time-frequency domain to isolate frequency bands containing the highest energy components [10][53][58][59], assuming the highest energy components corresponded to normal cardiac sounds. Although the use of frequency information is promising, the assumption that cardiac sounds which contribute to the cyclostationary behaviour of the cardiac cycle occur only in particular frequency bands may not always apply in this research. For example, murmurs associated with some heart conditions could contribute to the cyclostationary behaviour of the cardiac cycle, and could occur in different frequency bands than normal cardiac sounds.

2.2.5 Use of Wavelet Transform

Some PCG segmentation methods have used the wavelet transform to preprocess PCG prior to segmentation [10][28][34][44][49][52][53][64][68], or to classify cardiac sounds post-segmentation (not discussed). Although the use of time-frequency domain information made available by the wavelet transform is promising, several parameters or options must be considered, such as: type of wavelet transform, wavelet family and order, decomposition levels, and reconstruction method.

2.2.6 Limited Dataset

Some PCG segmentation methods have used limited datasets [11][21][43][44][45] [49][52][55][64]. The performance or accuracy of such methods may have been evaluated using only a small number of PCGs or a small range of pathologies. Some methods were tested using a dataset of fewer than six PCGs [11][43][45], some methods

did not specify the number of PCGs in the dataset [21][49][52][64], some methods did not specify the types of PCGs tested [21][55], and some methods did not specify dataset size nor the types of PCGs tested [44].

Some research studies have limited their evaluation of PCG segmentation methods by using relatively clean PCGs that lack non-cardiac noises. Using only clean PCGs does not sufficiently test the robustness of a segmentation method, since the segmentation method would not be tested for PCGs containing confounding noises.

Although some methods have shown potential for segmentation of noisy PCGs, more testing using a larger number and variety of PCGs is required. In particular, a segmentation method was described in [45] as invariant to amplitude and frequency variations of heart sounds, and used eigen-value spectrum to locate heart sounds in the presence of murmurs; however, segmentation results were presented for only five PCGs, which may not represent a sufficiently wide range of noise conditions and/or murmur types.

2.2.7 Synchronous Segmentation

Some PCG segmentation methods have attempted to provide synchronous segmentation [9][55] or refined boundaries of normal cardiac sounds [4][30][35]. Most works have not aimed for synchronous segmentation that would be useful for averaging cardiac cycles; such methods only detect and classify the normal cardiac sounds, then label the intervals between the normal cardiac sounds as systole and diastole. In [55], normal cardiac sounds were considered successfully labelled if the center of a classified

(predicted) sound is within 50ms of the center of an annotated (control or validated) sound. Although [4], [30], and [35], attempted to locate more precise boundaries of normal cardiac sounds post-segmentation, synchronous segmentation was not the primary aim.

2.2.8 Quantitative Results

Some PCG segmentation methods have been described without reporting quantitative results [23][32][38][43][44][45][49][52]. Furthermore, there is no standard method for evaluating segmentation results in an objective, quantitative, repeatable manner.

2.3 Requirements of a Robust Phonocardiogram Segmentation Algorithm

In this research, a robust PCG segmentation algorithm should meet several criteria:

(i) uses only a PCG, and does not require the use of any auxiliary signals;

(ii) does not follow any assumptions regarding the intensity of normal cardiac sounds relative to the intensity of noise;

(iii) does not follow any assumptions regarding the relative intensity between S1 and S2;

(iv) does not follow any assumptions regarding the relative duration of systole and diastole;

(v) uses information in the time-frequency domain for preprocessing prior to segmentation;

(vi) tested using a dataset containing a large number of PCGs, representative of a large variety of heart conditions and pathologies, and including varying types and degrees of noise;

(vii) provides synchronous segmentation;

(viii) segmentation results evaluated in an objective, quantitative, repeatable manner.

The original Sliding Window Autocorrelation (SWA) segmentation algorithm satisfies most of these criteria. Modifications to the SWA will satisfy the criteria that are not met by the original SWA. A detailed description of the original SWA follows in the next chapter.

3 SLIDING WINDOW AUTOCORRELATION SEGMENTATION ALGORITHM

The work described in this dissertation is built upon an existing phonocardiogram (PCG) segmentation algorithm, called the *Sliding Window Autocorrelation* (SWA) [9]. The SWA algorithm is designed to perform automatic synchronous segmentation of PCGs exhibiting varying complexity, such as the presence of murmur noise, non-biological noise, or variable heart rate.

The SWA assumes the variability of systole duration is less than the variability of diastole duration; that is, the timing within a heartbeat has less variability than the timing between heartbeats. The SWA relies on the cyclostationary nature of heartbeats in PCGs, and extensively uses correlations of similar windows of heartbeats.

The SWA consists of three stages: *Heart Rate Estimation* (section 3.2), *Heartbeat Template Location* (section 3.3), and *Heartbeat Boundary Prediction* (section 3.4). A block diagram showing how the three stages are interconnected can be seen in Figure 3.1.

As a preprocessing stage, the Heart Rate Estimation stage estimates the heartbeat period in a given PCG, to set parameters used by the other stages. Both the Heartbeat Template Location and Heartbeat Boundary Prediction stages rely heavily on the *similarity correlation operator* (section 3.1), which generates coefficients indicating the degree of similarity between two windows within a given PCG.

In order to segment a given PCG, the SWA requires passing through the given PCG twice. The first pass corresponds to the Heartbeat Template Location stage, which generates the first set of similarity correlations, and locates a representative heartbeat or

heartbeat template within the given PCG. The second pass corresponds to the Heartbeat Boundary Prediction stage, which generates the second set of similarity correlations (using the heartbeat template), and predicts the locations of heartbeat boundaries within the given PCG.

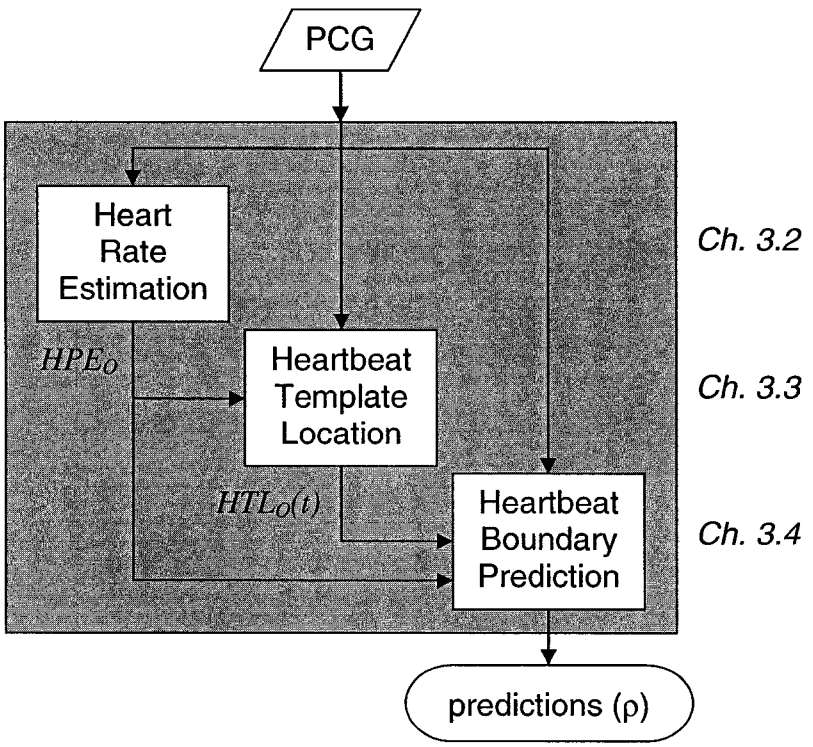

Figure 3.1: Block diagram of original Sliding Window Autocorrelation (SWA).

3.1 Similarity Correlation Operator

Central to the performance of the SWA is the similarity correlation operator [9]. As with conventional cross-correlation, the similarity correlation provides an indication of the degree of similarity between two windows of a PCG. A *similarity correlation* is generated by sliding a short *template window* (e.g. part of the PCG corresponding to a single heartbeat) across a longer *search window*. A peak in a similarity correlation

indicates a high degree of similarity between the template window and a portion of the search window. By observing the time offset at which the peak occurs in the similarity correlation, along with knowledge of where the search window occurs within the PCG, the time at which a highly similar portion occurs in the PCG could be predicted. An example of a similarity correlation can be seen in Figure 3.2.

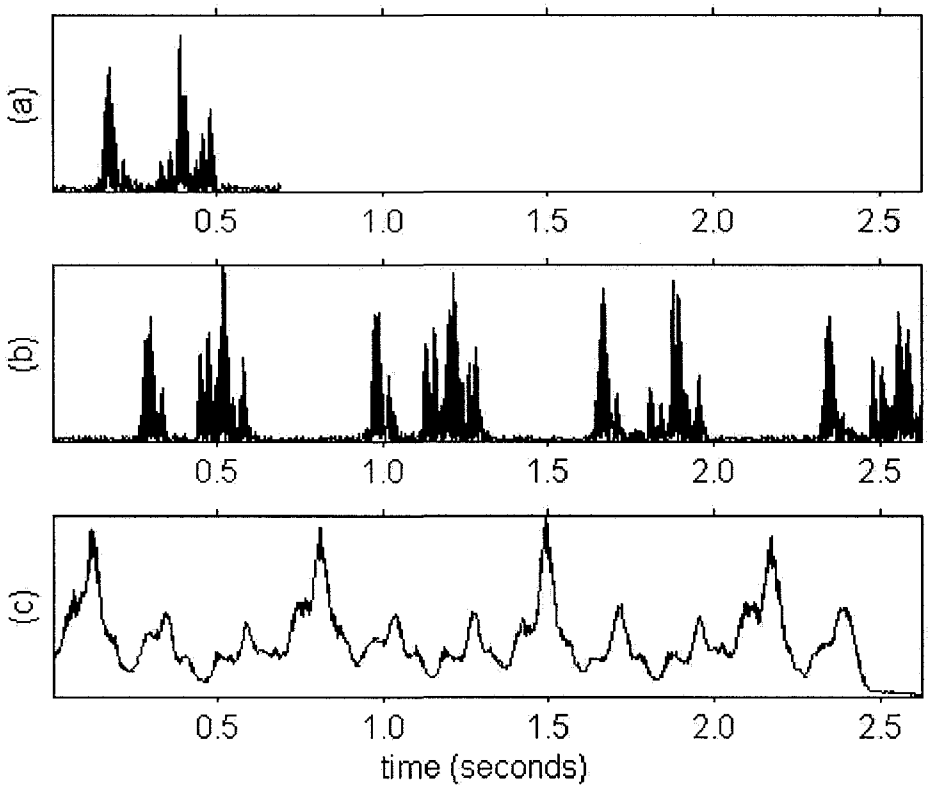

Figure 3.2: Example of a similarity correlation: (a) template window; (b) search window; (c) similarity correlation.

Conventional cross-correlation has a notable disadvantage, in that it is affected by varying energy within the two windows. For example, a PCG may contain cardiac cycles which have a similar intensity pattern, but which vary in absolute intensity. Such heartbeat-to-heartbeat energy variation can cause the conventional cross-correlation to

incorrectly indicate a high degree of similarity between heart sounds of differing types (i.e. S1 and S2). The similarity correlation, however, attempts to compensate for heartbeat-to-heartbeat magnitude variations, by scaling the cross-correlation by the energy of each window.

For the SWA, similarity correlations were calculated on the normalized signal magnitude of a PCG, which could be calculated using Eq. (3.1)-(3.3). Given the original waveform $s(t)$ of a digitized PCG of length N samples, the DC component $\overline{s(t)}$ is first removed, as in Eq. (3.1). It should be noted that round brackets are used to denote discrete time signals (not continuous time signals) throughout this thesis dissertation. (Although square brackets are usually used to denote discrete time signals, square brackets are used in this thesis dissertation to denote step units for the peak offset sequence described in ch. 3.3.) The resulting waveform $s_{AC}(t)$ is scaled by the inverse of its RMS, yielding a normalized waveform $s_{norm}(t)$, as in Eq. (3.2). The absolute magnitude of $s_{norm}(t)$ is taken, yielding the normalized signal magnitude $w(t)$, as in Eq. (3.3).

$$s_{AC}(t) = s(t) - \overline{s(t)} \tag{3.1}$$

$$s_{norm}(t) = \frac{s_{AC}(t)}{\sqrt{\frac{1}{N}\sum_{t=0}^{N-1}[s_{AC}(t)]^2}} \tag{3.2}$$

$$w(t) = |s_{norm}(t)| \tag{3.3}$$

Using $w(t)$, the similarity correlation $G(\tau)$ can be calculated using Eq. (3.4)-(3.8). The two windows to be correlated are $w_1(t)$ and $w_2(t)$, which are of length N_1 and N_2 samples, respectively. By convention, $N_1 \leq N_2$. Using $w_1(t)$ zero-padded to length N_2, the conventional cross-correlation $R(\tau)$ is calculated, as shown in Eq. (3.4). $G(\tau)$ shown in Eq. (3.8) is scaled by magnitudes derived in Eq. (3.5) to (3.7).

$$R(\tau) = \sum_{t=0}^{N_2-\tau-1} w_2(t+\tau)w_1(t) \text{ , for } 0 \leq \tau < N_2 \tag{3.4}$$

$$E = \sum_{t=0}^{N_1-1} [w_1(t)]^2 \tag{3.5}$$

$$L(t) = \begin{Bmatrix} 1, & 0 \leq t < N_1 \\ 0, & N_1 \leq t < N_2 \end{Bmatrix} \tag{3.6}$$

$$M(\tau) = \sum_{t=0}^{N_2-\tau-1} [w_2(t+\tau)]^2 L(t) \text{ , for } 0 \leq \tau < N_2 \tag{3.7}$$

$$G(\tau) = \frac{1}{\sqrt{E}} \frac{R(\tau)}{\sqrt{M(\tau)}} \text{ , for } 0 \leq \tau < N_2 \tag{3.8}$$

3.2 Heart Rate Estimation Stage

The Heart Rate Estimation (HRE) stage estimates the heartbeat period of a given PCG prior to segmentation. The *estimated heartbeat period* HPE_0 is the reciprocal of the estimated heart rate, and corresponds to the time offset of the peak in a tapered autocorrelation of the PCG waveform. The estimated heartbeat period is used to set parameters in the later stages of the SWA.

HPE_O is calculated using Eq. (3.9)-(3.14). Using the square magnitude $x(t)$ of the given PCG waveform of length N samples, the HRE stage generates an autocorrelation $R_{xx}(\tau)$. The time offset range corresponding to a reasonable heartbeat period is emphasized by multiplying $R_{xx}(\tau)$ by a tapered window $T_R(\tau)$, which generates a tapered autocorrelation $R_{xx,T}(\tau)$. $T_R(\tau)$ also removes the inherent peak located within τ_{null} of the beginning of $R_{xx}(\tau)$. An exponential taper used in the HRE stage is defined by Eq. (3.11), where C is the time constant of the taper. The time offset $\tau_{\max}$ of the highest magnitude peak in $R_{xx,T}(\tau)$ is a likely estimate of heartbeat period, since $\tau_{\max}$ represents the time between S1 of the first heartbeat and S1 of the second heartbeat in the PCG. An example of $x(t)$, $R_{xx}(\tau)$, $T_R(\tau)$, $R_{xx,T}(\tau)$, and $\tau_{\max}$ can be seen in Figure 3.3.

$$x(t) = [w(t)]^2 \tag{3.9}$$

$$R_{xx}(\tau) = \sum_{t=0}^{N-\tau-1} x(t+\tau)x(t) \text{ , for } 0 \le \tau < N_2 \tag{3.10}$$

$$T_R(\tau) = \begin{Bmatrix} \frac{\tau}{C} \times e^{-\tau/C}, \tau >= \tau_{null} \\ 0, \tau < \tau_{null} \end{Bmatrix} \text{ , for } 0 \le \tau < N_2 \tag{3.11}$$

$$R_{xx,T}(\tau) = R_{xx}(\tau)T_R(\tau) \text{ , for } 0 \le \tau < N_2 \tag{3.12}$$

$$\tau_{\max} = \arg\max_{\tau} \{R_{xx,T}(\tau)\} \tag{3.13}$$

$$HPE_O = \tau_{\max} \tag{3.14}$$

The time constant C could be chosen based on *a priori* patient information in order to account for the physiological properties of a patient's heart. For example, pediatric patients usually have faster heart rates than adult patients, and so may require a smaller time constant to represent a "faster" taper that can effectively attenuate the peak at twice the HPE_0.

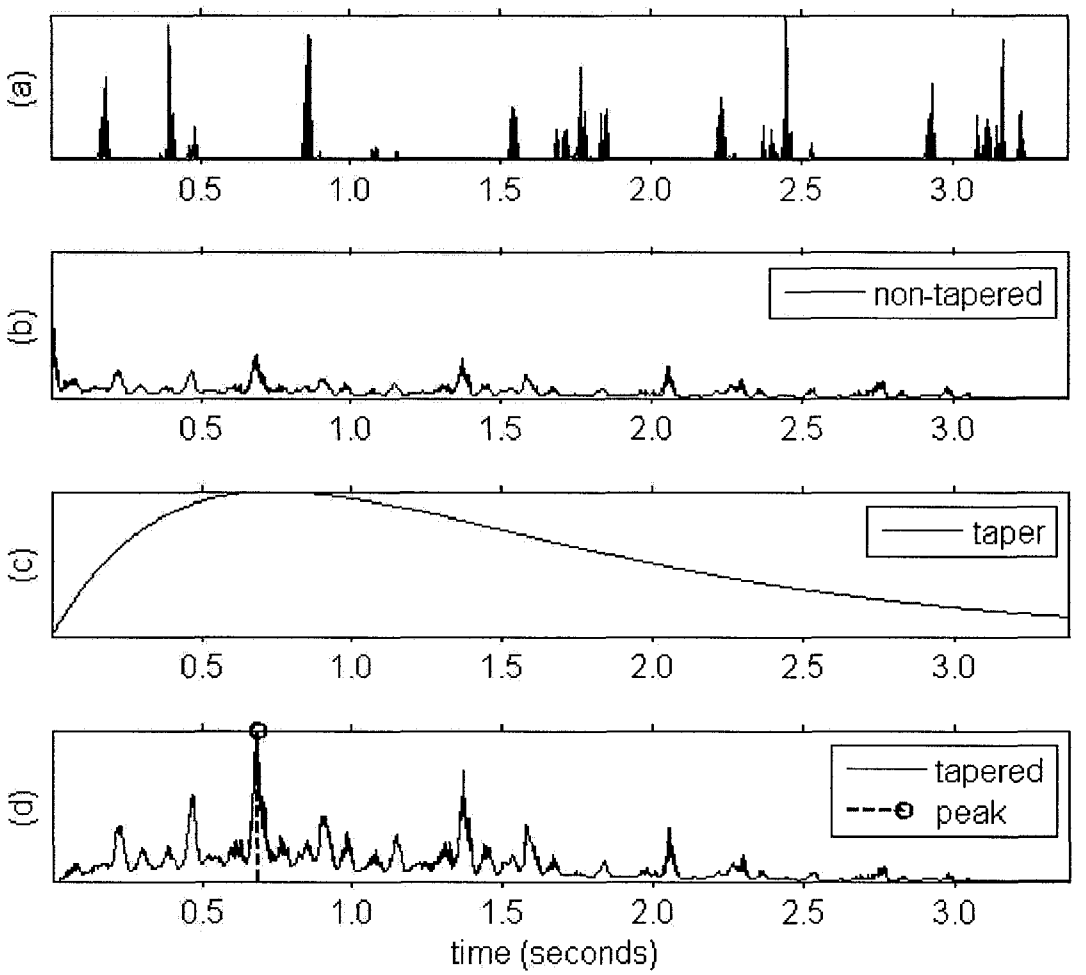

Figure 3.3: Example of heartbeat period estimate HPE_0 generation: (a) square magnitude $x(t)$; (b) autocorrelation $R_{xx}(\tau)$; (c) taper $T_R(\tau)$; (d) tapered autocorrelation $R_{xx,T}(\tau)$ and highest magnitude peak. In (d), τ_{max} corresponds to the time offset of the highest magnitude peak.

Variations of the HRE stage involve generating an autocorrelation from waveforms other than the square magnitude, such as the Hilbert magnitude (i.e. magnitude of the Hilbert transform) and the absolute magnitude. In previous work [9], the square magnitude generated the highest overall accuracy in the HRE stage. For this reason, in this work, the HRE stage uses only the square magnitude.

3.3 Heartbeat Template Location Stage

The accurate location of a representative heartbeat template $HTL_O(t)$ is essential to the performance of the Heartbeat Boundary Prediction stage, since it is used to predict locations of potential heartbeat boundaries in a given PCG.

The Heartbeat Template Location (HTL) stage generates the first set of similarity correlations. At each "*step*" or interval of 40 ms (corresponding to length $N_{step} = 160$ samples assuming sampling rate of 4000 Hz) within the normalized signal magnitude $w(t)$ of length N samples (previously expressed in Eq. (3.3)), a similarity correlation is performed. The number of steps I is calculated using Eq. (3.15). The sample location u of each step i is calculated using Eq. (3.16).

$$I = \left\lceil \frac{N}{N_{step}} \right\rceil \tag{3.15}$$

$$u = i \times N_{step} \text{ , for } 0 \le i < I \tag{3.16}$$

At each step i, the template window $w_1^i(t)$ and the search window $w_2^i(t)$ are defined using Eq. (3.17) and (3.18), and the resulting similarity correlation $G^i(\tau)$ is

calculated using Eq. (3.4)-(3.8). $G^i(\tau)$ is multiplied by a taper $T_G(\tau)$ defined by Eq. (3.19), which generates a tapered similarity correlation $G_T^i(\tau)$ expressed in Eq. (3.20). An example of $G_T^i(\tau)$ can be seen in Figure 3.4. The time offset $\tau_{\max}^i$ of the highest magnitude peak in $G_T^i(\tau)$, or *peak offset*, is determined by Eq. (3.21).

$$w_1^i(t) = \{w(t) : u \le t < (u + N_1)\}\ ,\ N_1 = \lfloor 0.7 HPE_O \rfloor \tag{3.17}$$

$$w_2^i(t) = \{w(t) : u \le t < (u + N_2)\}\ ,\ N_2 = \lfloor 1.8 HPE_O \rfloor \tag{3.18}$$

$$T_G(\tau) = \tau \times e^{-\tau / HPE_O}\ \text{, for } 0 \le \tau < N_2 \tag{3.19}$$

$$G_T^i(\tau) = G^i(\tau) T_G(\tau)\ \text{, for } 0 \le \tau < N_2 \tag{3.20}$$

$$\tau_{\max}^i = \arg\max_{\tau} \{G_T^i(\tau)\} \tag{3.21}$$

The peak offsets $\tau_{\max}^i$ for all steps $i = 0...(I-1)$, when taken in sequence, are referred to as the *peak offset sequence* $P_o[i]$ expressed in Eq. (3.22). An example of $P_o[i]$ can be seen in Figure 3.5.

$$P_o[i] \equiv \tau_{\max}^i\ \text{, where } i = 0...(I-1) \tag{3.22}$$

The portion $P_o[a,b]$ of the peak offset sequence between steps a and b is defined by Eq. (3.23), which corresponds to length N_{span} samples defined by Eq. (3.24). The *range of variability* $D[a,b]$ of the peak offset sequence between steps a and b can be defined by Eq. (3.25).

$$P_o[a,b] = \{P_o[i] : a \le i \le b\} \tag{3.23}$$

$$N_{span} = (b-a) \times N_{step} \tag{3.24}$$

$$D[a,b] = \max\{P_o[a,b]\} - \min\{P_o[a,b]\} \tag{3.25}$$

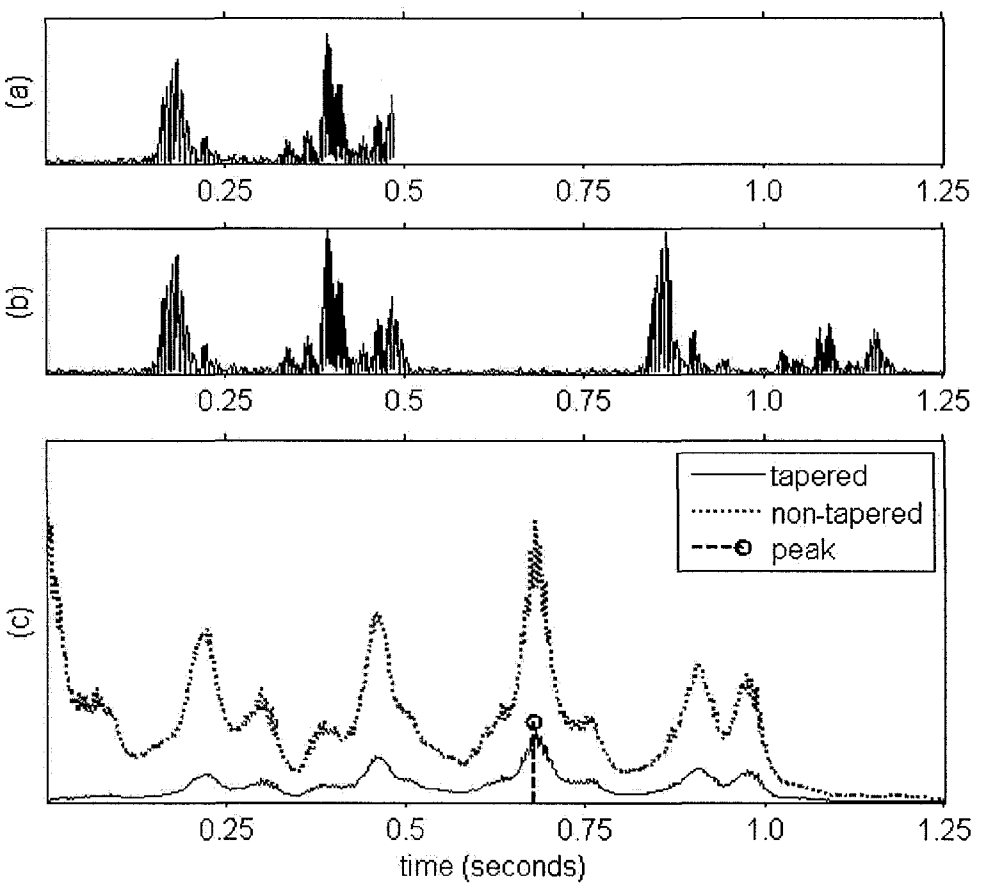

Figure 3.4: Example of tapered similarity correlation generation: (a) template window $w_1^i(t)$; (b) search window $w_2^i(t)$; (c) similarity correlation $G^i(\tau)$, tapered similarity correlation $G_T^i(\tau)$, and time offset $\tau_{\max}^i$ of highest magnitude peak.

Within $P_o[i]$, adjacent steps which have comparable $\tau_{\max}^i$ likely belong to the same heartbeat, whereas relatively large changes of $\tau_{\max}^i$ occur approximately at locations

of heartbeat boundaries. Adjacent steps which have $\tau^i_{\max}$ differ by at most 0.2% of HPE_O are grouped as a "*span*". Each span j can be characterized by Eq. (3.26)-(3.28), and satisfy the empirical criteria expressed in Eq. (3.29) and (3.30).

$$P_o^j[a^j,b^j]=\{P_o[i]: a^j \le i \le b^j\} \tag{3.26}$$

$$N^j_{span}=(b^j-a^j)\times N_{step} \tag{3.27}$$

$$D[a^j,b^j]=\max\{P_o^j[a^j,b^j]\}-\min\{P_o^j[a^j,b^j]\} \tag{3.28}$$

$$0.1HPE_O \le N^j_{span} \le 0.8HPE_O \tag{3.29}$$

$$D[a^j,b^j] \le 0.002HPE_O \tag{3.30}$$

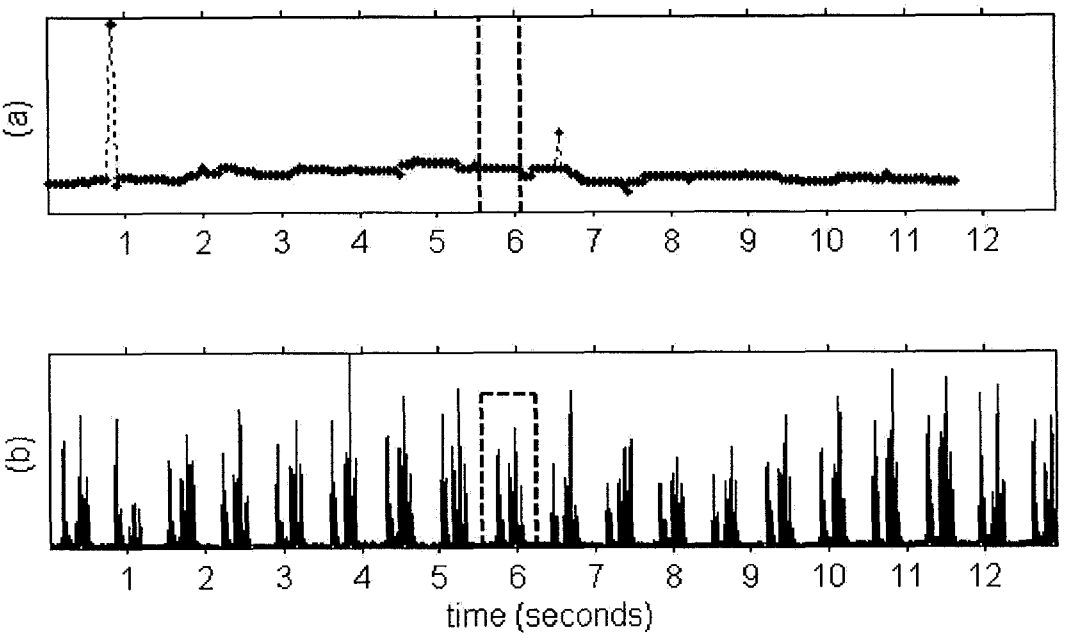

Figure 3.5: Example of peak offset sequence and corresponding PCG: (a) peak offset sequence $P_o[i]$ with longest span enclosed by dashed lines; (b) heartbeat template $HTL_O(t)$ enclosed by dashed box.

The *longest span* ℓ satisfies the additional empirical criteria of Eq. (3.31).

$$\ell = \arg\max_{j} \{N_{span}^{j}\} \tag{3.31}$$

If there are multiple spans with the same longest length, the span with smallest $D[a^j, b^j]$ is selected as the longest span. An example of ℓ can be seen in Figure 3.5.

If there are no valid spans in $P_o[i]$, then the rest of the SWA is skipped, and no predictions are made for the PCG; hence, the PCG is considered un-segmentable. Otherwise, the heartbeat template starts at the beginning of the longest span (u^{ℓ}), and has length N_{HTL} equal to HPE_O, as characterized by Eq. (3.32) and (3.33). An example of the heartbeat template can be seen in Figure 3.5 and Figure 3.6.

$$u^{\ell} = a^{\ell} \times N_{step} \tag{3.32}$$

$$HTL_O(t) = \{w(t) : u^{\ell} \le t < (u^{\ell} + N_{HTL})\} \ , \ N_{HTL} = HPE_O \tag{3.33}$$

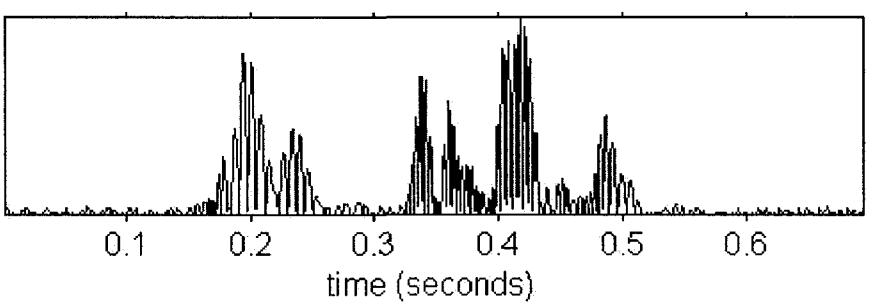

Figure 3.6: Example of heartbeat template $HTL_O(t)$. This is the same heartbeat template seen in Figure 3.5 (b).

3.4 Heartbeat Boundary Prediction Stage

The Heartbeat Boundary Prediction (HBP) stage generates the second set of similarity correlations, where similarity correlations are performed iteratively towards the right and left of the heartbeat template $HTL_O(t)$. The time offsets of the peaks of these similarity correlations correspond to the locations of heartbeat boundary predictions in a PCG.

By convention, the start of the heartbeat template (u^ℓ) is selected as the first heartbeat boundary prediction p_0. For each iteration k, the template window $w_1(t)$ is defined as $HTL_O(t)$, while the search window $w_2^k(t)$ is positioned dependent on the previous heartbeat boundary prediction. Towards the right of $w_1(t)$, k is noted by a positive integer, and so the previous boundary prediction is p_{k-1}. Towards the right of $w_1(t)$, $w_2^k(t)$ is positioned between 60% to 180% of HPE_O after p_{k-1}, as expressed in Eq. (3.36). Towards the left of $w_1(t)$, k is noted by a negative integer, and so the previous boundary prediction is p_{k+1}. Towards the left of $w_1(t)$, $w_2^k(t)$ is positioned between 0% to 150% of HPE_O before p_{k+1}, as expressed in Eq. (3.37). $G^k(\tau)$ is the similarity correlation between $w_1(t)$ and $w_2^k(t)$. Examples of similarity correlations $G^k(\tau)$ towards the right and left of $w_1(t)$ can be seen in Figure 3.7.

$$p_0 = u^\ell \tag{3.34}$$

$$w_1(t) = HTL_O(t) \tag{3.35}$$

$$w_2^k(t) = \{w(t) : (p_{k-1} + 0.6HPE_O) \le t < (p_{k-1} + 1.8HPE_O)\},$$
$$N_2 = 1.2HPE_O, k = 1,2,3,... \tag{3.36}$$

$$w_2^k(t) = \{w(t) : (p_{k+1} - 1.5HPE_O) \le t < p_{k+1}\},$$
$$N_2 = 1.5HPE_O, k = -1,-2,-3,... \tag{3.37}$$

$$\tau_{\max}^k = \arg\max_{\tau}\{G^k(\tau)\} \tag{3.38}$$

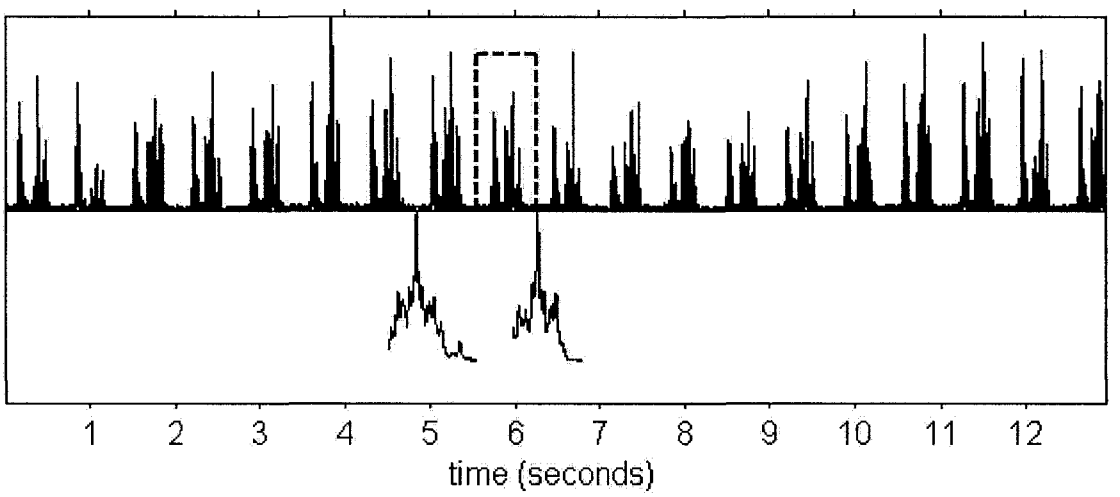

Figure 3.7: Examples of similarity correlations $G^k(\tau)$ toward the right and left of template window $w_1(t)$. The upper half of the plot shows the same PCG as previously seen in Figure 3.5 (b). $w_1(t)$ is enclosed by dashed box. The lower half of the plot shows $G^{-1}(\tau)$ and $G^1(\tau)$.

The time offset $\tau_{\max}^k$ of the highest magnitude peak in $G^k(\tau)$ corresponds to the time difference from a neighbouring heartbeat boundary. Along with knowledge of the actual position of $w_1(t)$ within a PCG, $\tau_{\max}^k$ is used to determine the time at which heartbeat boundary prediction p_k occurs in the PCG, as expressed in Eq. (3.39) and

(3.40) for iterations towards the right and left of $w_1(t)$, respectively. In this manner, the PCG is segmented, as seen in Figure 3.8.

$$p_k = p_{k-1} + 0.6HPE_O + \tau^k_{\max} \ , \ k = 1,2,3,... \tag{3.39}$$

$$p_k = p_{k+1} - 1.5HPE_O + \tau^k_{\max} \ , \ k = -1,-2,-3,... \tag{3.40}$$

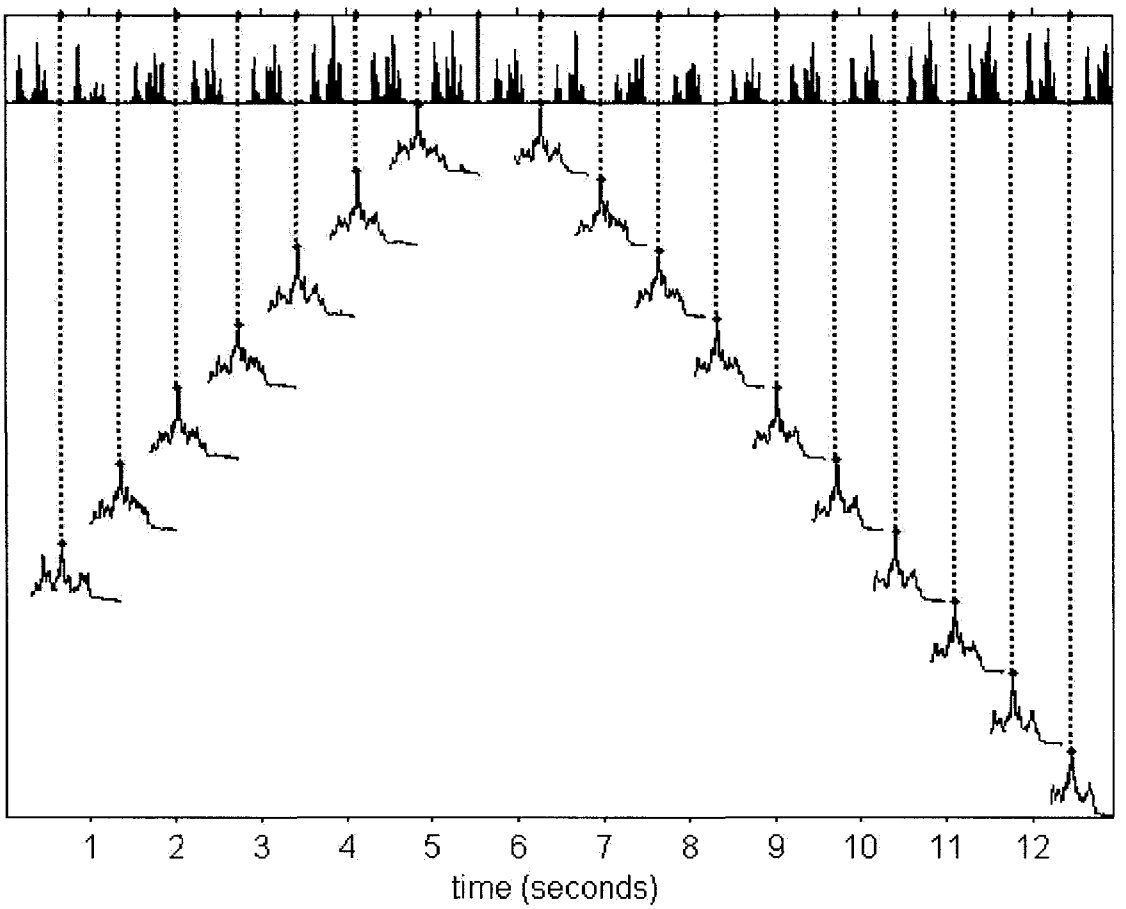

Figure 3.8: PCG segmented using highest magnitude peaks of similarity correlations. The upper portion of the plot shows the same PCG as previously seen in Figure 3.7. The similarity correlations are shifted downwards for clarity.

Iterations continue towards the right and left of $w_1(t)$ until p_k is located within HPE_O of the end and beginning of the PCG. These criteria for discontinuing, or stopping, iterations at the end and beginning of the PCG are expressed in Eq. (3.41) and (3.42), respectively. Any $G^k(\tau)$ which extend beyond the end or beginning of the PCG are truncated. The final set ρ of heartbeat boundary predictions is expressed in Eq. (3.43).

$$p_k > (N - HPE_O) \tag{3.41}$$

$$p_k < HPE_O \tag{3.42}$$

$$\rho = \{p_k : k = ...,-2,-1,0,1,2,...\} \tag{3.43}$$

3.5 Comparison of SWA to Energy-Based Methods

Previously in [9], the SWA was compared to an energy-based segmentation method called the Peak Energy Detector (PED). The PED worked well for PCGs containing clearly visible S1 and S2 [9]. Typical to energy-based segmentation methods, the PED relied on heuristics and energy thresholds. Due to this reliance, the PED did not work well when the energy of S1 was significantly less than the energy of S2, nor when the energy of S1 was comparable to (and hence mistaken for) the energy of a murmur [9].

The SWA worked better than the PED for PCGs containing: impulse noise (such as motion artifacts or background noise), intermittent noise (such as respiration), low intensity S1, low signal-to-noise ratio, loud and inconsistent holodiastolic murmur [9]. A significant difference in segmentation performance was observed between the SWA and

the PED. Whereas the SWA correctly segmented 83% of cardiac cycles in a dataset, the PED correctly segmented only 69% of cardiac cycles in the same dataset [9]. Since the SWA achieved approximately 14% improvement in segmentation over the PED, it was expected that the SWA would also out-perform other energy-based segmentation methods [9].

4 DATA AND METHODS FOR EVALUATION

In this chapter, the dataset and methods used to assess the Sliding Window Autocorrelation (SWA) segmentation algorithm are described. The dataset (section 4.1) contains a relatively large number of phonocardiograms representing a wide variety of heart pathologies and noise conditions. For evaluation purposes, the actual heartbeat boundaries of each phonocardiogram (PCG) were manually located, and referred to as *gold standard* heartbeat boundaries (section 4.2). The heartbeat period estimate generated by the first stage of the SWA is evaluated based on the range of actual heartbeat periods in the PCG (section 4.3). The *Automatic Scoring Method* (section 4.4) evaluates the heartbeat boundary predictions generated by the third stage of the SWA, using the gold standard heartbeat boundaries. The Automatic Scoring Method evaluates the accuracy of synchronous segmentation in an objective and quantitative manner, and can be used to assess other segmentation algorithms. Segmentation results for the original SWA (section 4.6) indicate that the performance of the SWA can be improved (section 4.7).

4.1 Dataset

The dataset used to assess the Sliding Window Autocorrelation (SWA) segmentation algorithm contains phonocardiograms (PCGs) which represent a wide variety of heart pathologies and noise conditions. The dataset includes PCGs which exhibit heartbeat-to-heartbeat variability in: heart sound intensity and duration, heart rate, murmur intensity and duration, non-cardiac noise intensity and duration. Such variability

of data is required to test if the SWA is sufficiently robust to be used in realistic clinical situations, where the acquisition environment may be prone to noise.

The dataset contains PCGs from four sources. Three of the data sources were from collections of PCGs intended for auscultation training [3][13][56]. The PCGs from these three sources were originally digitized at various sampling rates (8000-22050 Hz) and linear quantization (12-bit or 16-bit). The fourth source was the Children's Hospital of Eastern Ontario (CHEO) located in Ottawa, Ontario, Canada. The PCGs from CHEO were originally acquired from pediatric patients, using a Littman electronic stethoscope at sampling rate of 4000 Hz and 12-bit linear quantization. (Permission to use the PCGs from CHEO was obtained by a previous graduate student who compiled the original dataset.) The PCGs from all four sources were filtered, sub-sampled at 4000 Hz, and re-quantized to 16 bits per sample (mono).

Each PCG was characterized by the non-expert author (i.e. with no significant medical background) in terms of: source, heart pathology, duration, number of heartbeats, heartbeat period (average, variability), heart sounds (intensity variability, relative intensity), murmur (timing, overlap, configuration, relative duration, relative intensity), noise (timing, overlap, relative intensity, occurrence), and segmentability. In this work, *variability of heartbeat periods* is equivalent to the standard deviation of the heartbeat periods. *Intensity variability of heart sounds* indicates whether there is significant heartbeat-to-heartbeat variability of S1 and/or S2 intensity. *Relative intensity of heart sounds* indicates the qualitative relationship between the intensity of S1 and S2. *Relative duration of murmur* indicates whether murmur has shorter or longer duration than normal

heart sounds. For both murmur and noise, *overlap* indicates with which normal heart sounds the murmur or noise overlaps in the time domain. For both murmur and noise, *relative intensity* indicates whether murmur or noise has greater or lower intensity than normal heart sounds. *Occurrence* of noise indicates whether the noise occurs sporadically at only a few instances in the PCG or whether the noise occurs in a regular manner throughout the PCG. *Segmentability* indicates the degree to which manual and automatic segmentation are expected to succeed.

Furthermore, Figure 4.1 shows the number of PCGs with fast heart rate and/or high variability of heart rate in the dataset. In this work, *fast heart rate* corresponds to any heartbeat period shorter than 500 ms, and *high variability of heart rate* corresponds to greater than 100 ms standard deviation of heartbeat periods.

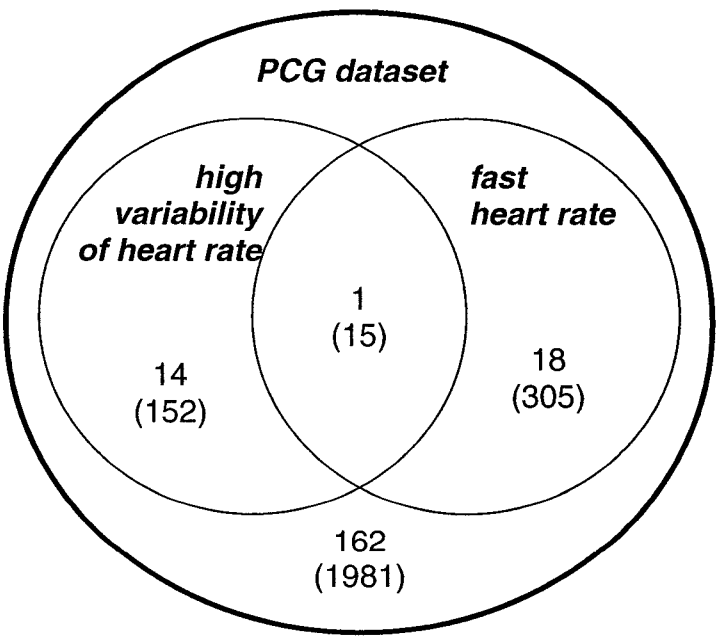

Figure 4.1: Number of PCGs (and cardiac cycles) with fast heart rate and/or high variability of heart rate in the dataset.

Each PCG was assigned to a particular class (1-4), based on segmentability. *Class 1* contained PCGs for which both manual and automatic segmentation are expected to succeed for all heartbeats. *Class 2* contained PCGs for which manual segmentation is expected to succeed for all heartbeats, whereas automatic segmentation is expected to succeed for most heartbeats. *Class 3* contained PCGs for which manual segmentation is expected to succeed for all heartbeats, whereas automatic segmentation is expected to succeed for fewer than half of the heartbeats. *Class 4* contained PCGs for which both manual and automatic segmentation are expected to succeed for fewer than half of the heartbeats. Examples of PCGs from each of the four classes can be seen in Figure 4.2. Since accurate manual segmentation of highly variable PCGs in class 4 could not be guaranteed, PCGs in class 4 were excluded from the dataset.

The entire dataset contained 195 PCGs (2453 cardiac cycles). Table 4.1 lists the number of PCGs and cardiac cycles per source. Table 4.2 lists the ranges of: PCG duration, number of cardiac cycles per PCG, average heartbeat period per PCG, and standard deviation of heartbeat period per PCG. Table 4.3 lists the number of PCGs and cardiac cycles per class.

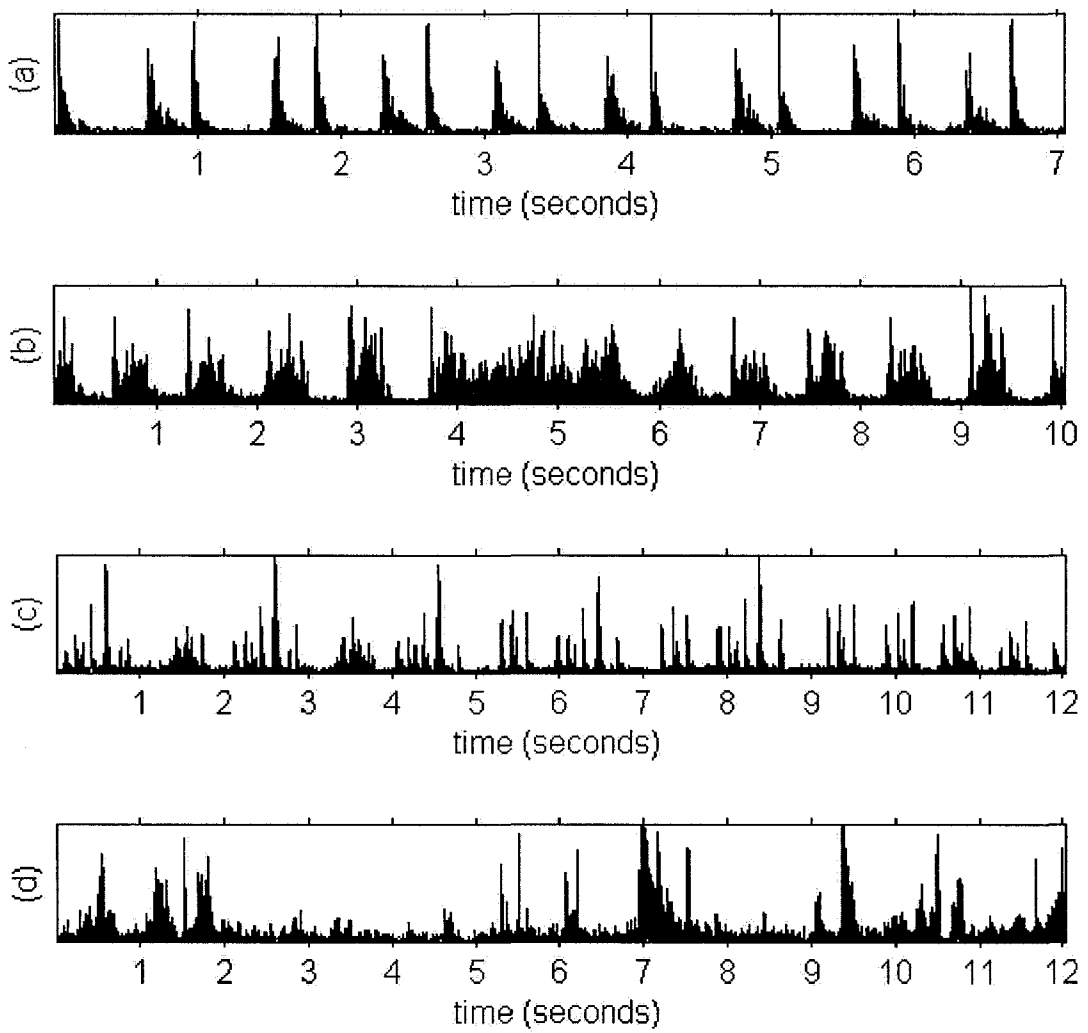

Figure 4.2: Example signal magnitude of PCGs from: (a) class 1, (b) class 2, (c) class 3, (d) class 4.

Table 4.1: Number of PCGs and cardiac cycles per source.

Source	[56]	[13]	[3]	CHEO	Total
# PCGs	74	54	61	6	195
# Cardiac Cycles	1229	316	825	83	2453

Table 4.2: Ranges of various PCG metrics.

Per PCG	Range
Duration	2.070 seconds – 22.595 seconds
# Cardiac Cycles	2 – 34
Average Heartbeat Period	0.297 seconds – 1.801 seconds
Standard Deviation of Heartbeat Period	0.00075 seconds – 0.366 seconds

Table 4.3: Number of PCGs and cardiac cycles in dataset;

(a) including class 4;

Class	1	2	3	4	Total
# PCGs	100	68	27	4	199
# Cardiac Cycles	935	1092	426	76	2529

(b) excluding class 4.

Class	1	2	3	Total
# PCGs	100	68	27	195
# Cardiac Cycles	935	1092	426	2453

4.2 Gold Standard Heartbeat Boundaries

The gold standard heartbeat boundaries were used as references by the Automatic Scoring Method, to evaluate the heartbeat boundary predictions generated by the Sliding Window Autocorrelation (SWA) segmentation algorithm. The gold standard heartbeat boundaries were also used to evaluate the heartbeat period estimate generated by the Heart Rate Estimation stage of the SWA. The heartbeat periods observed in a PCG (as described in section 4.1) correspond to the amount of time between neighbouring gold

standard heartbeat boundaries in the PCG. Gold standard heartbeat boundaries (simply referred to as GSBs) represent the beginning of cyclostationary cardiac cycles in PCG.

GSBs were manually located by the non-expert author (i.e. with no significant medical background), by visual and aural (audio) inspection of the original waveform of digitized PCGs. A visual software utility was developed which allowed cardiac cycles in a PCG to be bounded, superimposed, and shifted to optimize the alignment of sound features in the cardiac cycles. Using this utility, GSBs were positioned a short time before S1 in a synchronous manner. In complex PCGs, GSBs were allowed to be located a short time after S1, if the starting edge of S1 was indistinguishable due to murmur. This is acceptable in the context of this research, since the criterion for synchronous segmentation (namely that the timing between the GSB and the beginning of S1 is consistent for all heartbeats in a PCG) is retained. The absolute position of a GSB is not a primary concern.

The final set γ of GSBs in a PCG is expressed as Eq. (4.1), where g_z is the sample position of the z^{th} GSB, and Z is the total number of GSBs in the PCG.

$$\gamma = \{g_z : z = 1,..., Z\} \tag{4.1}$$

4.3 Evaluation of Heart Rate Estimation Stage

The accuracy of the Heart Rate Estimation (HRE) stage was evaluated by comparing the heartbeat period estimate HPE_O with an upper limit and a lower limit. For a given PCG, HPE_O was considered correct if it occurred between, or within 10ms of, the upper and lower limits. The upper and lower limits can be chosen as one of the

following options: (i) the maximum and minimum heartbeat periods observed in the PCG, respectively; (ii) the mean heartbeat period observed in the PCG, ± one standard deviation, respectively. The heartbeat periods observed in the PCG are computed as the difference between consecutive GSBs (described in section 4.2). For this evaluation, option (ii) is generally a stricter requirement than option (i). The overall accuracy of the HRE stage can be expressed as the percentage of PCGs with correct HPE_O out of all PCGs.

The appropriateness of the HPE_O in specifying a suitable search window range for the Heartbeat Boundary Prediction (HBP) stage of the SWA was also evaluated. For a given PCG, the HPE_O was considered appropriate if the search window range (i.e. $0.6\,HPE_O$ to $1.8\,HPE_O$) enclosed the lower and upper limits previously described. For this evaluation, option (i) is generally a stricter requirement than option (ii). The overall appropriateness of the HPE_O in specifying a suitable search window range for the HBP stage can be expressed as a percentage of PCGs with appropriate HPE_O out of all PCGs.

4.4 Automatic Scoring Method – Evaluation of Synchronous Segmentation

For the purpose of this work, it was not essential to represent the beginning of a heartbeat as the start of systole, since the primary concern was the alignment of cardiac sounds (i.e. S1 and S2) within multiple PCG segments.

Consider a set ρ of heartbeat boundary predictions in a given PCG as defined by Eq. (3.43), and a set γ of gold standard heartbeat boundaries in the same PCG as defined

by Eq. (4.1). In this section, a heartbeat boundary prediction is simply referred to as a *prediction*, where the k^{th} prediction is located at sample p_k in the PCG. Also, a gold standard heartbeat boundary is simply referred to as a *gold standard*, where the z^{th} gold standard is located at sample g_z in the PCG.

The Automatic Scoring Method evaluates each prediction in a given PCG based on a *prediction-gold standard difference* (simply referred to as PGD), which is denoted as $d(k,z)$ in Eq. (4.2), and corresponds to the time difference between prediction k and gold standard z.

$$d(k,z) = p_k - g_z \tag{4.2}$$

For a heartbeat h under consideration, z_h and k_h denote the gold standard and prediction, respectively, associated with the heartbeat. For the given heartbeat h, the single value $d(k_h,z_h)$ alone does not determine whether the heartbeat was segmented correctly; rather, it must be considered in relation to the PGD of all other heartbeats in the same PCG. Hence, in a given PCG, all correctly synchronously segmented heartbeats must have consistent PGD, in order to enable the proper alignment of multiple heartbeats that is required prior to further analyses (i.e. murmur detection).

In this work, the SWA aimed to perform synchronous segmentation in the sense that each correctly segmented heartbeat in a given PCG should have the same PGD as every other correctly segmented heartbeat in the same PCG. The PGD common to the correctly segmented heartbeats is designated Q. In the given PCG, the most commonly observed PGD, or *mode* PGD, is chosen as Q. Realistically, a heartbeat in the given PCG

is considered correctly segmented if it has PGD within a reasonable *deviation* δ from Q. The set η of correctly segmented heartbeats in a given PCG is expressed in Eq. (4.3).

$$\eta = \{h : (Q - \delta) \leq d(k_h, z_h) \leq (Q + \delta)\} \tag{4.3}$$

A value δ corresponding to between 35 ms and 50 ms was considered reasonable, since synchronous segmentation can be achieved by heartbeat boundaries located during isovolumetric contraction, which has typical duration between 70 ms and 100 ms [8]. Another reasonable δ may correspond to 10 ms, since humans can distinguish between sounds that are separated by an interval of 20 ms [67]. In this work, segmentation results were generated for a range of δ corresponding to between 10 ms and 50 ms.

By convention, in order to limit the number of gold standards which a prediction could possibly predict, a prediction k_h and associated gold standard z_h must be within *vicinity* v of each other, as expressed in Eq. (4.4).

$$\left| d(k_h, z_h) \right| \leq v \tag{4.4}$$

Since correct predictions are expected to be separated by the heartbeat period, the location of a prediction k_h is expected to be within one heartbeat period of the associated gold standard z_h. Hence, for all predictions in the given PCG, the longest predicted heartbeat period (calculated as the longest duration between two consecutive predictions) was considered an acceptable v, as expressed in Eq. (4.5).

$$v = \max\{|\Delta p_k|\} \tag{4.5}$$

4.4.1 Scoring Procedure

Each prediction (k) and gold standard (z) in a given PCG is scored taking into consideration: prediction-gold standard difference (PGD), vicinity (v), and deviation (δ) from the mode PGD (Q). The total number of predictions in a given PCG is denoted by K, and the total number of gold standards in the given PCG is denoted by Z. An example of a PCG depicting gold standards, predictions, PGDs, vicinity, deviation, and mode PGD can be seen in Figures 4.3 through to 4.6.

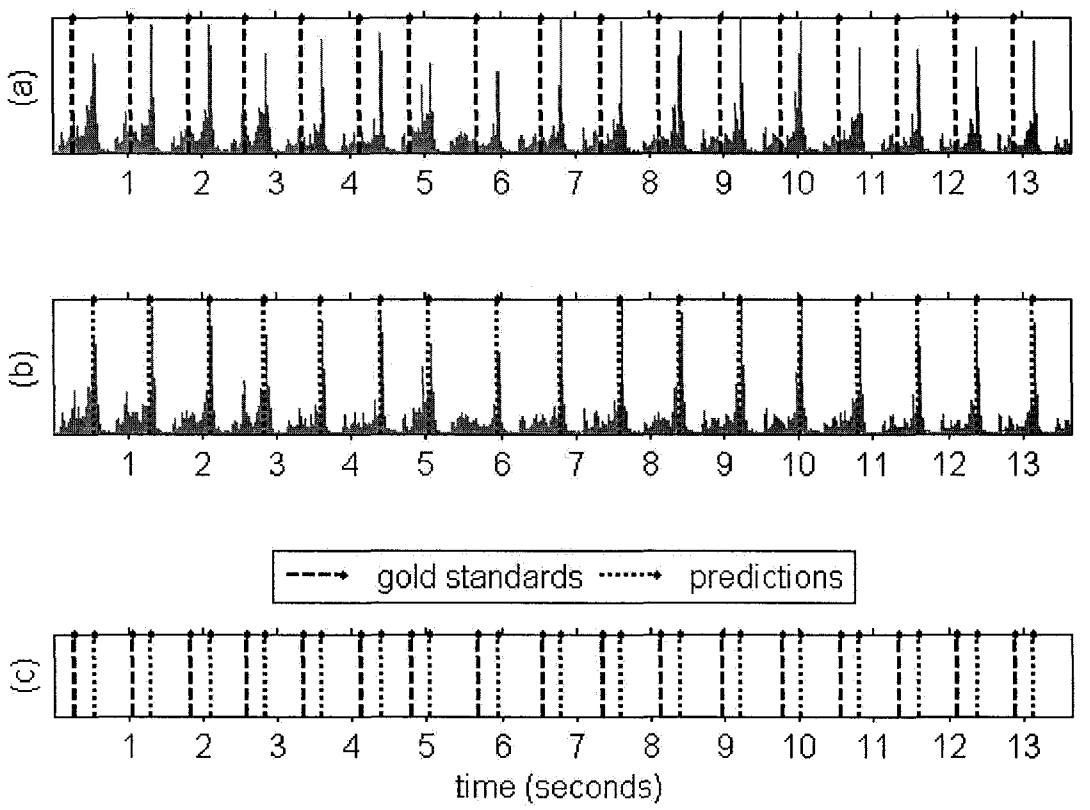

Figure 4.3: Example PCG depicting gold standards and predictions: (a) gold standards only; (b) predictions only; (c) both gold standards and predictions. Subplots (a) and (b) show the same PCG as previously seen in Figure 3.8.

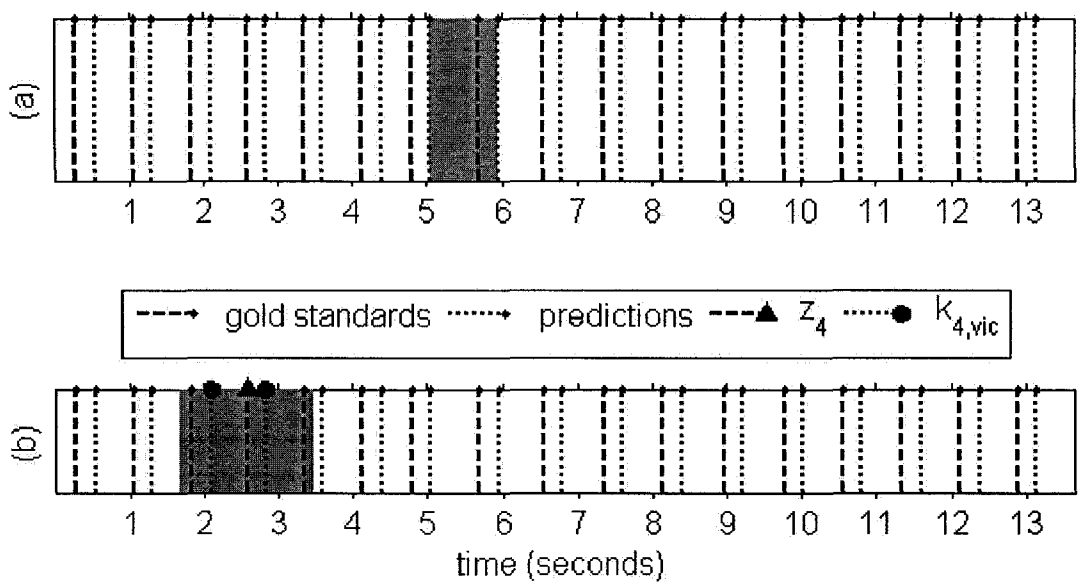

Figure 4.4: Example of vicinity v (shown as shaded area): (a) equivalent to longest duration between two consecutive predictions; (b) around the fourth gold standard z_4. Two predictions are within the vicinity of z_4, so there are two PGDs associated with z_4. This figure continues from the example previously seen in Figure 4.3.

Any gold standard not within the vicinity of any prediction was considered *unused*. The set γ_{unused} of unused gold standards is defined by Eq. (4.6).

$$\gamma_{unused} = \{g_z : z \ni |d(k,z)| > v, k = 1,...,\mathrm{K}\} \tag{4.6}$$

Any prediction not within the vicinity of any gold standard was also considered *unused*. The set ρ_{unused} of unused predictions is defined by Eq. (4.7).

$$\rho_{unused} = \{p_k : k \ni |d(k,z)| > v, z = 1,...,\mathrm{Z}\} \tag{4.7}$$

For each gold standard z_h in the given PCG, the set $\rho_{h,vic}$ of predictions $k_{h,vic}$ within the vicinity of z_h was determined, as expressed in Eq. (4.8) and (4.9).

$$k_{h,vic} = \{k : |d(k,z_h)| \leq v\} \tag{4.8}$$

$$\rho_{h,vic} = \{p_k : k = k_{h,vic}\} \tag{4.9}$$

In a perfect segmentation scenario, only one prediction $k_{h,vic}$ occurs within the vicinity before a gold standard z_h. A PGD $d(k, z_h)$ was calculated for each $k = k_{h,vic}$.

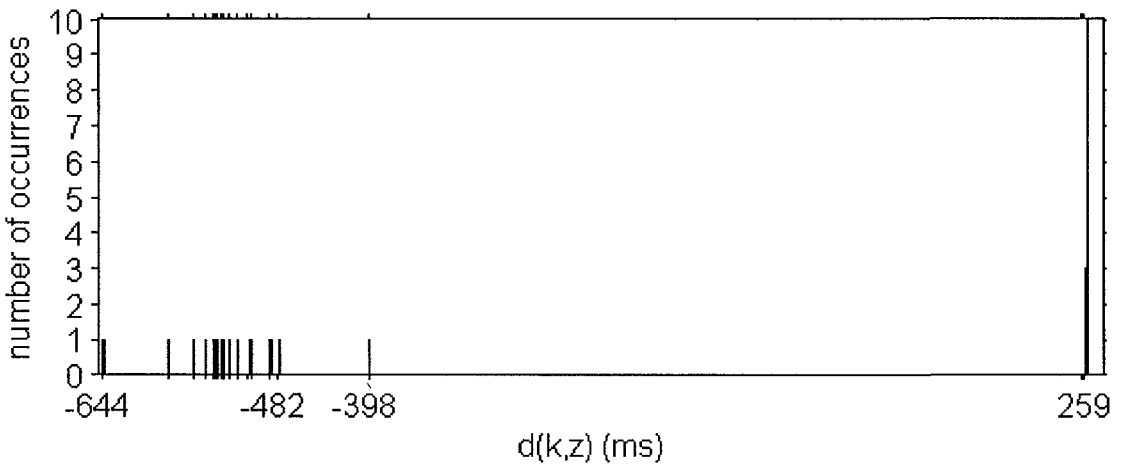

Figure 4.5: Example of PGD distribution for gold standards and predictions within vicinity v of each other. Only a few PGD values are labeled. This PGD distribution continues from the example previously seen in Figure 4.4.

Out of all the gold standards in the given PCG, the mode PGD was determined, and expressed as Q in Eq. (4.10).

$$Q = \text{mode}\{d(k, z), \forall k = k_{h,vic}, \forall z = z_h, \forall h\} \tag{4.10}$$

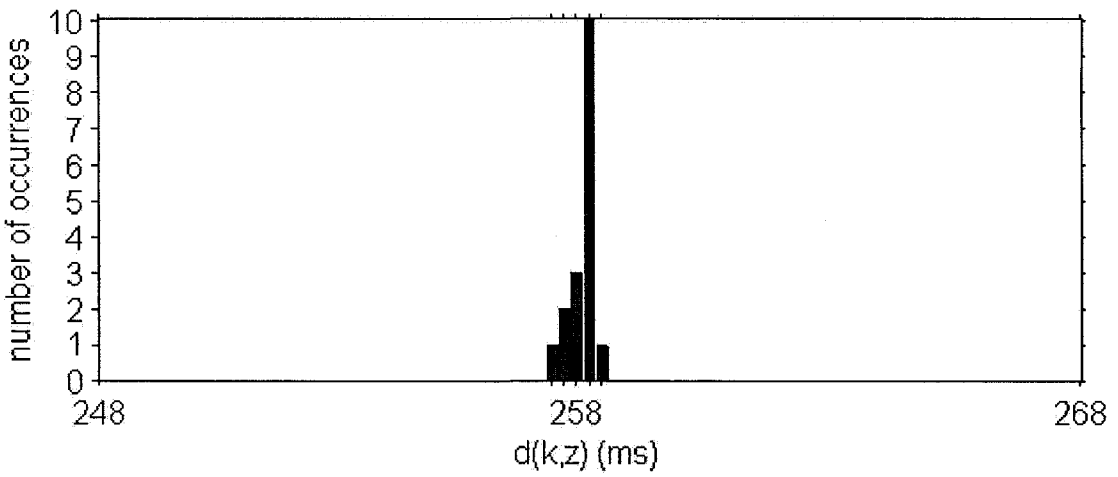

Figure 4.6: Example of PGD distribution for gold standards and predictions within vicinity v and deviation δ = 10 ms of each other. Mode PGD is Q = 258 ms. This PGD distribution continues from the example previously seen in Figure 4.5.

A gold standard z_h (and associated prediction $k_h \in k_{h,vic}$) with PGD within reasonable deviation δ of the mode PGD Q was considered *correct*. More formally, the heartbeat h corresponding to the gold standard z_h was correctly segmented; the set η of correctly segmented heartbeats is defined previously in Eq. (4.3). The set $\gamma_{correct}$ of correct gold standards and the set $\rho_{correct}$ of correct predictions are defined in Eq. (4.11) and (4.12), respectively.

$$\gamma_{correct} = \{g_z : \forall z = z_h, \ni (Q-\delta) \le d(k_h, z_h) \le (Q+\delta)\} \tag{4.11}$$

$$\rho_{correct} = \{p_k : \forall k = k_h, \ni (Q-\delta) \le d(k_h, z_h) \le (Q+\delta)\} \tag{4.12}$$

A gold standard z_h (and associated prediction $k_h \in k_{h,vic}$) with PGD beyond reasonable deviation δ of the mode PGD Q was considered *incorrect*. More formally, the heartbeat h corresponding to the gold standard z_h was incorrectly segmented; the set

$\overline{\eta}$ of incorrectly segmented heartbeats is defined in Eq. (4.15). The set $\gamma_{incorrect}$ of incorrect gold standards and the set $\rho_{incorrect}$ of incorrect predictions are defined in Eq. (4.13) and (4.14), respectively.

$$\gamma_{incorrect} = \{g_z : \forall z = z_h, \exists\, d(k_h, z_h) < (Q-\delta), \exists\, d(k_h, z_h) > (Q+\delta)\} \quad (4.13)$$

$$\rho_{incorrect} = \{p_k : \forall k = k_h, \exists\, d(k_h, z_h) < (Q-\delta), \exists\, d(k_h, z_h) > (Q+\delta)\} \quad (4.14)$$

$$\overline{\eta} = \{h : d(k_h, z_h) < (Q-\delta), d(k_h, z_h) > (Q+\delta)\} \quad (4.15)$$

4.4.2 Scoring Metrics

For a given PCG, the following metrics are considered:

(i) number of correct gold standards ($Z_{correct}$);

(ii) number of incorrect gold standards ($Z_{incorrect}$);

(iii) number of unused gold standards (Z_{unused});

(iv) number of *unpredicted* gold standards ($Z_{incorrect} + Z_{unused}$);

(v) total number of gold standards ($Z_{correct} + Z_{incorrect} + Z_{unused}$);

(vi) number of correct predictions ($K_{correct}$);

(vii) number of incorrect predictions ($K_{incorrect}$);

(viii) number of unused predictions (K_{unused});

(ix) number of *faulty* predictions ($K_{incorrect} + K_{unused}$);

(x) total number of predictions ($K_{correct} + K_{incorrect} + K_{unused}$).

The metrics for gold standards are collected using several rules. If a gold standard is correctly predicted by multiple predictions, it is counted as one correct gold standard. If a gold standard is incorrectly predicted by multiple predictions, it is counted as one incorrect gold standard. If a gold standard is correctly predicted by a prediction, but is also incorrectly predicted by another prediction, it is counted as one correct gold standard.

Likewise, the metrics for predictions are collected using similar rules. If a prediction is correct for multiple gold standards, it is counted as one correct prediction. If a prediction is incorrect for multiple gold standards, it is counted as one incorrect prediction. If a prediction is correct for a gold standard, but also incorrect for another gold standard, it is counted as one correct prediction.

For each class of PCGs, the metrics are aggregated from individual PCGs, and converted to percentages. For the entire dataset, the metrics are aggregated from individual classes, and converted to percentages.

4.4.3 Scoring Statistics

The synchronous segmentation accuracy is expressed as the percentage of correct gold standards out of all gold standards, as in Eq. (4.16).

$$accuracy = 100 \times \frac{Z_{correct}}{Z_{correct} + Z_{incorrect} + Z_{unused}} \tag{4.16}$$

The synchronous segmentation accuracy measured by the Automatic Scoring Method was used to assess the work described in subsequent chapters.

4.5 Naming Convention for SWA Variations

A naming convention is defined in order to differentiate between the original SWA and variations of the SWA discussed in later chapters. The names of the original SWA and variations of the SWA adhere to the following notation: $SWA(HPE_V, HTL_V)$, where the subscript V indicates the variation. Using this notation, the original SWA is referred to as $SWA(HPE_O, HTL_O)$ throughout this dissertation.

4.6 Results of Original SWA Segmentation Algorithm

The accuracy of the original Heart Rate Estimation (HRE) stage was evaluated, as described in ch. 4.3. The appropriateness of the original heartbeat period estimate HPE_O in specifying a suitable search window range for the Heartbeat Boundary Prediction (HBP) stage was evaluated, as described in ch. 4.3. Results can be seen in ch. 4.6.1.

The original Sliding Window Autocorrelation (SWA) segmentation algorithm, or $SWA(HPE_O, HTL_O)$, was evaluated for synchronous segmentation accuracy, as described in ch. 4.4. The scoring metrics and scoring statistics were determined for δ = 10 ms and δ = 50 ms, and can be seen in ch. 4.6.2.

4.6.1 Heart Rate Estimation Stage

Results of evaluating the accuracy of the original HRE stage are shown in Table 4.4. Results of evaluating the appropriateness of HPE_O in specifying a suitable search window range for the HBP stage are shown in Table 4.5.

Table 4.4: Number of PCGs with correct HPE_O. Limits based on: (i) maximum and minimum heartbeat periods; (ii) mean and standard deviation of heartbeat periods.

Dataset	# PCGs	# PCGs with correct HPE_O	
		(i)	(ii)
Class 1	100	97 (97.0%)	92 (92.0%)
Class 2	68	62 (91.1%)	60 (88.2%)
Class 3	27	21 (77.7%)	17 (62.9%)
Overall	195	180 (92.3%)	169 (86.6%)

Table 4.5: Number of PCGs with appropriate HPE_O for HBP stage. Limits based on: (i) maximum and minimum heartbeat periods; (ii) mean and standard deviation of heartbeat periods.

Dataset	# PCGs	# PCGs with appropriate HPE_O	
		(i)	(ii)
Class 1	100	97 (97.0%)	97 (97.0%)
Class 2	68	61 (89.7%)	61 (89.7%)
Class 3	27	22 (81.8%)	22 (81.8%)
Overall	195	180 (92.3%)	180 (92.3%)

4.6.2 Synchronous Segmentation

Results of evaluating the synchronous segmentation accuracy of $SWA(HPE_O, HTL_O)$, for δ = 10 ms and δ = 50 ms, are shown in Table. 4.6.

Table 4.6: Scoring metrics and statistics for original SWA.

Dataset	# PCGs	# Cardiac Cycles	# Cardiac Cycles Correctly Segmented (Segmentation Accuracy)	
			$SWA(HPE_O, HTL_O)$	
			δ = 10 ms	δ = 50 ms
Class 1	100	935	819 (87.5%)	889 (95.0%)
Class 2	68	1092	893 (81.7%)	986 (90.2%)
Class 3	27	426	293 (68.7%)	337 (79.1%)
Overall	195	2453	2005 (81.7%)	2212 (90.1%)

4.7 Discussion of Original SWA Segmentation Algorithm

As expected, the results seen in Table 4.4 confirm that option (ii) is more strict than option (i) when evaluating accuracy of the HRE stage. The results seen in Table 4.5 show that neither option (i) nor option (ii) was more strict in evaluating the appropriateness of HPE_O.

As seen in Table 4.6, the overall segmentation accuracy of $SWA(HPE_O, HTL_O)$ was 81.7% and 90.1%, for δ = 10 ms and δ = 50 ms, respectively. In general, less precision (i.e. higher δ) allowed more predictions to be considered correct, thereby increasing the calculated segmentation accuracy.

Although the SWA can successfully segment PCGs in most cases, it does not work for every case. Prior to this research, the proportion of cardiac cycles incorrectly segmented due to various causes have not been quantified.

Incorrect and/or inappropriate heartbeat period estimate HPE_0 calculated in the HRE stage could cause incorrect segmentation, since the heartbeat template length in the HTL stage and the search window length in the HBP stage both rely on this parameter. Since HPE_0 represents the period of the first cardiac cycle at the beginning of a given PCG, HPE_0 may not be representative of all the cardiac cycles in the given PCG. Furthermore, HPE_0 does not take into account heart rate variations that could occur throughout the given PCG.

The heartbeat template $HTL_0(t)$ may not be representative of all cardiac cycles in a given PCG if, for example, the template contains aberrant noise or there is significant heartbeat-to-heartbeat sound magnitude variation. If the template does not encompass an S1 and S2 in order, then it may not correlate well with all cardiac cycles in the PCG. For example, if the template contains only a partial cardiac cycle or more than one cardiac cycle, then the number of boundaries will be over-predicted or under-predicted, respectively.

In the HBP stage, the fixed range of the search window may not be sufficient if the heart rate is highly variable within a given PCG. Furthermore, the second-highest peak magnitude (rather than the highest peak magnitude) in a similarity correlation has been observed to correspond with the location of a correct prediction. If the second-highest peak magnitude is comparable to the highest peak magnitude, then an alternate search window may need to be considered with respect to the second-highest peak magnitude.

The dataset includes PCGs containing varying degrees and types of noise. The original SWA did not include preprocessing to remove noise prior to segmentation. Cardiac noise, such as murmur, may not negatively affect segmentation if it is present in the majority of heartbeats in a given PCG. Aberrant noise, however, may negatively affect segmentation if the intensity of noise is comparable to or greater than the intensity of regular heart sounds.

The work outlined in this dissertation will attempt to address some of the causes of incorrect segmentation by the SWA, and improve upon the original SWA algorithm.

5 MANUAL AVERAGE HEARTBEAT PERIOD ESTIMATE AND HEARTBEAT TEMPLATE

5.1 Introduction

Prior to this research, the causes of incorrect segmentation by the Sliding Window Autocorrelation (SWA) segmentation algorithm (described in ch. 3) have not been quantified. Two identified causes of incorrect segmentation are: incorrect heartbeat period estimate HPE_O generated by the Heart Rate Estimation stage (described in ch. 3.3), which is used to set parameters of the later stages; and incorrect heartbeat template $HTL_O(t)$ generated by the Heartbeat Template Location stage (described in ch. 3.4), which is used to predict the boundaries between heartbeats. Improving the Heart Rate Estimation stage and/or the Heartbeat Template Location stage will improve the SWA.

Ideally, a heartbeat period estimate should represent the various heart rates observed throughout a given PCG. However, in the original SWA, HPE_O corresponds to the period of only the first heartbeat in a PCG. Furthermore, ideally, a heartbeat template should represent the magnitudes observed in all heartbeats throughout a given PCG. However, in the original SWA, $HTL_O(t)$ corresponds to the magnitude of only a single heartbeat in a PCG. The overall performance of the SWA is expected to improve with the use of a more representative heartbeat period estimate, as well as a more representative heartbeat template.

The aim of this chapter is to quantify the effect of optimized heartbeat period estimate and optimized heartbeat template on the overall performance of the SWA. This

will substantiate the hypothesis that heartbeat period estimate and heartbeat template are areas of improvement for the SWA. Additionally, a reasonable upper bound for the expected performance increase associated with these improvements will be established.

This chapter describes methods for generating an average heartbeat period HPE_M and an average heartbeat template $HTL_M(t)$, both based on the gold standard heartbeat boundaries which were manually located (described in ch. 4.2). Multiple revised SWA, which use HPE_M (instead of HPE_O) and/or $HTL_M(t)$ (instead of $HTL_O(t)$), are described and evaluated.

5.2 Methods

Methods for generating an average heartbeat period HPE_M and an average heartbeat template $HTL_M(t)$ are described in ch. 5.2.1. Methods used to evaluate these refinements are described in ch. 5.2.2.

5.2.1 Refinements to SWA

For a given PCG containing Z gold standard heartbeat boundaries (simply referred to as GSBs), HPE_M corresponds to the average time duration between GSBs in set γ described in Eq. (4.1), and is calculated in Eq. (5.1).

$$HPE_M = \frac{1}{Z-1}\sum_{z=1}^{Z-1}\left(g_{z+1} - g_z\right) \tag{5.1}$$

For a given PCG, $HTL_M(t)$ corresponds to the average magnitude of heartbeats delineated by GSBs in set γ. The longest observed length between neighbouring GSBs is

expressed as N_{HTL} in Eq. (5.2). Prior to averaging, heartbeats $w_z(t)$ with length shorter than N_{HTL} are zero-padded to length N_{HTL}, as expressed in Eq. (5.3).

$$N_{HTL} = \max\{(g_{z+1} - g_z), z = 1...(Z-1)\} \tag{5.2}$$

$$w_z(t) = \begin{Bmatrix} w(g_z + t - 1), 1 \le t \le (g_{z+1} - g_z) \\ 0, (g_{z+1} - g_z) < t \le N_{HTL} \end{Bmatrix} \tag{5.3}$$

The last heartbeat $w_{z=Z}(t)$ is excluded from $HTL_M(t)$, since it may represent a partial heartbeat with significantly more zero-padding than the other heartbeats in a given PCG. Also, if a partial heartbeat is located prior to the first GSB $g_{z=1}$ in a given PCG, the partial heartbeat is also excluded from $HTL_M(t)$. $HTL_M(t)$ is expressed in Eq. (5.4), and has length equal to N_{HTL}.

$$HTL_M(t) = \frac{1}{Z-1}\sum_{z=1}^{Z-1} w_z(t) \text{ , for } 1 \le t \le N_{HTL} \tag{5.4}$$

When $HTL_M(t)$ is used in the existing framework of the SWA, a starting position is required for $HTL_M(t)$. Specifically, in the Heartbeat Boundary Prediction (HBP) stage (described in ch. 3.4), the start of the heartbeat template is selected as the first heartbeat boundary prediction p_0. The first GSB $g_{z=1}$ in the given PCG is considered the start of $HTL_M(t)$; hence, $g_{z=1}$ is selected as p_0. As such, the HBP stage needs to search iteratively only to the right of the heartbeat template.

5.2.2 Evaluation of Revised SWA

The accuracy and appropriateness of HPE_M were evaluated, in the same manner as HPE_O, as described in ch. 4.3.

Two revised SWA were evaluated: $SWA(HPE_M, HTL_O)$, and $SWA(HPE_M, HTL_M)$. To quantify the effect of ideal heartbeat period estimate on overall performance of SWA, $SWA(HPE_M, HTL_O)$ which used HPE_M (instead of HPE_O) was evaluated. To quantify the effect of ideal heartbeat template on overall performance of SWA, as well as determine the highest possible overall performance of SWA, $SWA(HPE_M, HTL_M)$ which used HPE_M (instead of HPE_O) and $HTL_M(t)$ (instead of $HTL_O(t)$) was evaluated, where the length of $HTL_M(t)$ was truncated to HPE_M. Figure 5.1 illustrates the block diagram representative of $SWA(HPE_M, HTL_O)$ and $SWA(HPE_M, HTL_M)$.

Each revised SWA was evaluated using the dataset, Automatic Scoring Method (for δ = 10 ms and δ = 50 ms), and scoring statistics previously described in ch. 4.2, ch. 4.3, and ch. 4.4, respectively.

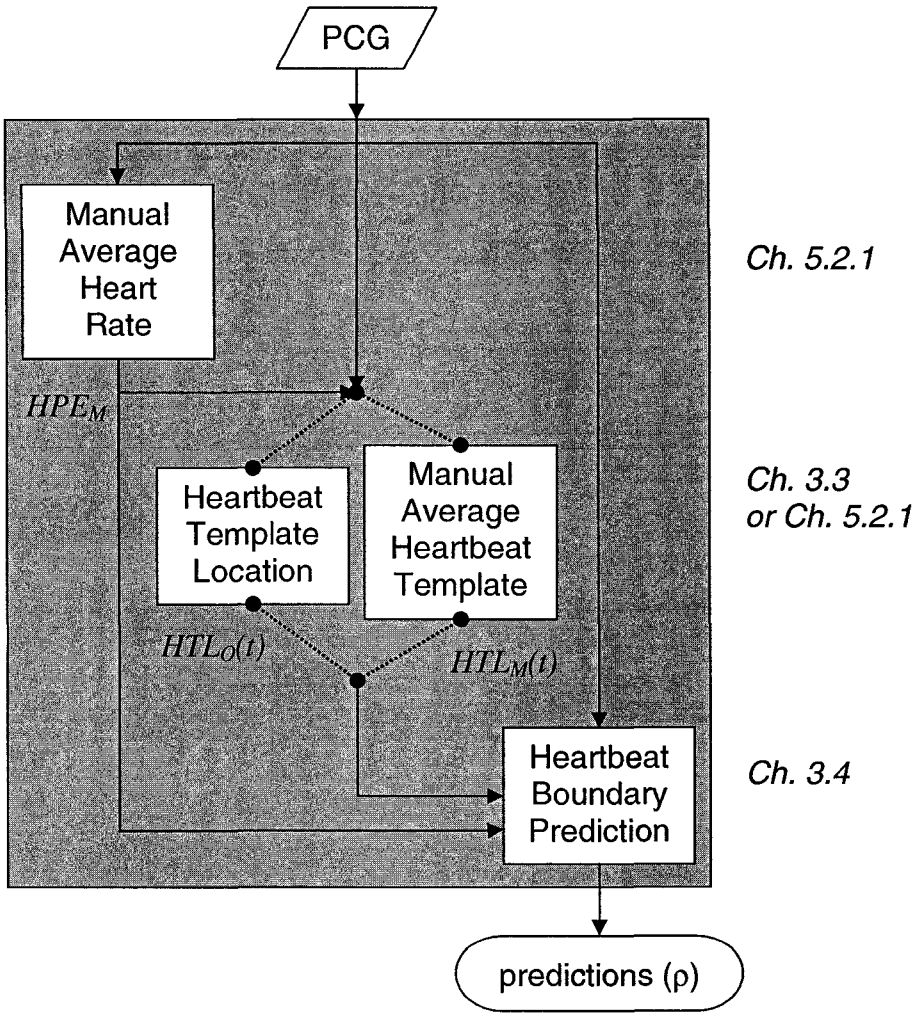

Figure 5.1: Block diagram of revised SWA, using manual average heartbeat period. Representative of $SWA(HPE_M, HTL_O)$ and $SWA(HPE_M, HTL_M)$.

5.3 Results

Results of evaluating the accuracy and appropriateness of HPE_M are shown in Table 5.1 and Table 5.2, respectively. The scoring statistics for $SWA(HPE_M, HTL_O)$ and $SWA(HPE_M, HTL_M)$, described in ch. 5.2.2, are shown in Table 5.3. For reference

purposes, results for the original $SWA(HPE_O, HTL_O)$, which were previously reported in ch. 4.6.2, are shown in Table 5.4.

The change in number of cardiac cycles correctly segmented between $SWA(HPE_O, HTL_O)$ and $SWA(HPE_M, HTL_O)$ are shown in Table 5.5. The change in number of cardiac cycles correctly segmented between $SWA(HPE_M, HTL_O)$ and $SWA(HPE_M, HTL_M)$ are shown in Table 5.6.

Table 5.1: Number of PCGs with correct HPE_M. Limits based on: (i) maximum and minimum heartbeat periods; (ii) mean and standard deviation of heartbeat periods.

Dataset	# PCGs	# PCGs with correct HPE_M	
		(i)	(ii)
Class 1	100	100 (100%)	100 (100%)
Class 2	68	68 (100%)	68 (100%)
Class 3	27	27 (100%)	27 (100%)
Overall	195	195 (100%)	195 (100%)

Table 5.2: Number of PCGs with appropriate HPE_M for HBP stage. Limits based on: (i) maximum and minimum heartbeat periods; (ii) mean and standard deviation of heartbeat periods.

Dataset	# PCGs	# PCGs with appropriate HPE_M	
		(i)	(ii)
Class 1	100	100 (100%)	100 (100%)
Class 2	68	68 (100%)	67 (98.5%)
Class 3	27	27 (100%)	27 (100%)
Overall	195	195 (100%)	194 (99.4%)

Table 5.3: Scoring statistics for $SWA(HPE_M, HTL_O)$ and $SWA(HPE_M, HTL_M)$.

Dataset	# PCGs	# Cardiac Cycles	# Cardiac Cycles Correctly Segmented (Segmentation Accuracy)			
			$SWA(HPE_M, HTL_O)$		$SWA(HPE_M, HTL_M)$	
			δ = 10 ms	δ = 50 ms	δ = 10 ms	δ = 50 ms
Class 1	100	935	827 (88.4%)	909 (96.8%)	919 (98.2%)	929 (99.3%)
Class 2	68	1092	925 (84.7%)	1028 (94.1%)	1034 (94.6%)	1069 (97.8%)
Class 3	27	426	311 (73.0%)	377 (88.4%)	373 (87.5%)	402 (94.3%)
Overall	195	2453	2063 (84.1%)	2311 (94.2%)	2326 (94.8%)	2400 (97.8%)

Table 5.4: Scoring statistics for original $SWA(HPE_O, HTL_O)$.

Dataset	# PCGs	# Cardiac Cycles	# Cardiac Cycles Correctly Segmented (Segmentation Accuracy)	
			$SWA(HPE_O, HTL_O)$	
			δ = 10 ms	δ = 50 ms
Class 1	100	935	819 (87.5%)	889 (95.0%)
Class 2	68	1092	893 (81.7%)	986 (90.2%)
Class 3	27	426	293 (68.7%)	337 (79.1%)
Overall	195	2453	2005 (81.7%)	2212 (90.1%)

Table 5.5: Change in number of cardiac cycles correctly segmented between $SWA(HPE_O, HTL_O)$ and $SWA(HPE_M, HTL_O)$. *Improve* indicates not correctly segmented in $SWA(HPE_O, HTL_O)$, but correctly segmented in $SWA(HPE_M, HTL_O)$. *Decline* indicates correctly segmented in $SWA(HPE_O, HTL_O)$, but not correctly segmented in $SWA(HPE_M, HTL_O)$. *No Change* indicates not correctly segmented in both $SWA(HPE_O, HTL_O)$ and $SWA(HPE_M, HTL_O)$.

Dataset	# Cardiac Cycles	# Cardiac Cycles					
		$\delta = 10$ ms			$\delta = 50$ ms		
		Improve	*Decline*	*No Change*	*Improve*	*Decline*	*No Change*
Class 1	935	46 (4.9%)	38 (4.0%)	70 (7.5%)	24 (2.6%)	7 (0.7%)	22 (2.4%)
Class 2	1092	85 (7.8%)	53 (4.9%)	114 (10.4%)	64 (5.9%)	22 (2.0%)	42 (3.8%)
Class 3	426	60 (14.1%)	42 (9.9%)	73 (17.1%)	67 (15.7%)	27 (6.3%)	22 (5.2%)
Overall	2453	191 (7.7%)	133 (5.4%)	257 (10.4%)	155 (6.3%)	56 (2.2%)	86 (3.5%)

Table 5.6: Change in number of cardiac cycles correctly segmented between $SWA(HPE_M, HTL_O)$ and $SWA(HPE_M, HTL_M)$. *Improve* indicates not correctly segmented in $SWA(HPE_M, HTL_O)$, but correctly segmented in $SWA(HPE_M, HTL_M)$. *Decline* indicates correctly segmented in $SWA(HPE_M, HTL_O)$, but not correctly segmented in $SWA(HPE_M, HTL_M)$. *No Change* indicates not correctly segmented in both $SWA(HPE_M, HTL_O)$ and $SWA(HPE_M, HTL_M)$.

Dataset	# Cardiac Cycles	# Cardiac Cycles					
		$\delta = 10$ ms			$\delta = 50$ ms		
		Improve	*Decline*	*No Change*	*Improve*	*Decline*	*No Change*
Class 1	935	97 (10.4%)	5 (0.5%)	11 (1.2%)	26 (2.8%)	3 (0.3%)	3 (0.3%)
Class 2	1092	131 (12.0%)	22 (2.0%)	36 (3.3%)	54 (4.9%)	13 (1.2%)	10 (0.9%)
Class 3	426	82 (19.2%)	20 (4.7%)	33 (7.7%)	47 (11.0%)	22 (5.2%)	2 (0.5%)
Overall	2453	310 (12.6%)	47 (1.9%)	80 (3.2%)	127 (5.1%)	38 (1.5%)	15 (0.6%)

5.4 Discussion

As expected, the overall accuracy (as defined in ch. 4.3) of the manual average heartbeat period estimate HPE_M was 100%, for both options (i) and (ii). Only a single PCG had an inappropriate HPE_M when using option (ii); this was caused by the upper bound of the search window range, which was only 3 ms too short for the single PCG. This evaluation confirmed HPE_M represents the optimized or best possible heartbeat period estimate.

Without the effect of inaccurate heartbeat period estimate, the overall segmentation accuracy of the SWA increased by 2.4% and 4.1%, for δ = 10 ms and δ = 50 ms, respectively. This was observed by comparing $SWA(HPE_M, HTL_O)$ against $SWA(HPE_O, HTL_O)$. Hence, the use of a more representative heartbeat period estimate is expected to increase the overall segmentation accuracy of the SWA.

Nonetheless, the use of HPE_M did not improve all the segmentation errors associated with $HTL_O(t)$. Segmentation errors still occurred due to heartbeat template magnitude variations and heartbeat template location in the cardiac cycle (previously discussed in ch. 4.7). Such errors persisted regardless of δ, but improved through the use of $HTL_M(t)$.

As expected, the segmentation accuracy of $SWA(HPE_M, HTL_M)$ was quite high, since HPE_M and $HTL_M(t)$ represent the best possible heartbeat period estimate and heartbeat template that can be generated by the SWA, respectively.

Without the effect of inaccurate heartbeat period estimate, the use of the manual average heartbeat template $HTL_M(t)$ increased the overall segmentation accuracy of the SWA by 10.7% and 3.6%, for δ = 10 ms and δ = 50 ms, respectively. This was observed by comparing $SWA(HPE_M, HTL_M)$ against $SWA(HPE_M, HTL_O)$. The number of cardiac cycles improved by $SWA(HPE_M, HTL_M)$ significantly outnumbered those which declined from $SWA(HPE_M, HTL_O)$, as seen in Table 5.6. The majority of cardiac cycles which declined through the use of $SWA(HPE_M, HTL_M)$ in classes 2-3 were related to segmentation errors of the Heartbeat Boundary Prediction (HBP) stage (previously discussed in ch. 4.7), which persisted regardless of δ.

As expected, the use of $HTL_M(t)$ improved segmentation accuracy and avoided errors associated with $HTL_O(t)$, such as heartbeat template magnitude variations and heartbeat template location in cardiac cycle. In general, the presence of heartbeat-to-heartbeat sound intensity variations and aberrant noise in $HTL_M(t)$ was less pronounced than in $HTL_O(t)$. Also, the intensity pattern of cardiac cycles in a given PCG were more similar to $HTL_M(t)$ than $HTL_O(t)$. In the HBP stage of $SWA(HPE_M, HTL_M)$, similarity correlation curves and their peak coefficients exhibited more consistency among the cardiac cycles in a given PCG, resulting in improved synchronous segmentation performance. Thus, the hypothesis that SWA performance could be improved through the use of a more representative heartbeat template, such as $HTL_M(t)$, was confirmed.

5.5 Conclusions

Refinements of the Heart Rate Estimation stage and Heartbeat Template Location stage were presented in this chapter. Improvements in these two stages were shown to improve the segmentation accuracy of the Sliding Window Autocorrelation (SWA) algorithm.

Overall, the use of an optimized heartbeat period estimate HPE_M improved the segmentation accuracy of the SWA by 2.4% (δ = 10 ms) to 4.1% (δ = 50 ms). Thus, the overall performance of the SWA can be improved with the use of a more representative heartbeat period estimate.

Overall, without the effect of inaccurate heartbeat period estimate, the use of an optimized heartbeat template $HTL_M(t)$ improved the segmentation accuracy of the SWA by 3.6% (δ = 50 ms) to 10.7% (δ = 10 ms). Thus, the overall performance of the SWA can be improved with the use of a more representative heartbeat template.

When both the heartbeat period estimate and heartbeat template were optimized, the highest overall segmentation accuracy achieved by the SWA was 94.8% (δ = 10 ms) to 97.8% (δ = 50 ms). This corresponded to an improvement over the original SWA of 7.7% (δ = 50 ms) to 13.3% (δ = 10 ms). Hence, the upper bound for expected segmentation accuracy achievable by any revised SWA is 97.8%.

The average heartbeat period estimate HPE_M and the average heartbeat template $HTL_M(t)$ described in this chapter were generated using information from manual segmentation. However, in a realistic scenario, the availability of manual segmentation

information cancels the need for automated segmentation. Hence, automated methods are required for improving the Heart Rate Estimation stage and Heartbeat Template Location stage. The next chapter investigates automated methods for improving the location of the original heartbeat template.

6 HEARTBEAT TEMPLATE SHIFT COMPETITION

6.1 Introduction

The original Heartbeat Template Location (HTL) stage of the Sliding Window Autocorrelation (SWA) segmentation algorithm (described in ch. 3.2) locates a heartbeat template that is representative of a single cardiac cycle in a given PCG. However, the heartbeat template is not guaranteed to contain an *ordered S1-S2 pair*, which is a contiguous section of the given PCG in which S1 of a heartbeat is followed closely by S2 of the same heartbeat. For example, it was observed on several occasions that the heartbeat template contained an ordered S2-S1 pair (i.e. S2 of a heartbeat followed by S1 of the proceeding heartbeat), or even a sole S2. The overall performance of the SWA is expected to improve if an ordered S1-S2 pair can be successfully located and contained within the heartbeat template.

The aim of this chapter is to improve the HTL stage by locating a heartbeat template that contains an ordered S1-S2 pair. As previously discussed in the Heartbeat Boundary Prediction (HBP) stage of the SWA (described in ch. 3.3), similarity correlation coefficients indicate the degree of similarity between the heartbeat template and the cardiac cycles in the given PCG. Furthermore, the peak similarity correlation coefficient is used to determine the heartbeat boundaries. It is expected that a heartbeat template containing an ordered S1-S2 pair will generate higher peak similarity correlation coefficients than a heartbeat template containing an ordered S2-S1 pair or a sole S2. The proposed methodology generates a small pool of possible heartbeat templates. Out of this

pool, the heartbeat template that generates the highest average peak similarity correlation coefficient in the HBP stage can be considered as most likely to contain an ordered S1-S2 pair. In this manner of competition, the most appropriately located heartbeat template can be determined.

Within the existing framework of the SWA, a pool of possible heartbeat templates can be derived in a systematic manner. Possible heartbeat templates can occupy a time range that is offset from an existing heartbeat template. More specifically, the time range of an existing heartbeat template can be incrementally shifted (up to one heartbeat period) such that each possible heartbeat template corresponds with an incremental shift.

This chapter describes methods for generating shifted heartbeat templates using the original heartbeat template $HTL_O(t)$ (described in ch. 3.3). The competition for selecting the most appropriately shifted heartbeat template out of a pool of possible heartbeat templates is also described. When the pool of possible heartbeat templates are derived from $HTL_O(t)$, the most appropriately shifted heartbeat template is designated $HTL_{OS}(t)$. Multiple revised SWA, which use $HTL_{OS}(t)$ (instead of $HTL_O(t)$), are described and evaluated.

6.2 Methods

The method for generating shifted heartbeat templates, using the original heartbeat template $HTL_O(t)$, is described in ch. 6.2.1. A competitive criterion for selecting the most appropriately shifted heartbeat template out of a pool of possible heartbeat templates is described in ch. 6.2.2. The methods used to evaluate the

performance of multiple revised SWA, which use $HTL_{OS}(t)$ (instead of $HTL_O(t)$), are described in ch. 6.2.3.

6.2.1 Refinements to SWA – Heartbeat Template Shift

The set of $HTL_{O,\lambda}(t)$, where λ may be a positive or negative integer, represents the possible heartbeat templates derived from $HTL_O(t)$. To generate the set of $HTL_{O,\lambda}(t)$, the time range of $HTL_O(t)$ is shifted in increments (of N_{inc} samples, corresponding to 10 ms) backwards and forwards in time, up to a maximum offset (of N_{offset} samples, corresponding to the heartbeat period estimate). The time range of $HTL_O(t)$ was previously expressed in Eq. (3.32)-(3.33). $u^{\ell,\lambda}$ represents the beginning of a shifted time range, as expressed in Eq (6.1). $HTL_{O,\lambda}(t)$ is expressed in Eq. (6.2). The heartbeat period estimate specified by the revised SWA (i.e. either HPE_O or HPE_M) is used to set N_{offset} and N_{HTL}.

$$u^{\ell,\lambda} = u^{\ell} + (\lambda N_{inc}) \;,\; \ni \left|\lambda N_{inc}\right| < N_{offset} \tag{6.1}$$

$$HTL_{O,\lambda}(t) = \{w(t) : u^{\ell,\lambda} \le t < (u^{\ell,\lambda} + N_{HTL})\} \tag{6.2}$$

6.2.2 Refinements to SWA – Heartbeat Template Competition

The competitive criterion for selecting the most appropriately shifted heartbeat template $HTL_{OS}(t)$ out of a pool of possible heartbeat templates $HTL_{O,\lambda}(t)$ is described. Each possible heartbeat template $HTL_{O,\lambda}(t)$ is used as a heartbeat template in the HBP

stage, as described in ch. 3.4. The peak magnitudes of the similarity correlations $G^k(\tau)$ from the HBP stage are averaged, resulting in a mean peak similarity correlation coefficient $\mu_{O,\lambda}$. Each possible heartbeat template $HTL_{O,\lambda}(t)$ has an associated $\mu_{O,\lambda}$ value. The $HTL_{O,\lambda}(t)$ with the highest value of $\mu_{O,\lambda}$ is selected as $HTL_{OS}(t)$, as expressed in Eq. (6.3) and Eq. (6.4).

$$\lambda_{\max} = \arg\max_{\lambda}\{\mu_{O,\lambda}\} \tag{6.3}$$

$$HTL_{OS}(t) = HTL_{O,\lambda_{\max}}(t) \tag{6.4}$$

6.2.3 Evaluation of Revised SWA

To quantify the effect of using the shift competition with the original heartbeat template on the overall performance of the SWA, two revised SWA were evaluated: $SWA(HPE_M, HTL_{OS})$, and $SWA(HPE_O, HTL_{OS})$. Without the effect of incorrect heartbeat period estimate, $SWA(HPE_M, HTL_{OS})$ which used HPE_M (instead of HPE_O) and $HTL_{OS}(t)$ (instead of $HTL_O(t)$) was evaluated. With the effect of the original heartbeat period estimate, $SWA(HPE_O, HTL_{OS})$ which used $HTL_{OS}(t)$ (instead of $HTL_O(t)$) was evaluated. Figure 6.1 illustrates the block diagram representative of $SWA(HPE_M, HTL_{OS})$ and $SWA(HPE_O, HTL_{OS})$.

Each revised SWA was evaluated using the dataset, Automatic Scoring Method (for δ = 10 ms and δ = 10 ms), and scoring statistics previously described in ch. 4.2, ch. 4.3, and ch. 4.4, respectively.

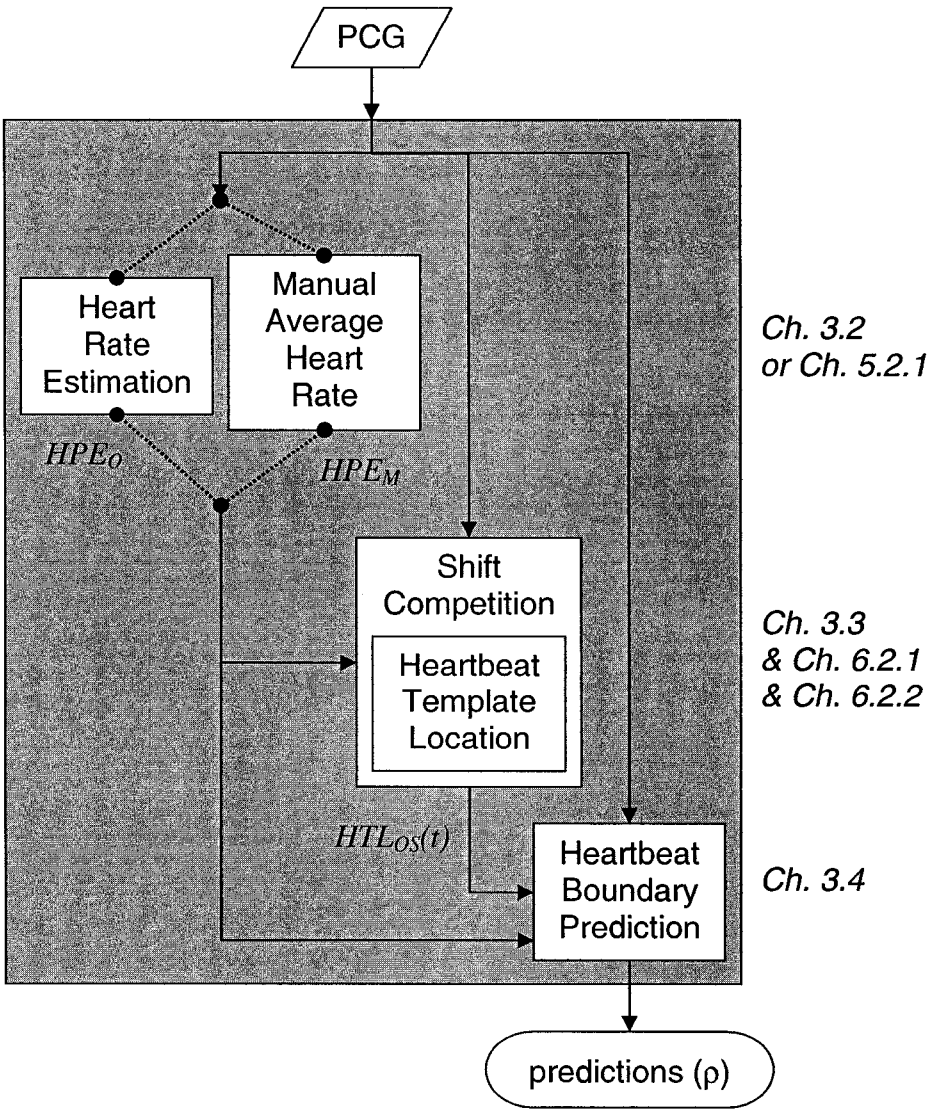

Figure 6.1: Block diagram of revised SWA, using original heartbeat template with shift competition. Representative of $SWA(HPE_O, HTL_{OS})$ and $SWA(HPE_M, HTL_{OS})$.

6.3 Results

The scoring statistics for $SWA(HPE_M, HTL_{OS})$ and $SWA(HPE_O, HTL_{OS})$, described in ch. 6.2.3, are shown in Table 6.2 and Table 6.3. For reference purposes, previously reported results for $SWA(HPE_M, HTL_M)$, $SWA(HPE_M, HTL_O)$, and $SWA(HPE_O, HTL_O)$, are shown in Table 6.1 through to Table 6.3. (Revised SWA marked by * were previously reported in ch. 4.6.2; ** in ch. 5.3.)

Table 6.1: Scoring statistics for $SWA(HPE_M, HTL_M)$**.

Dataset	# PCGs	# Cardiac Cycles	# Cardiac Cycles Correctly Segmented (Segmentation Accuracy)	
			$SWA(HPE_M, HTL_M)$	
			δ = 10 ms	δ = 50 ms
Class 1	100	935	919 (98.2%)	929 (99.3%)
Class 2	68	1092	1034 (94.6%)	1069 (97.8%)
Class 3	27	426	373 (87.5%)	402 (94.3%)
Overall	195	2453	2326 (94.8%)	2400 (97.8%)

Table 6.2: Scoring statistics for $SWA(HPE_M, HTL_O)$**, and $SWA(HPE_M, HTL_{OS})$.

Dataset	# PCGs	# Cardiac Cycles	# Cardiac Cycles Correctly Segmented (Segmentation Accuracy)			
			$SWA(HPE_M, HTL_O)$		$SWA(HPE_M, HTL_{OS})$	
			δ = 10 ms	δ = 50 ms	δ = 10 ms	δ = 50 ms
Class 1	100	935	827 (88.4%)	906 (96.8%)	856 (91.5%)	909 (97.2%)
Class 2	68	1092	925 (84.7%)	1028 (94.1%)	937 (85.8%)	1011 (92.5%)
Class 3	27	426	311 (73.0%)	377 (88.4%)	317 (74.4%)	385 (90.3%)
Overall	195	2453	2063 (84.1%)	2311 (94.2%)	2110 (86.0%)	2305 (93.9%)

Table 6.3: Scoring statistics for $SWA(HPE_O, HTL_O)$*, and $SWA(HPE_O, HTL_{OS})$.

Dataset	# PCGs	# Cardiac Cycles	# Cardiac Cycles Correctly Segmented (Segmentation Accuracy)			
			$SWA(HPE_O, HTL_O)$		$SWA(HPE_O, HTL_{OS})$	
			δ = 10 ms	δ = 50 ms	δ = 10 ms	δ = 50 ms
Class 1	100	935	819 (87.5%)	889 (95.0%)	842 (90.0%)	888 (94.9%)
Class 2	68	1092	893 (81.7%)	986 (90.2%)	928 (84.9%)	999 (91.4%)
Class 3	27	426	293 (68.7%)	337 (79.1%)	293 (68.7%)	339 (79.5%)
Overall	195	2453	2005 (81.7%)	2212 (90.1%)	2063 (84.1%)	2226 (90.7%)

6.4 Discussion

In general, the use of the shift competition in conjunction with the original heartbeat template improved the overall segmentation accuracy of the SWA.

When unaffected by inaccurate heartbeat period estimate, the use of the shift competition generated an increase in overall segmentation accuracy of 1.9% for δ = 10 ms. This was observed by comparing the performance of $SWA(HPE_M, HTL_O)$ and $SWA(HPE_M, HTL_{OS})$, seen in Table 6.2. However, for δ = 50 ms, the use of the shift competition generated a decrease in overall segmentation accuracy, primarily due to 17 incorrectly predicted cardiac cycles in class 2. Upon closer analysis, these 17 cardiac cycles were incorrectly predicted due to partial correlations occurring at the end of PCG, which is an error attributed to the Heartbeat Boundary Prediction stage (as discussed in ch. 4.7). Also, since the decrease in overall segmentation accuracy was only 0.3%, the

use of the shift competition was not considered detrimental to the performance of the SWA.

Furthermore, when affected by potentially inaccurate heartbeat period estimate, the use of the shift competition generated an increase in overall segmentation accuracy of 2.4% and 0.6%, for δ = 10 ms and δ = 50 ms, respectively. This was observed by comparing the performance of $SWA(HPE_O, HTL_O)$ and $SWA(HPE_O, HTL_{OS})$, seen in Table 6.3. The segmentation accuracy of each class was increased, and class 2 had the greatest increase in segmentation accuracy. Hence, the use of the shift competition with the original heartbeat template improved the overall performance of the SWA. This result also suggests that the original heartbeat templates were generally suitable, as there was not a large increase in overall segmentation accuracy for δ = 50 ms. However, the shift competition did improve the precision of the heartbeat boundaries, as there was a greater increase in overall segmentation accuracy for δ = 10 ms.

As expected, the use of the shift competition in conjunction with the optimized heartbeat period estimate HPE_M had greater overall segmentation accuracy than when used in conjunction with the original heartbeat period estimate HPE_O. As seen in Table 6.2 and Table 6.3, the overall segmentation accuracy of $SWA(HPE_M, HTL_{OS})$ was greater than $SWA(HPE_O, HTL_{OS})$ by 1.9% and 3.2%, for δ = 10 ms and δ = 50 ms, respectively. Hence, further improvements to the heartbeat period estimate are expected to generate at most 1.9% to 3.2% increase in overall segmentation accuracy, when used in conjunction with the shift competition and original heartbeat template.

As expected, the use of the shift competition, in conjunction with either heartbeat period estimate, had lower overall segmentation accuracy than the optimized $SWA(HPE_M, HTL_M)$. As seen in Table 6.1 and Table 6.2, the overall segmentation accuracy of $SWA(HPE_M, HTL_M)$ was greater than $SWA(HPE_M, HTL_{OS})$ by 8.8% and 3.9%, for δ = 10 ms and δ = 50 ms, respectively. Hence, further improvements to the location of the original heartbeat template are expected to generate at most 3.9% to 8.8% increase in overall segmentation accuracy, when used in conjunction with the optimized heartbeat period estimate.

Possible improvements to the shift competition could include a larger maximum offset for shifting the time range of $HTL_O(t)$, which was described in ch. 6.2.1. Currently, the maximum offset of HPE_O may be insufficient if $HTL_O(t)$ occurs among cardiac cycles with heartbeat period greater than HPE_O.

6.5 Conclusions

Refinements of the Heartbeat Template Location stage were presented in this chapter, and were shown to improve the segmentation accuracy of the Sliding Window Autocorrelation (SWA) algorithm.

Overall, the use of the shift competition in conjunction with the original heartbeat template location, i.e. $HTL_{OS}(t)$, increased the overall segmentation accuracy of the SWA by 0.6% (δ = 50 ms) to 2.4% (δ = 10 ms). Thus, the overall segmentation accuracy of the SWA can be improved with the use of the heartbeat template shift competition.

The heartbeat template shift competition described in this chapter sought to locate a heartbeat template containing cardiac sounds which contribute to the cyclostationary behaviour of the cardiac cycle; specifically, an ordered S1-S2 pair. Nonetheless, the heartbeat template encloses only a single cardiac cycle within a given PCG. Hence, the intensity of heart sounds contained in the heartbeat template may not be representative of all the cardiac cycles in the given PCG, due to heartbeat-to-heartbeat intensity variations. Methods are required for generating a heartbeat template with heart sound intensities representative of all the cardiac cycles in a given PCG. The next chapter investigates automated methods for generating an averaged heartbeat template and an averaged heartbeat period estimate.

7 AUTOMATIC AVERAGE HEARTBEAT PERIOD ESTIMATE AND HEARTBEAT TEMPLATE

7.1 Introduction

The segmentation accuracy of the Sliding Window Autocorrelation (SWA) segmentation algorithm (described in ch. 3) can be increased by using more representative heartbeat period estimate and heartbeat template. As demonstrated in ch.5, segmentation accuracy was increased by using average heartbeat period and average heartbeat template, which were computed from the gold standard heartbeat boundaries (GSBs) obtained by manual segmentation. As an automatic segmentation algorithm, the SWA cannot make use of a heartbeat period estimate and a heartbeat template that are based on the GSBs, since GSBs are not available as predictive information to any PCG segmentation algorithm.

In order to achieve the performance improvements associated with the use of an average heartbeat period and an average heartbeat template, it is necessary to generate both in an automatic manner. The overall performance of the SWA is expected to improve with the use of an average heartbeat period estimate and an average heartbeat template that are automatically generated. However, automatically generated variables are not expected to yield as great an improvement as variables based on the GSBs, because errors in the automated process are inevitable.

This chapter describes methods for automatically generating an average heartbeat period estimate HPE_A and an average heartbeat template $HTL_A(t)$. A variation of the

heartbeat template shift competition, for generating shifted heartbeat templates using $HTL_A(t)$ (instead of $HTL_O(t)$), is described. When the pool of possible heartbeat templates are derived from $HTL_A(t)$, the most appropriately shifted heartbeat template is designated $HTL_{AS}(t)$, with corresponding heartbeat period estimate HPE_{AS}. Multiple revised SWA which use HPE_A (instead of HPE_O) and/or $HTL_A(t)$ (instead of $HTL_O(t)$), with and without the shift competition, are described and evaluated.

7.2 Methods

Methods for automatically generating an average heartbeat period estimate HPE_A and an average heartbeat template $HTL_A(t)$ are described in ch. 7.2.1. Methods for generating shifted heartbeat templates using $HTL_A(t)$ are described in ch. 7.2.2. Multiple revised SWA are described, which use HPE_A (instead of HPE_O) and/or $HTL_A(t)$ (instead of $HTL_O(t)$), with and without the shift competition. The methods used to evaluate the performance of multiple revised SWA are described in ch. 7.2.3.

7.2.1 Refinements to SWA – Average Heartbeat Template and Period Estimate

For a given PCG, HPE_A and $HTL_A(t)$ are generated simultaneously in an automatic manner. Starting at the beginning of the PCG, the first heartbeat is estimated, and is used to initialize the running average heartbeat period $HPE_{A,m}$ and the running average heartbeat template $HTL_{A,m}(t)$. The PCG is then modified by discarding the first estimated heartbeat. Next, the heartbeat at the beginning of the modified PCG is

estimated, used to update $HPE_{A,m}$ and $HTL_{A,m}(t)$, and subsequently discarded from the modified PCG; this continues iteratively until the modified PCG no longer contains any heartbeats. A flowchart illustrating this high-level description can be seen in Figure 7.1.

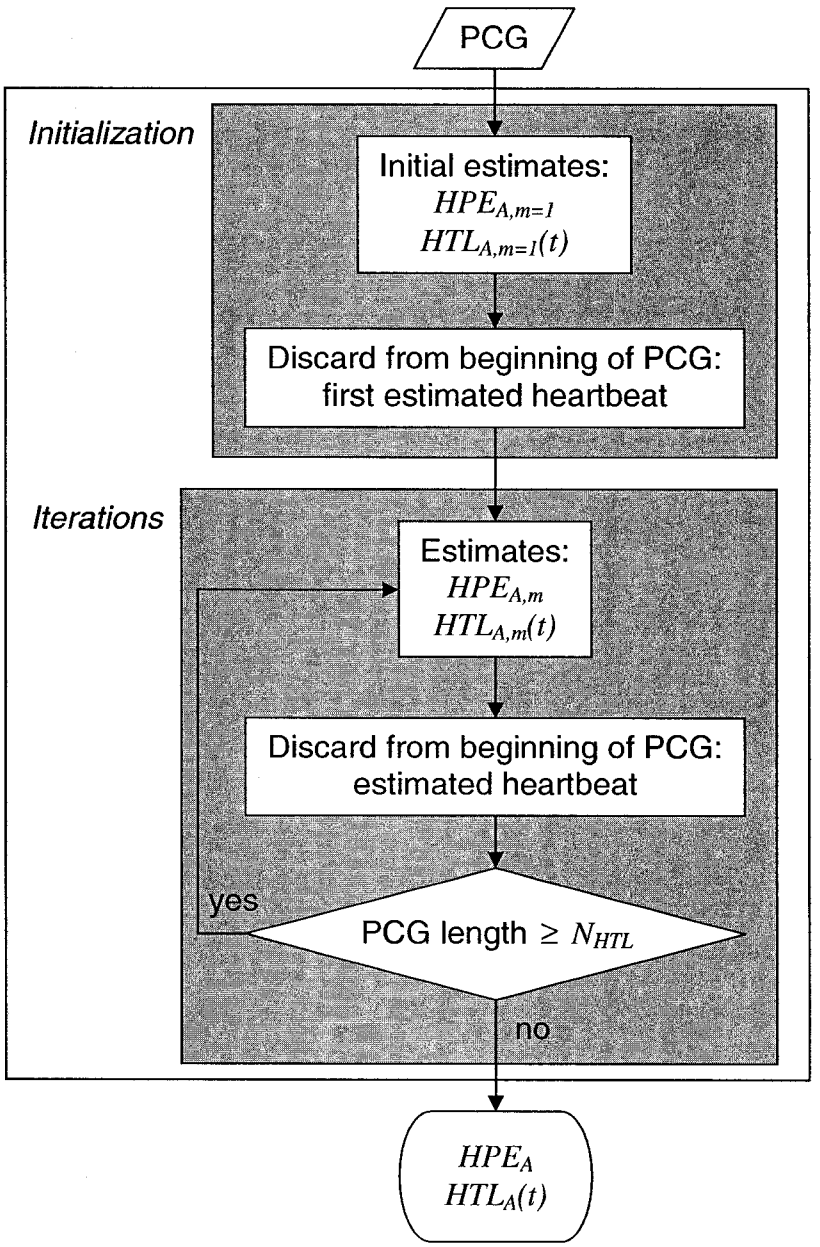

Figure 7.1: Flowchart of process for simultaneously generating automatic average heartbeat period estimate and automatic average heartbeat template, showing initialization and iterations.

Using $w(t)$ of length N samples (as described in ch. 3.1), the period of the first heartbeat in the given PCG is estimated as q_1, which corresponds to the time offset $\tau_{\max}$

of the highest magnitude peak in the tapered autocorrelation $R_{ww,T}(\tau)$, as expressed in Eq. (7.1). The tapered autocorrelation $R_{ww,T}(\tau)$ is generated using the same method as the original HRE stage (described in ch. 3.2) with taper time constant $C = 0.75$, except using the normalized signal magnitude $w(t)$ in place of the square magnitude $x(t)$ in Eq. (3.10) to Eq. (3.13).

At this point, q_1 initializes the running average heartbeat period estimate $HPE_{A,m}$, as expressed in Eq. (7.2). Also, the magnitude of the corresponding first heartbeat in the given PCG initializes the running average heartbeat template $HTL_{A,m}(t)$, as expressed in Eq. (7.3). The length of $HTL_{A,m}(t)$ is represented by $N_{HTL,m}$.

$$q_1 = \tau_{\max} = \arg\max_{\tau}\{R_{ww,T}(\tau)\} \tag{7.1}$$

$$HPE_{A,m=1} = q_1 \tag{7.2}$$

$$HTL_{A,m=1}(t) = w(t) \text{ , for } 1 \le t \le q_1 \tag{7.3}$$

The portion at the beginning of $w(t)$ corresponding to the first heartbeat is discarded, resulting in a shortened $w_s(t)$ with length N_s, as expressed in Eq. (7.4). This marks the end of initialization.

$$w_s(t) = \{w(n) : q_1 < n \le N, t = (n - q_1)\} \tag{7.4}$$

For each iteration, where m indicates the current iteration, a similarity correlation $G^m(\tau)$ is generated between the shortened $w_s(t)$ and $HTL_{A,m-1}(t)$. As expressed in Eq.

(7.5), $G_T^m(\tau)$ is generated by multiplying $G^m(\tau)$ by the tapered window $T_R(\tau)$ of Eq. (3.11), which uses time constant $C = 0.75$. The time offset $\tau_{\max}^m$ of the highest magnitude peak in $G_T^m(\tau)$ is a likely estimate of q_m, which is the period of the next heartbeat $w_m(t)$ in the given PCG, expressed in Eq. (7.7). If the length of $w_m(t)$ is shorter than $N_{HTL,m-1}$, then $w_m(t)$ is zero-padded to $N_{HTL,m-1}$, as expressed in Eq. (7.8).

$$G_T^m(\tau) = G^m(\tau) T_R(\tau) \text{ , for } 0 \le \tau < N_s \tag{7.5}$$

$$\tau_{\max}^m = \arg\max_{\tau} \{G_T^m(\tau)\} \tag{7.6}$$

$$q_m = \tau_{\max}^m \tag{7.7}$$

$$w_m(t) = \begin{Bmatrix} w_s(t) : 1 \le t \le q_m \\ 0 : q_m < t \le N_{HTL,m-1} \end{Bmatrix} \text{ , if } q_m < N_{HTL,m-1} \tag{7.8}$$

q_m and $w_m(t)$ contribute to $HPE_{A,m}$ and $HTL_{A,m}(t)$, respectively, as expressed in Eq. (7.9) and (7.10). It should be noted that if the length of $w_m(t)$ is greater than $N_{HTL,m-1}$, $HTL_{A,m-1}(t)$ is zero-padded to q_m, prior to Eq. (7.10). Hence, $N_{HTL,m}$ reflects either $N_{HTL,m-1}$ or q_m, whichever is greater. The portion at the beginning of $w_s(t)$ corresponding to $w_m(t)$ is discarded, as expressed in Eq. (7.11).

$$HPE_{A,m} = HPE_{A,m-1} + q_m \tag{7.9}$$

$$HTL_{A,m}(t) = HTL_{A,m-1}(t) + w_m(t) \text{ , for } 1 \le t \le N_{HTL,m} \tag{7.10}$$

$$w_s(t) = \{w_s(n) : q_m < n \leq N_s, t = (n - q_m)\} \tag{7.11}$$

N_s is updated to reflect the shortened length of the remaining $w_s(t)$. This marks the end of iteration m.

Subsequent iterations, each represented by Eq. (7.5)-(7.11), continue until the length of the remaining $w_s(t)$ no longer meets or exceeds the length of $HTL_{A,m}(t)$. This stopping condition is expressed in Eq. (7.12).

$$N_s < N_{HTL,m} \tag{7.12}$$

At this point, the final HPE_A and $HTL_A(t)$ are calculated as in Eq. (7.13) and (7.14), respectively, where M represents the total number of iterations.

$$HPE_A = \frac{HPE_{A,m=M}}{M} \tag{7.13}$$

$$HTL_A(t) = \frac{HTL_{A,m=M}(t)}{M} \tag{7.14}$$

When $HTL_A(t)$ is used in the existing framework of the SWA, a starting position is required for $HTL_A(t)$. Specifically, in the Heartbeat Boundary Prediction stage (described in ch. 3.4), the start of the heartbeat template is selected as the first heartbeat boundary prediction p_0. The start of $HTL_A(t)$ is considered equivalent to the start of the initial running average heartbeat template, which is represented by q_0. Since the initial running average heartbeat template starts at the beginning of the given PCG, q_0 is equivalent to the position of the first sample in $w(t)$, i.e. $q_0 = 1$. Hence, $p_0 = q_0 = 1$.

7.2.2 Modifications to Shift Competition – Average Heartbeat Template

The shifting required to generate a pool of possible heartbeat templates from $HTL_A(t)$ is slightly different from $HTL_O(t)$, previously described in ch. 6.2.1.

The set of $HTL_{A,\lambda}(t)$ represents the possible heartbeat templates derived using $HTL_A(t)$. To generate the set of $HTL_{A,\lambda}(t)$, q_0 (described in ch. 7.2.1) is shifted in increments (of N_{inc} samples, corresponding to 10 ms) forwards in time, up to a maximum offset (of N_{offset} samples, corresponding to the heartbeat period estimate). $q_{0,\lambda}$ represents a shifted q_0, as expressed in Eq. (7.15), for which there is a corresponding automatic averaged heartbeat template $HTL_{A,\lambda}(t)$.

$$q_{0,\lambda} = q_0 + (\lambda N_{inc}) \ , \ \exists \left|\lambda N_{inc}\right| < N_{offset} \tag{7.15}$$

A 3-step process is required to generate $HTL_{A,\lambda}(t)$ and corresponding $HPE_{A,\lambda}$. First, a shortened $w_\lambda(t)$ is generated by discarding the portion at the beginning of $w(t)$ prior to $q_{0,\lambda}$. Second, $w_\lambda(t)$ replaces $w(t)$ in the automated process described in ch. 7.2.1, and generates $HTL_A(t)$ and corresponding HPE_A. Third, $HTL_{A,\lambda}(t)$ and $HPE_{A,\lambda}$ are set equal to $HTL_A(t)$ and HPE_A from the second step, respectively. The length of $HTL_{A,\lambda}(t)$ is truncated to N_{HTL}. The heartbeat period estimate specified by the revised SWA (i.e. either HPE_O, HPE_M, or $HPE_{A,\lambda}$) is used to set N_{offset} and N_{HTL}.

The competitive criterion for selecting the most appropriately shifted heartbeat template $HTL_{AS}(t)$ out of a pool of possible heartbeat templates $HTL_{A,\lambda}(t)$ is the same as

described in ch. 6.2.2, for selecting $HTL_{OS}(t)$ out of a pool of $HTL_{O,A}(t)$. HPE_{AS} is the heartbeat period estimate corresponding to $HTL_{AS}(t)$.

7.2.3 Evaluation of Revised SWA

To quantify the effect of using the automatic average heartbeat template on the overall performance of the SWA, three revised SWA were evaluated: $SWA(HPE_M, HTL_A)$, $SWA(HPE_A, HTL_A)$, and $SWA(HPE_O, HTL_A)$. To quantify the effect of using the automatic average heartbeat template in conjunction with the shift competition, three additional revised SWA were evaluated: $SWA(HPE_M, HTL_{AS})$, $SWA(HPE_{AS}, HTL_{AS})$, and $SWA(HPE_O, HTL_{AS})$.

The first three revised SWA used $HTL_A(t)$, as follows. Without the effect of inaccurate heartbeat period estimate, $SWA(HPE_M, HTL_A)$ was evaluated, where the length of $HTL_A(t)$ was truncated to HPE_M. With the effect of automatic average heartbeat period estimate, $SWA(HPE_A, HTL_A)$ was evaluated, where the length of $HTL_A(t)$ was truncated to HPE_A. With the effect of original heartbeat period estimate, $SWA(HPE_O, HTL_A)$ was evaluated, where the length of $HTL_A(t)$ was truncated to HPE_O. Figure 7.2 illustrates the block diagram representative of $SWA(HPE_M, HTL_A)$, $SWA(HPE_A, HTL_A)$, and $SWA(HPE_O, HTL_A)$.

The remaining three revised SWA used $HTL_{AS}(t)$. The description of the first three revised SWA applies to the remaining three revised SWA, except $HTL_A(t)$ is

replaced by $HTL_{AS}(t)$, and HPE_A is replaced by HPE_{AS}. Figure 7.3 illustrates the block diagram representative of $SWA(HPE_M, HTL_{AS})$, $SWA(HPE_{AS}, HTL_{AS})$, and $SWA(HPE_O, HTL_{AS})$.

Each revised SWA was evaluated using the dataset, Automatic Scoring Method (for δ = 10 ms and δ = 50 ms), and scoring statistics previously described in ch. 4.2, ch. 4.3, and ch. 4.4, respectively. The accuracy and appropriateness of HPE_A and HPE_{AS} were evaluated, in the same manner as HPE_O, as described in ch. 4.3.

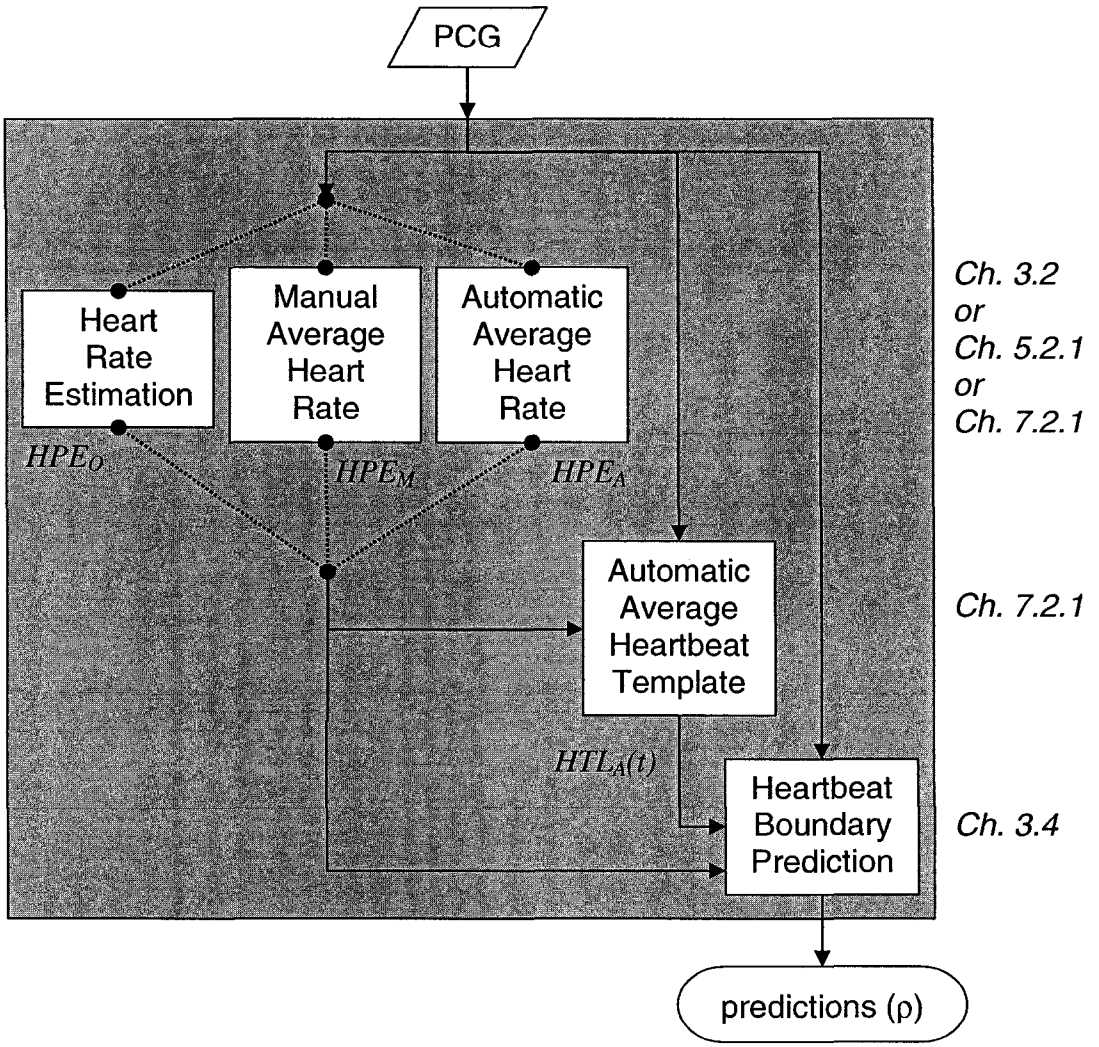

Figure 7.2: Block diagram of revised SWA, using automatic average heartbeat template. Representative of $SWA(HPE_O, HTL_A)$, $SWA(HPE_M, HTL_A)$, and $SWA(HPE_A, HTL_A)$.

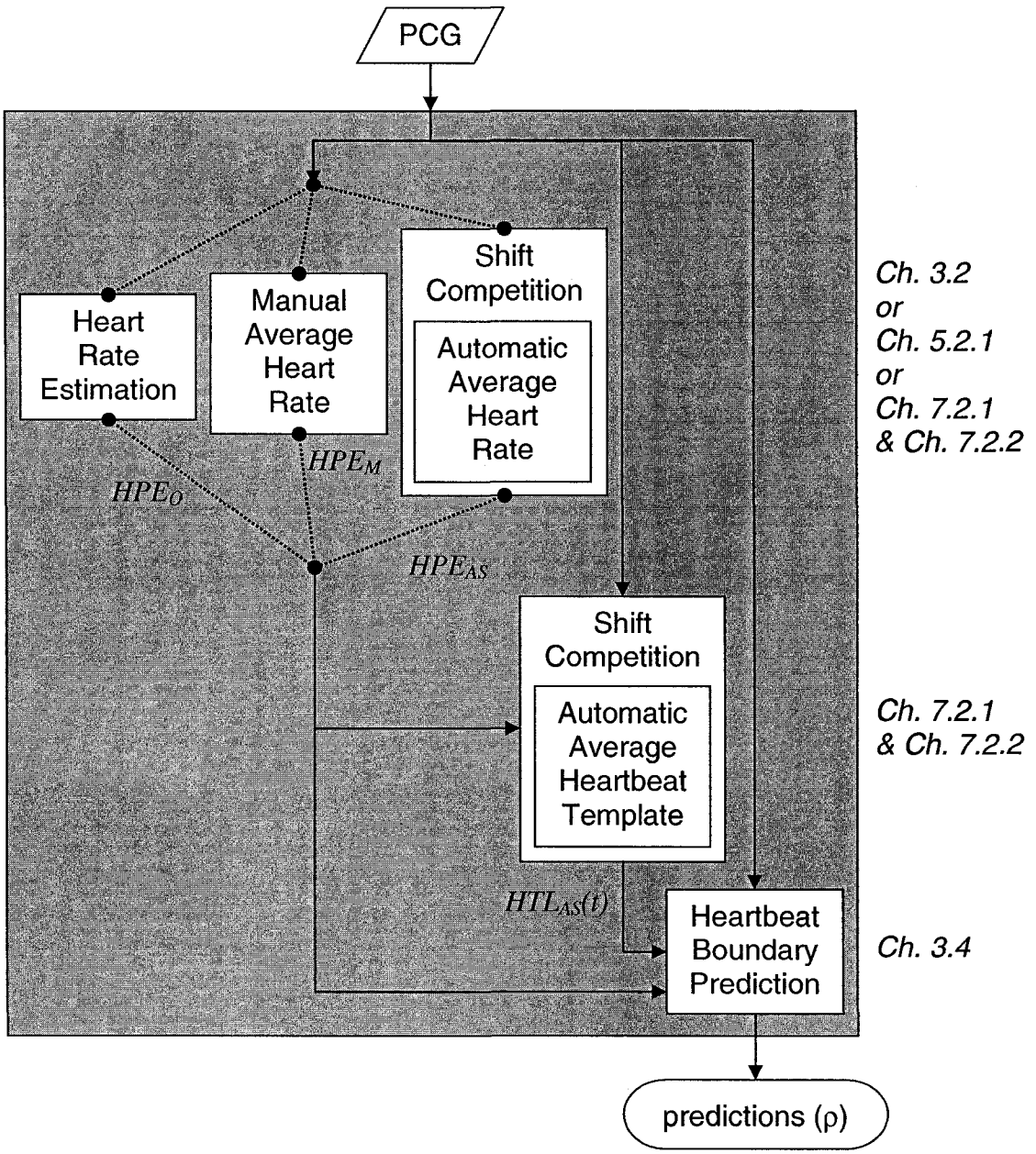

Figure 7.3: Block diagram of revised SWA, using automatic average heartbeat template with shift competition. Representative of $SWA(HPE_O, HTL_{AS})$, $SWA(HPE_M, HTL_{AS})$, and $SWA(HPE_{AS}, HTL_{AS})$.

7.3 Results

The scoring statistics for the revised SWA described in ch. 7.2.3 are shown in Table 7.3, Table 7.5, and Table 7.6. For reference purposes, previously reported results of other revised SWA are shown in Table 7.1, Table 7.2, and Table 7.4. (Revised SWA marked by * were previously reported in ch. 4.6.2; ** in ch. 5.3; *** in ch. 6.3.) Results of evaluating the accuracy and appropriateness of HPE_A and HPE_{AS} are shown in Table 7.7 and Table 7.8, respectively.

Table 7.1: Scoring statistics for $SWA(HPE_M, HTL_M)$ **.

Dataset	# PCGs	# Cardiac Cycles	# Cardiac Cycles Correctly Segmented (Segmentation Accuracy)	
			$SWA(HPE_M, HTL_M)$	
			δ = 10 ms	δ = 50 ms
Class 1	100	935	919 (98.2%)	929 (99.3%)
Class 2	68	1092	1034 (94.6%)	1069 (97.8%)
Class 3	27	426	373 (87.5%)	402 (94.3%)
Overall	195	2453	2326 (94.8%)	2400 (97.8%)

Table 7.2: Scoring statistics for $SWA(HPE_M, HTL_O)$**, and $SWA(HPE_M, HTL_{OS})$***.

Dataset	# PCGs	# Cardiac Cycles	# Cardiac Cycles Correctly Segmented (Segmentation Accuracy)			
			$SWA(HPE_M, HTL_O)$		$SWA(HPE_M, HTL_{OS})$	
			δ = 10 ms	δ = 50 ms	δ = 10 ms	δ = 50 ms
Class 1	100	935	827 (88.4%)	906 (96.8%)	856 (91.5%)	909 (97.2%)
Class 2	68	1092	925 (84.7%)	1028 (94.1%)	937 (85.8%)	1011 (92.5%)
Class 3	27	426	311 (73.0%)	377 (88.4%)	317 (74.4%)	385 (90.3%)
Overall	195	2453	2063 (84.1%)	2311 (94.2%)	2110 (86.0%)	2305 (93.9%)

Table 7.3: Scoring statistics for $SWA(HPE_M, HTL_A)$, and $SWA(HPE_M, HTL_{AS})$.

Dataset	# PCGs	# Cardiac Cycles	# Cardiac Cycles Correctly Segmented (Segmentation Accuracy)			
			$SWA(HPE_M, HTL_A)$		$SWA(HPE_M, HTL_{AS})$	
			δ = 10 ms	δ = 50 ms	δ = 10 ms	δ = 50 ms
Class 1	100	935	828 (88.5%)	915 (97.8%)	853 (91.2%)	915 (97.8%)
Class 2	68	1092	895 (81.9%)	986 (90.2%)	965 (88.3%)	1043 (95.5%)
Class 3	27	426	310 (72.7%)	376 (88.2%)	340 (79.8%)	406 (95.3%)
Overall	195	2453	2033 (82.8%)	2277 (92.8%)	2158 (87.9%)	2364 (96.3%)

Table 7.4: Scoring statistics for $SWA(HPE_O, HTL_O)$*, and $SWA(HPE_O, HTL_{OS})$***.

Dataset	# PCGs	# Cardiac Cycles	# Cardiac Cycles Correctly Segmented (Segmentation Accuracy)			
			$SWA(HPE_O, HTL_O)$		$SWA(HPE_O, HTL_{OS})$	
			δ = 10 ms	δ = 50 ms	δ = 10 ms	δ = 50 ms
Class 1	100	935	819 (87.5%)	889 (95.0%)	842 (90.0%)	888 (94.9%)
Class 2	68	1092	893 (81.7%)	986 (90.2%)	928 (84.9%)	999 (91.4%)
Class 3	27	426	293 (68.7%)	337 (79.1%)	293 (68.7%)	339 (79.5%)
Overall	195	2453	2005 (81.7%)	2212 (90.1%)	2063 (84.1%)	2226 (90.7%)

Table 7.5: Scoring statistics for $SWA(HPE_O, HTL_A)$, and $SWA(HPE_O, HTL_{AS})$.

Dataset	# PCGs	# Cardiac Cycles	# Cardiac Cycles Correctly Segmented (Segmentation Accuracy)			
			$SWA(HPE_O, HTL_A)$		$SWA(HPE_O, HTL_{AS})$	
			δ = 10 ms	δ = 50 ms	δ = 10 ms	δ = 50 ms
Class 1	100	935	823 (88.0%)	904 (96.6%)	846 (90.4%)	910 (97.3%)
Class 2	68	1092	874 (80.0%)	975 (89.2%)	954 (87.3%)	1028 (94.1%)
Class 3	27	426	269 (63.1%)	315 (73.9%)	306 (71.8%)	349 (81.9%)
Overall	195	2453	1966 (80.1%)	2194 (89.4%)	2106 (85.8%)	2287 (93.2%)

Table 7.6: Scoring statistics for $SWA(HPE_A, HTL_A)$, and $SWA(HPE_{AS}, HTL_{AS})$.

Dataset	# PCGs	# Cardiac Cycles	# Cardiac Cycles Correctly Segmented (Segmentation Accuracy)			
			$SWA(HPE_A, HTL_A)$		$SWA(HPE_{AS}, HTL_{AS})$	
			δ = 10 ms	δ = 50 ms	δ = 10 ms	δ = 50 ms
Class 1	100	935	794 (84.9%)	877 (93.7%)	835 (89.3%)	897 (95.9%)
Class 2	68	1092	888 (81.3%)	973 (89.1%)	925 (84.7%)	1000 (91.5%)
Class 3	27	426	284 (66.6%)	326 (76.5%)	301 (70.6%)	344 (80.7%)
Overall	195	2453	1966 (80.1%)	2176 (88.7%)	2061 (84.0%)	2241 (91.3%)

Table 7.7: Number of PCGs with correct HPE_A and appropriate HPE_A. Evaluated using limits based on: (i) maximum and minimum heartbeat periods; (ii) mean and standard deviation of heartbeat periods.

Dataset	# PCGs	# PCGs with:			
		correct HPE_A		appropriate HPE_A	
		(i)	(ii)	(i)	(ii)
Class 1	100	82 (82.0%)	76 (76.0%)	97 (97.0%)	98 (98.0%)
Class 2	68	47 (69.1%)	38 (55.8%)	64 (94.1%)	66 (97.0%)
Class 3	27	18 (66.6%)	18 (66.6%)	21 (77.7%)	22 (81.4%)
Overall	195	147 (75.3%)	132 (67.6%)	182 (93.3%)	186 (95.3%)

Table 7.8: Number of PCGs with correct HPE_{AS} and appropriate HPE_{AS}. Evaluated using limits based on: (i) maximum and minimum heartbeat periods; (ii) mean and standard deviation of heartbeat periods.

Dataset	# PCGs	# PCGs with:			
		correct HPE_{AS}		appropriate HPE_{AS}	
		(i)	(ii)	(i)	(ii)
Class 1	100	89 (89.0%)	89 (89.0%)	99 (99.0%)	99 (99.0%)
Class 2	68	55 (80.8%)	51 (75.0%)	64 (94.1%)	66 (97.0%)
Class 3	27	20 (74.0%)	20 (74.0%)	21 (77.7%)	22 (81.4%)
Overall	195	164 (84.1%)	160 (82.0%)	184 (94.3%)	187 (95.8%)

7.4 Discussion

The use of the automatic average heartbeat template and automatic average heartbeat period estimate, without the use of the shift competition, is discussed in ch. 7.4.1. The use of the automatic average heartbeat template and automatic average heartbeat period estimate, in conjunction with the use of the shift competition, is discussed in ch. 7.4.2.

7.4.1 Without Shift Competition

In general, without the shift competition, the use of the automatic average heartbeat template $HTL_A(t)$ caused a decrease in the overall segmentation accuracy of the SWA, relative to the original heartbeat template $HTL_O(t)$. This was observed by comparing $SWA(HPE_M, HTL_A)$ against $SWA(HPE_M, HTL_O)$, and $SWA(HPE_O, HTL_A)$ against $SWA(HPE_O, HTL_O)$. Although there was slight increase in segmentation

accuracy for class 1, there was greater decrease in segmentation accuracy for classes 2 and 3.

Furthermore, the use of the automatic average heartbeat period estimate HPE_A also did not increase the overall segmentation accuracy of the SWA, relative to the original heartbeat period estimate HPE_O. This was observed by comparing $SWA(HPE_A, HTL_A)$ against $SWA(HPE_O, HTL_A)$. In fact, the overall correctness of HPE_A was lower than HPE_O, as seen in Table 7.7 and Table 4.7, respectively. Although, the overall appropriateness of HPE_A was greater than HPE_O, as seen in Table 7.7 and Table 4.8, respectively, higher appropriateness does not necessarily imply higher segmentation accuracy. An inappropriate heartbeat period estimate that is too short does not necessarily lead to poor segmentation accuracy, since over-prediction tends to occur. However, an inappropriate heartbeat period estimate that is too long will inevitably lead to poor segmentation accuracy due to under-prediction. While nearly all of the inappropriate HPE_A were too long, less than three-quarters of the inappropriate HPE_O were too long. As expected, of the PCGs that had incorrect and inappropriate HPE_A, 52.9% of the cardiac cycles were incorrectly predicted. Of the PCGs that had incorrect but appropriate HPE_A, only 8.8% of the cardiac cycles were incorrectly predicted. Of the PCGs that had correct and appropriate HPE_A, 9.0% of the cardiac cycles were incorrectly predicted.

The lower than expected performance associated with the use of the automatic average heartbeat template and automatic average heartbeat period estimate can be

attributed to one crucial assumption: that the beginning of a given PCG corresponds to the beginning of a complete cardiac cycle. In other words, the use of $HTL_A(t)$ assumes that S1 is the first sound encountered in a given PCG, with only a short portion of diastole preceding S1. However, for the real PCG data comprising the dataset, a complete cardiac cycle does not necessarily occur at the very beginning of a given PCG. In fact, the beginning of a given PCG could correspond to any position within a cardiac cycle.

Although the generation of $HTL_A(t)$ reduces the presence of aberrant noise in the heartbeat template, it does not correct misalignment of the cardiac cycle in the heartbeat template. If the beginning of the heartbeat template is correctly located at the beginning of a cardiac cycle in a given PCG, the automatic average heartbeat template $HTL_A(t)$ is expected to perform segmentation better than the original heartbeat template $HTL_O(t)$. In order for the heartbeat template to enclose the cardiac sounds that contribute to the cyclostationary behaviour of the cardiac cycle, the shift competition was used in conjunction with $HTL_A(t)$.

7.4.2 With Shift Competition

In general, the use of the automatic average heartbeat template in conjunction with the shift competition, or $HTL_{AS}(t)$, increased the overall segmentation accuracy of the SWA in two ways: (1) relative to $HTL_A(t)$ or the automatic average heartbeat template generated without the shift competition; (2) relative to $HTL_{OS}(t)$ or the original heartbeat template generated with the shift competition.

As expected, the use of the shift competition with the automatic average heartbeat template increased the segmentation accuracy of the SWA for each individual class, regardless of the heartbeat period estimate. This was observed by comparing $SWA(HPE_M, HTL_A)$ against $SWA(HPE_M, HTL_{AS})$, $SWA(HPE_O, HTL_A)$ against $SWA(HPE_O, HTL_{AS})$, and $SWA(HPE_A, HTL_A)$ against $SWA(HPE_{AS}, HTL_{AS})$.

As discussed in ch. 7.4.1, without the shift competition, the use of the automatic average heartbeat template $HTL_A(t)$ led to decreased overall segmentation accuracy of the SWA, relative to the original heartbeat template $HTL_O(t)$. However, with the shift competition, the use of $HTL_{AS}(t)$ increased the overall segmentation accuracy of the SWA, relative to $HTL_{OS}(t)$.

Without the effect of inaccurate heartbeat period estimate, the use of $HTL_{AS}(t)$ led to an overall increase of 1.9% and 2.4% over $HTL_{OS}(t)$, for δ = 10 ms and δ = 50 ms, respectively. This was observed by comparing $SWA(HPE_M, HTL_{AS})$ against $SWA(HPE_M, HTL_{OS})$. Further improvements to the heartbeat template are expected to increase the overall segmentation accuracy of the SWA by at most 1.5% (for δ = 50 ms) to 6.9% (for δ = 10 ms), as determined by comparing $SWA(HPE_M, HTL_{AS})$ against $SWA(HPE_M, HTL_M)$.

With the effect of potential inaccuracies in the original heartbeat period estimate, the use of $HTL_{AS}(t)$ led to an overall increase of 1.7% and 2.5% over $HTL_{OS}(t)$, for δ = 10 ms and δ = 50 ms, respectively. This was observed by comparing

$SWA(HPE_O, HTL_{AS})$ against $SWA(HPE_O, HTL_{OS})$. Hence, when used with the shift competition, the automatic average heartbeat template performed better than the original heartbeat template, even when susceptible to potential errors in heartbeat period estimate.

If the starting position of $HTL_{AS}(t)$ is different from that of $HTL_A(t)$, then the automatic average heartbeat period estimate will also be inherently different for $HTL_{AS}(t)$ and $HTL_A(t)$. It was expected that HPE_{AS} generated simultaneously with $HTL_{AS}(t)$ would be more correct and appropriate, than HPE_A generated simultaneously with $HTL_A(t)$. As expected, HPE_{AS} led to an increase of 8.8% (option i) and 14.4% (option ii) in correctness, as well as an increase of 1.0% (option i) and 0.5% (option ii) in appropriateness. This was observed by comparing the results of Table 7.7 and Table 7.8.

Nonetheless, when used in conjunction with $HTL_{AS}(t)$, the use of HPE_{AS} decreased the segmentation accuracy of the SWA, relative to the use of HPE_O. This was observed by comparing the performance of $SWA(HPE_{AS}, HTL_{AS})$ against $SWA(HPE_O, HTL_{AS})$. The greatest decline in segmentation accuracy was observed in class 2, and was caused by only three PCGs: one PCG containing 20 cardiac cycles had different murmur patterns for each half of the PCG; two PCGs containing a combined total of 45 cardiac cycles had incorrect and inappropriate HPE_{AS} which was twice the actual average heartbeat period HPE_M. Furthermore, the decline in segmentation accuracy observed in class 1 was caused by only one PCG containing 21 cardiac cycles, which also had incorrect and inappropriate HPE_{AS} twice the actual average heartbeat

period HPE_M. This confirmed that the automatic average heartbeat period estimate was not as correct as the original heartbeat period estimate. Hence, HPE_O performed better than HPE_{AS}, when used in conjunction with either a non-shifted heartbeat template or the heartbeat template shift competition.

In general, the automatic average heartbeat period estimate HPE_{AS} is able to account for magnitude variations among the cardiac cycles of a given PCG, but only if the magnitude variations do not occur regularly. For example, for PCG in which heart sound intensity variations occur for alternating cardiac cycles, HPE_{AS} recognizes a pair of neighbouring cardiac cycles as a single cyclostationary unit that repeats throughout the given PCG. A correct heartbeat period estimate, however, would recognize the pair as two distinct occurrences of the same cyclostationary unit (i.e. two distinct cardiac cycles). Hence, the regularity of heart sound intensity variations can cause incorrect and inappropriate HPE_{AS} which is twice the actual average heartbeat period HPE_M.

Thus, the best automatically generated heartbeat template is the automatic average heartbeat template generated with the use of the shift competition, or $HTL_{AS}(t)$. The best automatically generated heartbeat period estimate is the original heartbeat period estimate HPE_O. When used together, $SWA(HPE_O, HTL_{AS})$ achieved overall segmentation accuracy of 85.8% and 93.2%, for δ = 10 ms and δ = 50 ms, respectively. This corresponds to an increase of 4.1% and 3.1% over the original $SWA(HPE_O, HTL_O)$, for δ = 10 ms and δ = 50 ms, respectively.

Further improvements to the heartbeat period estimate, when used in conjunction with $HTL_{AS}(t)$, are expected to increase the overall segmentation accuracy of the SWA by at most 2.1% to 3.1%, for δ = 10 ms and δ = 50 ms, respectively. This was determined by comparing $SWA(HPE_O, HTL_{AS})$ against $SWA(HPE_M, HTL_{AS})$. Improvements to the automatic average heartbeat period are in progress.

7.5 Conclusions

Refinements of the Heart Rate Estimation stage and Heartbeat Template Location stage were presented in this chapter. Refinements of the Heartbeat Template Location stage were shown to improve the segmentation accuracy of the Sliding Window Autocorrelation (SWA) algorithm. However, refinements of the Heart Rate Estimation stage did not generate as great an improvement as anticipated.

Without the use of the shift competition, the use of an automatic average heartbeat period estimate HPE_A preserved the overall segmentation accuracy of the SWA. The use of an automatically averaged heartbeat template $HTL_A(t)$ did not improve, but also did not drastically reduce, the segmentation accuracy of the SWA. Both $HTL_A(t)$ and HPE_A rely on the unrealistic assumption that the beginning of each PCG corresponded to the beginning of a complete cardiac cycle.

With the use of the shift competition, the use of an automatic average heartbeat template $HTL_{AS}(t)$ improved the overall segmentation accuracy of the SWA by 3.1% (δ = 50 ms) to 4.1% (δ = 10 ms). Thus, the overall performance of the SWA can be

improved with the use of a more representative heartbeat template that is generated in an automated manner, in conjunction with improved heartbeat template location.

The best heartbeat period estimate and heartbeat template, both generated in an automated manner, were HPE_O and $HTL_{AS}(t)$. When used together, the highest overall segmentation accuracy achieved by the SWA was 85.8% (δ = 10 ms) to 93.2% (δ = 50 ms).

The combination of the shift competition and automatic average heartbeat template described in this chapter sought to: reinforce cardiac sounds which contribute to the cyclostationary behaviour of the cardiac cycle, and reduce the presence of aberrant noise in the heartbeat template. Nonetheless, aberrant noise present in the PCG data contributed to segmentation errors, regardless of the lack of noise in the heartbeat template. Hence, in order to make the PCG data suitable for segmentation, methods are required for de-noising PCG data prior to segmentation. The next chapter investigates several automated methods for preprocessing PCG data.

8 DATA PREPROCESSING

8.1 Introduction

The Sliding Window Algorithm (SWA) segmentation algorithm has been improved through the use of a heartbeat template generated using contributions from all cardiac cycles in a given PCG (described in ch. 7), thus reducing the effect of aberrant noise in the heartbeat template. The SWA has also been improved through the use of a shift competition (described in ch. 6 and ch. 7) that selects the most appropriately shifted heartbeat template, which is likely to contain the part of a heartbeat that is most common to the cardiac cycles in a given PCG.

The overall performance of the SWA is expected to further improve if noise can be successfully excluded from PCG undergoing segmentation. The aim of this chapter is to introduce preliminary work for the purpose of preprocessing and de-noising PCG prior to segmentation. Hence, the focus is changed from improving the segmentation algorithm to improving the data to be segmented.

It is proposed that noise occurring in frequency bands, and/or with energy levels, uncharacteristic of the heart sounds in a given PCG will be excluded. However, if noise and heart sounds occur in the same frequency band and have similar energy, then it may not be possible to identify and exclude noise from a given PCG.

This chapter describes methods for preprocessing PCG data with the intent of de-noising. Several preprocessing techniques are considered, such as bandpass filtering, wavelet decomposition, and Hilbert transform. For a given PCG, two preprocessed

waveforms are generated: (i) $w_{BP}(t)$; (ii) $w_P(t)$. The revised SWA which has demonstrated the highest segmentation accuracy so far, $SWA(HPE_O, HTL_{AS})$, can be applied to each preprocessed waveform individually. The performance of these preprocessing techniques, in conjunction with the use of $SWA(HPE_O, HTL_{AS})$, are evaluated.

8.2 Methods

Methods for preprocessing PCG data using bandpass filtering, wavelet decomposition, and Hilbert magnitude, are described in ch. 8.2.1. Revised SWA which use $w_{BP}(t)$ or $w_P(t)$, instead of the normalized signal magnitude $w(t)$, are described in ch. 8.2.2. Methods of evaluating the performance of these preprocessing techniques are described in ch. 8.2.3.

8.2.1 Preprocessing Techniques

In general, when a bandpass filter is applied to a signal, energy components occurring at frequencies outside the passband are attenuated [51]. A bandpass filter can be used to preprocess PCG data, with passband corresponding to the frequency range in which S1 and S2 are expected to occur. The frequency spectrum of S1 is known to contain peaks in the low frequency range of 10-50 Hz and the medium frequency range of 50-140 Hz [34]. The frequency spectrum of S2 is known to contain peaks in the low frequency range of 10-80 Hz, the medium frequency range of 80-200 Hz, and the high frequency range of 220-400 Hz [34]. Since the frequency spectrum of S1 and S2 intersect

for the range of 10-140 Hz, this frequency range is chosen as the passband for the bandpass filter.

To preprocess a given PCG using bandpass filtering, the normalized waveform $s_{norm}(t)$ of the PCG (previously introduced in Eq. (3.2)) is filtered using a Butterworth filter of order 3, with passband corresponding to 10-140 Hz. To achieve zero-phase distortion, the bandpass-filtered waveform is processed in both the forward and reverse directions, doubling the filter order to 6 (according to Matlab's *filtfilt* function) [39]. The resulting filtered waveform is designated $s_{BP}(t)$. The absolute magnitude of $s_{BP}(t)$ yields $w_{BP}(t)$, similar to how the absolute magnitude of $s_{norm}(t)$ yields $w(t)$ in Eq. (3.3). Hence, the preprocessed waveform $w_{BP}(t)$ is the normalized signal magnitude of the bandpass-filtered waveform of the given PCG.

In general, when a continuous wavelet transform (CWT) [41][61][63] is applied to a signal, a two-dimensional time-scale matrix of wavelet coefficients $W(r,t)$ is generated, where r represents scale and t represents time. The value of a scale r corresponds with a particular frequency f. $W(r,t)$ essentially represents the energy of particular frequency bands in the signal, relative to the time domain. When a CWT is applied to a signal, $W(r,t)$ essentially shows when, and the degree to which, particular frequencies occur during the signal.

Several parameters are required by the CWT, such as scales and wavelet type. The scales specified for the CWT dictate which frequency bands are represented in $W(r,t)$. In this work, scales were chosen to correspond with frequencies in the range of

10 Hz to 250 Hz, that were separated by at least 4 Hz. The wavelet type dictates, in part, the relationship between scale and frequency. More importantly, the shape of the wavelet should correlate well with the signal components which will be represented in $W(r,t)$. In this work, the Morlet wavelet was chosen since it correlates well with heart sounds, as previously justified by [34] and [52]. In this work, wavelet decomposition is used to determine $W(r,t)$ for the bandpass-filtered waveform $s_{BP}(t)$ of a given PCG.

The Hilbert transform [12][40] was previously used to preprocess PCGs in [9], which was the precursor to this work. Hence, the suitability of the Hilbert transform for preprocessing PCGs has already been established. In this work, the Hilbert magnitude of each scale or frequency band of $W(r,t)$ of a given PCG is determined, resulting in $W_H(r,t)$.

The coefficients of $W_H(r,t)$ are summed at each time unit, and the resulting waveform is designated $s_P(t)$, as expressed in Eq. (8.1), where X is the number of scales. $s_P(t)$ is normalized to ± 1, yielding the waveform $w_P(t)$, as in Eq. (8.2).

$$s_P(t) = \sum_{r=1}^{X} W_H(r,t) \tag{8.1}$$

$$w_P(t) = \frac{s_P(t)}{\max\{s_P(t)\}} \tag{8.2}$$

Hence, the preprocessed waveform $w_P(t)$ is the normalized time-aggregate of the Hilbert magnitude of wavelet coefficients, for the bandpass-filtered waveform of the given PCG.

8.2.2 Refinements to SWA

The revised SWA which has achieved the best segmentation performance thus far, and which uses only automatically generated parameters, is $SWA(HPE_O, HTL_{AS})$. Since $SWA(HPE_O, HTL_{AS})$ achieved the highest overall segmentation accuracy out of the various revised SWA (as discussed in ch. 7), it is used to evaluate each preprocessed waveform. Specifically, in each of the three stages of $SWA(HPE_O, HTL_{AS})$, the normalized signal magnitude $w(t)$ is replaced by $w_{BP}(t)$ or $w_P(t)$.

8.2.3 Evaluation of Preprocessing

Two configurations of the SWA were evaluated to quantify the effect of preprocessing PCG data on the overall performance of the SWA: (i) $SWA(HPE_O, HTL_{AS})\big|_{w_{BP}(t)}$ which used $w_{BP}(t)$ (instead of $w(t)$), to quantify the effect of bandpass filtering; (ii) $SWA(HPE_O, HTL_{AS})\big|_{w_P(t)}$ which used $w_P(t)$ (instead of $w(t)$), to quantify the effect of bandpass filtering, wavelet decomposition, and Hilbert transform. Figure 8.1 illustrates the block diagram representative of these two configurations.

Each configuration was evaluated using the dataset, Automatic Scoring Method (for δ = 10 ms and δ = 50 ms), and scoring statistics previously described in ch. 4.2, ch. 4.3, and ch. 4.4, respectively.

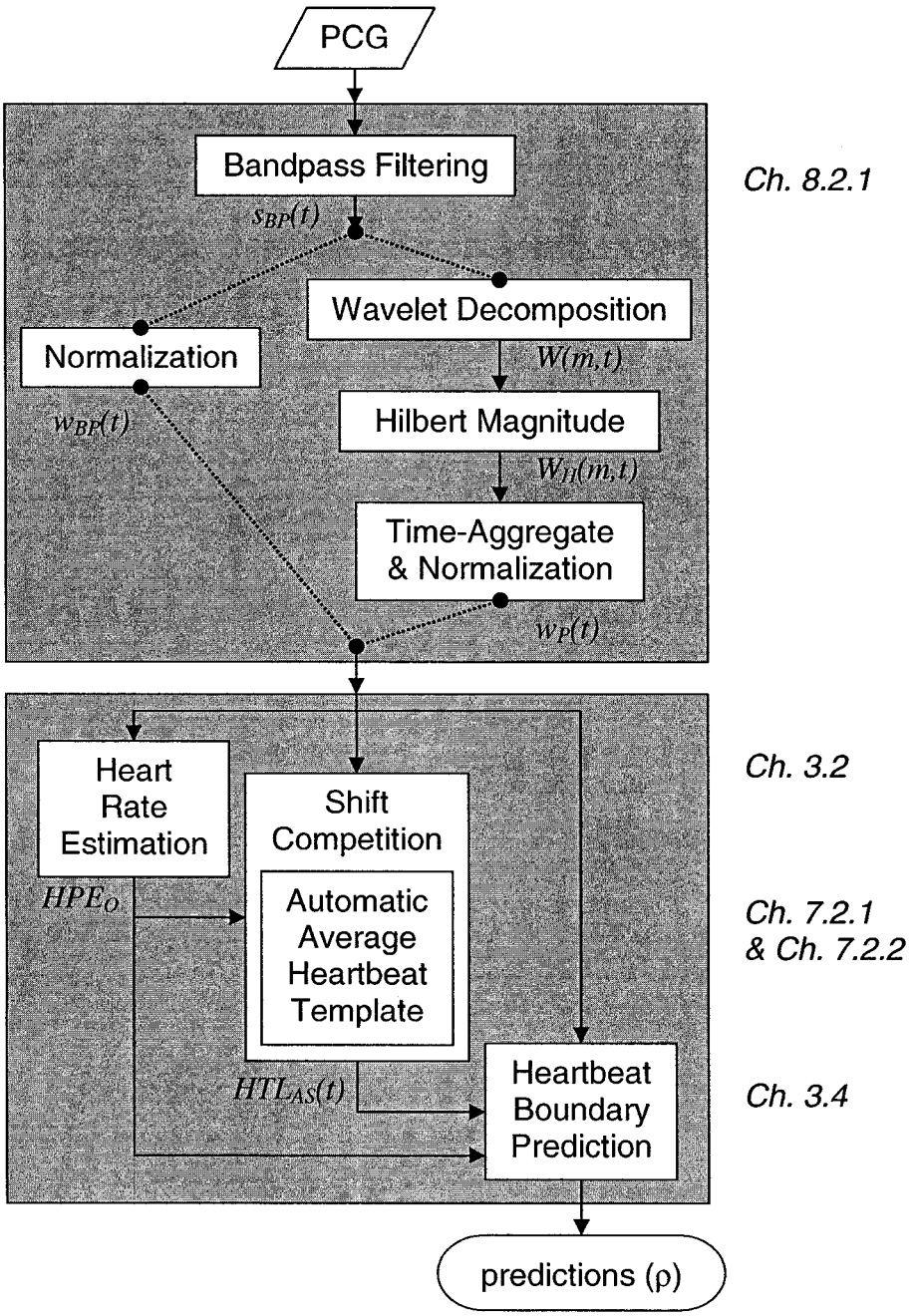

Figure 8.1: Block diagram of $SWA(HPE_O, HTL_{AS})$ with preprocessing, using original heartbeat period estimate and automatic average heartbeat template with shift competition.

8.3 Results

The scoring statistics for the two configurations of the revised SWA, described in ch. 8.2.3, are shown in Table 8.1. For reference purposes, previously reported results of $SWA(HPE_O, HTL_{AS})$ without preprocessing are shown in Table 8.2.

Table 8.1: Scoring statistics for $SWA(HPE_O, HTL_{AS})$, using: $w_{BP}(t)$, and $w_P(t)$.

Dataset	# PCGs	# Cardiac Cycles	# Cardiac Cycles Correctly Segmented (Segmentation Accuracy)			
			$SWA(HPE_O, HTL_{AS})\|_{w_{BP}(t)}$		$SWA(HPE_O, HTL_{AS})\|_{w_P(t)}$	
			δ = 10 ms	δ = 50 ms	δ = 10 ms	δ = 50 ms
Class 1	100	935	847 (90.5%)	910 (97.3%)	870 (93.0%)	912 (97.5%)
Class 2	68	1092	962 (88.0%)	1031 (94.4%)	980 (89.7%)	1034 (94.6%)
Class 3	27	426	313 (73.4%)	351 (82.3%)	313 (73.4%)	348 (81.6%)
Overall	195	2453	2122 (86.5%)	2292 (93.4%)	2163 (88.1%)	2294 (93.5%)

Table 8.2: Scoring statistics for $SWA(HPE_O, HTL_{AS})$, using $w(t)$.

Dataset	# PCGs	# Cardiac Cycles	# Cardiac Cycles Correctly Segmented (Segmentation Accuracy)	
			$SWA(HPE_O, HTL_{AS})\|_{w(t)}$	
			δ = 10 ms	δ = 50 ms
Class 1	100	935	846 (90.4%)	910 (97.3%)
Class 2	68	1092	954 (87.3%)	1028 (94.1%)
Class 3	27	426	306 (71.8%)	349 (81.9%)
Overall	195	2453	2106 (85.8%)	2287 (93.2%)

8.4 Discussion

In general, the use of preprocessing techniques improved the overall segmentation accuracy of the SWA.

In conjunction with the best performing SWA that relied only on automatically generated variables, the use of solely bandpass filtering generated an increase in overall segmentation accuracy of 0.7% and 0.2%, for δ = 10 ms and δ = 50 ms, respectively. This was observed by comparing the performance of $SWA(HPE_O, HTL_{AS})|_{w(t)}$ and $SWA(HPE_O, HTL_{AS})|_{w_{BP}(t)}$, seen in Table 8.2 and Table 8.1, respectively. The use of bandpass filtering, wavelet decomposition, and Hilbert transform, generated an increase in overall segmentation accuracy of 2.3% and 0.3%, for δ = 10 ms and δ = 50 ms, respectively. This was observed by comparing the performance of $SWA(HPE_O, HTL_{AS})|_{w(t)}$ and $SWA(HPE_O, HTL_{AS})|_{w_P(t)}$, seen in Table 8.2 and Table 8.1, respectively.

Thus, the use of bandpass filtering, wavelet decomposition, and Hilbert transform, generated greater improvement in overall segmentation accuracy than the use of solely bandpass filtering. However, the difference in overall segmentation accuracy between $SWA(HPE_O, HTL_{AS})|_{w_P(t)}$ and $SWA(HPE_O, HTL_{AS})|_{w_{BP}(t)}$ was only 1.6% and 0.1%, for δ = 10 ms and δ = 50 ms, respectively. Since the difference between using $w_{BP}(t)$ or

$w_P(t)$ was relatively small, the added complexity of $w_P(t)$ may not justify the small increase in performance.

8.5 Conclusions

Preliminary work in PCG preprocessing with the intent of de-noising was presented in this chapter, and was shown to improve the overall segmentation accuracy of the Sliding Window Autocorrelation (SWA) algorithm.

In conjunction with the best performing SWA that relied only on automatically generated variables, preprocessing improved the overall segmentation accuracy of the SWA by 2.3% (δ = 10 ms) to 0.3% (δ = 50 ms). Hence, the overall performance of the SWA can be improved with the use of a preprocessing stage that incorporates bandpass filtering, wavelet decomposition, and the Hilbert transform. The increase in segmentation accuracy when δ = 10 ms was appreciable, whereas the increase when δ = 50 ms was very low; this suggests the de-noising techniques described in this chapter aided in refining the precision of segmentation. Thus, the highest overall segmentation accuracy achieved by the SWA was 88.1% (δ = 10 ms) to 93.5% (δ = 50 ms).

The use of de-noising techniques described in this chapter, as part of the preprocessing stage of the best performing SWA, sought to combine improvements of the PCG data with improvements of the segmentation algorithm. The increased segmentation accuracy from these preliminary de-noising methods suggests that data preprocessing has potential. Nonetheless, flaws in both the PCG data and the segmentation algorithm still contributed to segmentation errors. Hence, additional methods are required for: further

preprocessing of PCG data, refining the automatic average heartbeat period estimate, and refining the behaviour of the Heartbeat Boundary Prediction stage. The next, final chapter discusses potential future work and outlines the general conclusions of this research.

9 CONCLUSIONS

In this thesis dissertation, the existing PCG segmentation algorithm called the Sliding Window Autocorrelation (SWA) was described in ch. 3. The dataset and Automatic Scoring Method used to evaluate the SWA were described in ch. 4. The effects of optimized heart rate estimation and optimized heartbeat template on the SWA were described in ch. 5. An extension to heartbeat template location of the SWA, based on a shifted heartbeat template competition, was described in ch. 6. Enhancements to heart rate estimation and heartbeat template location of the SWA, based on averaging, were described in ch. 7. A preliminary exploration of de-noising techniques for preprocessing PCG prior to segmentation was described in ch. 8.

This final chapter describes the main conclusions of this work (section 9.1) and potential future work (section 9.2).

9.1 Conclusions

Automated synchronous segmentation was achieved for PCG exhibiting varying degrees and types of noise. As hypothesized, enhancements to heartbeat template location improved the segmentation accuracy of the Sliding Window Autocorrelation (SWA) algorithm. An examination using the manually determined heartbeat period and heartbeat template supported this hypothesis. Specifically, improvements to the SWA were achieved by: (i) improving the automatic location and selection of a heartbeat template using a shift competition (hence addressing heart rate variability); (ii) improving the automatic generation of an averaged heartbeat template (hence addressing variability of

heart sound intensity); and (iii) de-noising PCG prior to segmentation (hence addressing non-cardiac noise presence).

In general, the use of the heartbeat template shift competition improved the segmentation accuracy of the SWA, for either automatically generated heartbeat template. With the use of the shift competition, the overall segmentation accuracy increased by: 3.8% (δ = 50 ms) to 5.7% (δ = 10 ms) for the automatic average heartbeat template; and, 0.6% (δ = 50 ms) to 2.4% (δ = 10 ms) for the original heartbeat template. Without the use of the shift competition, the automatic average heartbeat template did not improve the segmentation accuracy of the original SWA. However, with the use of the shift competition, the automatic average heartbeat template improved the segmentation accuracy of the SWA to a greater extent than the original heartbeat template. The automatic average heartbeat template with shift competition increased the overall segmentation accuracy by 3.1% (δ = 50 ms) to 4.1% (δ = 10 ms), whereas the original heartbeat template with shift competition increased the overall segmentation accuracy by only 0.6% (δ = 50 ms) to 2.4% (δ = 10 ms). Relative to the original heartbeat period estimate, the automatic average heartbeat period estimate did not improve the segmentation accuracy of the SWA. The use of data preprocessing techniques improved the segmentation accuracy of the SWA, by 0.3% (δ = 50 ms) to 2.3% (δ = 10 ms).

Through the use of a combination of enhancements (heartbeat template shift competition, automatic average heartbeat template, and data preprocessing), the SWA achieved correct segmentation, synchronous to within 10 ms of actual cardiac cycle

boundaries, for 88.1% of the 2453 cardiac cycles in a dataset of 195 PCGs. This corresponded to an overall improvement of 6.4% over the original SWA which did not use any enhancements. Within 50 ms of actual cardiac cycle boundaries, the SWA achieved correct synchronous segmentation of 93.5%, which corresponded to an overall improvement of 3.4%. A large proportion of the improvement (4.1% for δ = 10 ms, 3.1% for δ = 50 ms) was attributed to the use of the automatic average heartbeat template in conjunction with the shift competition. A relatively small proportion of the improvement (2.3% for δ = 10 ms, 0.3% for δ = 50 ms) was attributed to the use of data preprocessing techniques for de-noising PCG prior to segmentation. However, the de-noising results arise from only a preliminary exploration, so this area has potential to further improve the performance of the SWA.

The optimized SWA (which used manual average heartbeat period estimate and manual average heartbeat template) achieved correct segmentation, synchronous to within 10 ms of actual cardiac cycle boundaries, for 94.8% of the 2453 cardiac cycles in the dataset of 195 PCGs. This corresponded to an overall improvement of 6.7% over the highest segmentation accuracy achieved by the SWA using only automatically generated variables. Within 50 ms of cardiac cycle boundaries, the optimized SWA achieved correct synchronous segmentation of 97.8%, which corresponded to an overall improvement of 4.3%. Hence, further enhancements to the SWA are possible to further increase the overall segmentation accuracy.

At this point, errors in the automatic average heartbeat period estimate and Heartbeat Boundary Prediction (HBP) stage are the main obstacles to improving the

segmentation performance of the SWA. Although the manual average heartbeat period estimate increased the segmentation accuracy of the SWA, unfortunately the automatic average heartbeat period did not. A more accurate, automatic average heartbeat period estimate will also improve the simultaneously generated, automatic average heartbeat template. Several design specifications in the HBP stage cause poor segmentation, regardless of the correctness of the heartbeat period estimate or heartbeat template.

In conclusion, automatic segmentation of PCGs is an important stage in the automatic analysis of PCGs, especially automatic murmur analysis. This work provided a systematic and quantitative method for analyzing synchronous segmentation performance. The enhancements to the SWA increased the overall segmentation accuracy by 3.4% (δ = 50 ms) to 6.4% (δ = 10 ms) over the original SWA, resulting in overall segmentation accuracy of 88.1% (δ = 10 ms) to 93.5% (δ = 50 ms). Considering the high performance of the original SWA, these improvements are considerable, and represent a reduction in error of 34.3% (δ = 50 ms) to 34.9% (δ = 10 ms). Furthermore, compared to the majority of previous segmentation research which use PCGs with only low noise or a limited dataset, this work represents a thorough analysis on a large challenging dataset comprised of 195 PCGs (2453 cardiac cycles). Nonetheless, opportunities for further enhancements to the SWA still exist. The next, final section presents some of these possible opportunities.

9.2 Future Work

Potential future work includes further enhancements to heartbeat period estimation, heartbeat template location, data preprocessing, and heartbeat boundary prediction.

Heartbeat Period Estimate

I. **Consider secondary peak in correlation as possible heartbeat period estimate, in generating Automatic Average Heartbeat Period Estimate.**

This problem is similar to VI, except that the highest magnitude peak in a similarity correlation curve is automatically considered a heartbeat period estimate in the iterative process of generating the Automatic Average Heartbeat Period Estimate. The peak magnitude associated with a correct heartbeat period estimate may be surpassed by an unexpected peak. If this occurs regularly, the resulting Automatic Average Heartbeat Period Estimate may be incorrect and/or inappropriate. A possible solution to this problem involves considering not only the highest, but also the second-highest magnitude peak in a similarity correlation curve as a potential heartbeat period estimate.

Heartbeat Template Location

II. **Higher maximum offset for shifted heartbeat templates, in Heartbeat Template Shift Competition.**

Currently, the maximum offset for shifting heartbeat templates in the Heartbeat Template Shift Competition corresponds to the specified heartbeat period estimate. If the cardiac cycles at the beginning of a PCG have greater heartbeat period than the majority of other cardiac cycles in the PCG, the length of the heartbeat period estimate may not be sufficient to locate an ordered S1-S2 pair for a shifted template. The maximum offset could be increased, possibly to the maximum search window length from the Heartbeat Boundary Prediction stage, since the search window length is intended to represent the longest possible duration in which a neighbouring cardiac cycle could occur.

III. **Consider the starting locations of the estimated heartbeats, from generating Automatic Average Heartbeat Template, as a possible set of heartbeat boundary predictions.**

The process for generating the Automatic Average Heartbeat Template contains potential predictive information. If predictions generated in the automatic averaging process can match or surpass the segmentation accuracy achieved by predictions from the Heartbeat Boundary Prediction stage, then the inclusion of the HBP stage in the SWA may be redundant and no longer necessary.

Data Preprocessing

IV. **Exclude frequency bands exhibiting atypical regularity, when de-noising PCGs using wavelet-based methods.**

Sounds which occur at an interval uncharacteristic of the cyclostationary components in a PCG could indicate the presence of non-cardiac noise. The regularity at which sounds of comparable intensity occur in a frequency band can be characterized by the standard deviation and mean duration between thresholded sounds. A frequency band which exhibits regularity uncommon to other frequency bands can be excluded from the summation of wavelet coefficients.

Heartbeat Boundary Prediction

V. **Variable search window range in Heartbeat Boundary Prediction stage.**

The fixed length of the search window in the Heartbeat Boundary Prediction stage may not be sufficient for PCGs exhibiting highly variable heart rate. A trivial prediction will occur if the range of the search window does not reach the next cardiac cycle in a PCG, and the boundary of the next cardiac cycle may not be predicted correctly. Currently, the fixed length of the search window is defined by the heartbeat period estimate. A possible solution to this problem involves the use of an instantaneous heartbeat period estimate to define the length of the next search window. The process that generates

Automatic Average Heartbeat Period Estimate (ch. 7) could potentially provide information about the instantaneous heartbeat period estimate.

VI. **Consider secondary peak in similarity correlation as possible prediction, in Heartbeat Boundary Prediction stage.**

Currently, the highest magnitude peak in a similarity correlation curve is automatically considered a boundary prediction. Heartbeat-to-heartbeat magnitude variation may cause unexpected peaks in a similarity correlation curve. The peak magnitude associated with the location of a correct boundary prediction may be surpassed by an unexpected peak, and the boundary of the next cardiac cycle may not be predicted correctly. A possible solution to this problem involves considering not only the highest, but also the second-highest magnitude peak in a similarity correlation curve as a potential boundary prediction. This could be represented as a tree structure, where one branch corresponds with taking the highest magnitude peak, and another branch corresponds with taking the second-highest magnitude peak, as a boundary prediction. Competitive criteria can be used to select the most suitable set of boundary predictions out of a pool of possible sets.

VII. **Compensate correlation coefficients of partial search windows that overlap with the bounds of a PCG, in the Heartbeat Boundary Prediction stage.**

Currently, a search window that overlaps with the end (or beginning) of a PCG is truncated so as not to exceed the bounds of the PCG. The resulting

similarity correlation curve is also truncated. Nonetheless, due to the nature of cross correlation, the similarity correlation coefficients towards the end (or beginning) of the partial window are biased towards zero. The peak magnitude associated with the location of a correct boundary prediction may be reduced, and the boundary of the next cardiac cycle may not be predicted correctly. A method is required, for compensating the biased correlation coefficients, or possibly for iteratively truncating the template window.

VIII. **Competition between sets of predictions generated by different revised SWA, or a Prediction Set Competition.**

In the Heartbeat Template Shift Competition, a heartbeat template is selected from a pool of possible shifted heartbeat templates, based on the highest mean peak similarity correlation coefficient generated in the Heartbeat Boundary stage. Similarly, in the Prediction Set Competition, a set of predictions can be selected from a pool of possible sets, based on the highest mean peak similarity correlation coefficient generated in the Heartbeat Boundary Prediction stage. The pool of possible sets, however, can include sets of predictions from different revised SWA; so, the segmentation results of a given PCG will originate from whichever revised SWA performed best for that individual PCG. Currently, when evaluating segmentation performance, the segmentation results of each PCG originate from the same revised SWA.

REFERENCES

[1] Ahlstrom C., Hult P., Rask P., Karlsson J.-E., Nylander E., Dahlstrom U., and Ask P., "Feature extraction for systolic heart murmur classification," *Annals of Biomedical Engineering*, vol. 34, no. 11, pp. 1666-1677, 2006.

[2] Ahlstrom C., Lanne T., Ask P., and Johansson A., "A method for accurate localization of the first heart sound and possible applications," *Physiological Measurement*, vol. 29, pp. 417-428, 2008.

[3] Altman C. A., Nihill M. R., and Bricker J. T., *Pediatric Cardiac Auscultation*, CD-ROM. Lippincott Williams & Wilkins, 2000.

[4] Ari S., Kumar P., and Saha G., "On an algorithm for boundary estimation of commonly occurring heart valve diseases in time domain," in *3rd Annual IEEE India Conference*, 2006, pp. 1-5.

[5] Ari S., Kumar P., and Saha G., "A robust heart sound segmentation algorithm for commonly occurring heart valve diseases," *Journal of Medical Engineering & Technology*, vol. 32, pp. 456-465, 2008.

[6] Ari S., Sensharma K., and Saha G., "DSP implementation of a heart valve disorder detection system from a phonocardiogram signal," *Journal of Medical Engineering & Technology*, vol. 32, pp. 122-132, 2007.

[7] Baranek H. L., Lee H. C., Cloutier G., and Durand L.-G., "Automatic detection of sounds and murmurs in patients with Ionescu-Shiley aortic bioprostheses," *Medical and Biological Engineering and Computing*, vol. 27, pp. 449-455, 1989.

[8] Beers M. H., Ed., *The Merck Manual of Diagnosis and Therapy.* Whitehouse Station, NH: Merck Research Laboratories, 2006. (18th ed.) [Online] Available: http://www.merck.com

[9] Beirne P., "Unsupervised segmentation of heart sounds," M.A.Sc. thesis, Department of Computer and Systems Engineering, Carleton University, Ottawa, ON, Canada, 2006.

[10] Budd E. and Stevenson M., "PCG event detection and classification using right singular vectors," in *29th Canadian Medical and Biological Engineering Conference*, 2006.

[11] Carvalho P., Gil P., Henriques J., Eugenio L., and Antunes M., "Low complexity algorithm for heart sound segmentation using the variance fractal dimension," in *Proceedings of 4th Annual IEEE International Workshop on Intelligent Signal Processing*, 2005, pp. 194-199.

[12] Choi S. and Jiang Z., "Comparison of envelope extraction algorithms for cardiac sound signal segmentation," *Expert Systems with Applications*, vol. 34, pp. 1056-1069, 2008.

[13] Criley J. M., *The Physiological Origins of Heart Sounds and Murmurs*, CD-ROM. Lippincott Williams & Wilkins, 1997.

[14] Debbal S. M. and Bereksi-Reguig F., "Time-frequency analysis of the first and the second heartbeat sounds," *Applied Mathematics and Computation*, vol. 184, pp. 1041-1052, 2007.

[15] Delgado-Trejos E., Quiceno-Manrique A. F., Godino-Llorente J. I., Blanco-Velasco M., and Castellanos-Dominguez G., "Digital auscultation analysis for heart murmur detection," *Annals of Biomedical Engineering*, vol. 37, no. 2, pp. 337-353, 2009.

[16] Dokur Z. and Olmez T., "Heart sound classification using wavelet transform and incremental self-organizing map," *Digital Signal Processing*, vol. 18, pp. 951-959, 2008.

[17] El-Segaier M., Lilja O., Lukkarinen S., Sornmo L., Sepponen R., and Pesonen E., "Computer-based detection and analysis of heart sound and murmur," *Annals of Biomedical Engineering*, vol. 33, no. 7, pp. 937-942, 2005.

[18] El-Segaier M., Pesonen E., Lukkarinen S., Peters K., Sornmo L., and Sepponen R., "Detection of cardiac pathology: time intervals and spectral analysis," *Acta Paediatrica*, vol. 96, no. 7, pp. 1036-1042, 2007.

[19] Gardner W. A., Napolitano A., and Paura L., "Cyclostationarity: Half a century of research," *Signal Processing*, vol. 86, pp. 639-697, 2006.

[20] Gerbarg D. S., Holcomb F. W., Hofler J. J., Bading C. E., Schultz G. L., and Sears R. E., "Analysis of phonocardiogram by a digital computer," *Circulation Research*, vol. 11, pp. 569-576, 1962.

[21] Gupta C. N., Palaniappan R., Rajan S., Swaminathan S., and Krishnan S. M., "Segmentation and classification of heart sounds," in *18th Annual IEEE Canadian Conference on Electrical and Computer Engineering*, 2005, pp. 1674-1677.

[22] Gupta C. N., Palaniappan R., Swaminathan S., and Krishnan S. M., "Neural network classification of homomorphic segmented heart sounds," *Applied Soft Computing*, vol. 7, pp. 286-297, 2007.

[23] Haghighi-Mood A. and Torry J. N., "A sub-band energy tracking algorithm for heart sound segmentation," in *22nd Computers in Cardiology Conference*, 1995, pp. 501-504.

[24] Herold J., Schroeder R., Nasticzky F., Baier V., Mix A., Huebner T., and Voss A., "Diagnosing aortic valve stenosis by correlation analysis of wavelet filtered heart sounds," *Medical and Biological Engineering and Computing*, vol. 43, pp. 451-456, 2005.

[25] Hult P., Fjallbrant T., Wranne B., and Ask P., "Detection of the third heart sound using a tailored wavelet approach," *Medical and Biological Engineering and Computing*, vol. 42, pp. 253-258, 2004.

[26] Iwata A., Ishii N., and Suzumura N., "Algorithm for detection of the first and second heart sound by spectral tracking," *Medical and Biological Engineering and Computing*, vol. 18, pp. 19-26, 1980.

[27] Jiminez A., Ortiz M. R., Pena M. A., Charleston S., Aljama A. T., and Gonzalez R., "The use of wavelet packets to improve the detection of cardiac sounds from the fetal phonocardiogram," in *26th Computers in Cardiology Conference*, 1999, pp. 463-466.

[28] Kumar D., Carvalho P., Antunes M., Henriques J., Eugenio L., Schmidt R., and Habetha J., "Detection of S1 and S2 heart sounds by high frequency signatures,"

in *Proceedings of 28th Annual International Conference of the IEEE Engineering in Medicine and Biology Society*, 2006, pp. 1410-1416.

[29] Kumar D., Carvalho P., Antunes M., Henriques J., Maldonado M., Schmidt R., and Habetha J., "Wavelet transform and simplicity based heart murmur segmentation," in *33rd Computers in Cardiology Conference*, 2006, pp. 173-176.

[30] Kumar P., "Estimating boundaries of primary heart sounds for diagnosing heart valve disorders," in *3rd IET International Conference on Advances in Medical Signal and Information Processing*, 2006, pp. 1-4.

[31] Kurnaz M. N. and Olmez T., "Determination of features for heart sounds by using wavelet transforms," in *15th IEEE Symposium on Computer-Based Medical Systems*, 2002, pp. 155-158.

[32] Lehner R. J. and Rangayyan R. M., "A three-channel microcomputer system for segmentation and characterization of the phonocardiogram," *IEEE Transactions on Biomedical Engineering*, vol. BME-34, no. 6, pp. 485-489, 1989.

[33] Liang H., Lukkarinen S., and Hartimo I., "Heart sound segmentation algorithm based on heart sound envelogram," in *24th Computers in Cardiology Conference*, 1997, pp. 105-108.

[34] Liang H., Lukkarinen S., and Hartimo I., "A heart sound segmentation algorithm using wavelet decomposition and reconstruction," *Proceedings of 19th Annual International Conference of the IEEE Engineering in Medicine and Biology Society*, 1997, pp. 1630-1633.

[35] Liang H., Lukkarinen S., and Hartimo I., "A boundary modification method for heart sound segmentation algorithm," in *25th Computers in Cardiology Conference*, 1998, pp. 593-595.

[36] Liang H. and Hartimo I., "A feature extraction algorithm based on wavelet packet decomposition for heart sound signals," in *Proceedings of the IEEE-SP International Symposium on Time-Frequency and Time-Scale Analysis*, 1998, pp. 93-96.

[37] Lima C. S. and Barbosa D., "Automatic segmentation of the second cardiac sound by using wavelets and hidden Markov models," in *Proceedings of 30th Annual International Conference of the IEEE Engineering in Medicine and Biology Society*, 2008, pp. 334-337.

[38] Malarvili M. B., Kamarulafizam I., Hussain S., and Helmi D., "Heart sound segmentation algorithm based on instantaneous energy of electrocardiogram," in *30th Computers in Cardiology Conference*, 2003, pp. 327-330.

[39] MathWorks Inc., *Matlab Signal Processing Toolbox User's Guide*. Natick, MA: The MathWorks Inc., 2009. [Online] Available: http://www.mathworks.com/access/helpdesk/help/pdf_doc/signal/signal_tb.pdf

[40] McDonough R. N. and Whalen A.D., *Detection of signals in noise*. San Diego: Academic Press, 1995. (2nd ed.)

[41] Messer S. R., Agzarian J., and Abbott D., "Optimal wavelet denoising for phonocardiograms," *Microelectronics Journal*, vol. 32, pp. 931-941, 2001.

[42] Mohrman D. E. and Heller L. J., *Cardiovascular Physiology*. McGraw-Hill, 2003. (5^{th} ed.)

[43] Myint W. W. and Dillard B., "An electronic stethoscope with diagnostic capability," in *Proceedings of the 33^{rd} Southeastern Symposium on System Theory*, 2001, pp. 133-137.

[44] Nazeran H., "Wavelet-based segmentation and feature extraction of heart sounds for intelligent PDA-based phonocardiography," *Methods of Information in Medicine*, vol. 46, pp. 135-141, 2007.

[45] Nigam V. and Priemer R., "Simplicity based gating of heart sounds," in *Proceedings of the 48^{th} Midwest Symposium on Circuits and Systems*, 2005, pp. 1298-1301.

[46] Nigam V. and Priemer R., "A dynamic method to estimate the time split between the A2 and P2 components of the S2 heart sound," *Physiological Measurement*, vol. 27, pp. 553-567, 2006.

[47] Nigam V. and Priemer R., "A simplicity-based fuzzy clustering approach for detection and extraction of murmurs from the phonocardiogram," *Physiological Measurement*, vol. 29, pp. 33-47, 2008.

[48] Olmez T. and Dokur Z., "Classification of heart sounds using an artificial neural network," *Pattern Recognition Letters*, vol. 24, pp. 617-629, 2003.

[49] Omran S. and Tayel M., "A heart sound segmentation and feature extraction algorithm using wavelets," in *Proceedings of the 1^{st} International Symposium on Control, Communication and Signal Processing*, 2004, pp. 235-238.

[50] Peura R. A., "Blood pressure and sound," in *Medical Instrumentation: Application and Design*, Webster J. G., Ed. Hoboken, NJ: Wiley, 1998. (3rd ed.)

[51] Proakis J. G. and Manolakis D. G., *Digital Signal Processing*. Upper Saddle River, NJ: Prentice Hall, 2007. (4th ed.)

[52] Rajan S., Doraiswami R., Stevenson M., and Watrous R., "Wavelet based bank of correlators approach for phonocardiogram signal classification," in *Proceedings of the IEEE-SP International Symposium on Time-Frequency and Time-Scale Analysis*, 1998, pp. 77-80.

[53] Rajan S., Budd E., Stevenson M., and Doraiswami R., "Unsupervised and uncued segmentation of the fundamental heart sounds in phonocardiograms using a time-scale representation," in *Proceedings of 28th Annual International Conference of the IEEE Engineering in Medicine and Biology Society*, 2006, pp. 3732-3735.

[54] Reed T. R., Reed N. E., and Fritzson P., "Heart sound analysis for symptom detection and computer-aided diagnosis," *Simulation Modelling Practice and Theory*, vol. 12, pp. 129-146, 2004.

[55] Ricke A. D., Povinelli R. J., and Johnson M. T., "Automatic segmentation of heart sound signals using hidden Markov models," in *32nd Computers in Cardiology Conference*, 2005, pp. 953-956.

[56] Roy D. L. and Hoyt B., *EarsOn!*, CD-ROM. Halifax: Cor Sonics, 1997.

[57] Saha G. and Kumar P., "An efficient heart sound segmentation algorithm for cardiac diseases," in *Proceedings of the 1st Annual IEEE India Conference*, 2004, pp. 344-348.

[58] Sava H. and Durand L.-G., "Automatic detection of cardiac cycle based on an adaptive time-frequency analysis of the phonocardiogram," in *Proceedings of 19th Annual International Conference of the IEEE Engineering in Medicine and Biology Society*, 1997, pp. 1316-1319.

[59] Sava H., Pibarot P., and Durand L.-G., "Application of the matching pursuit method for structural decomposition and averaging of phonocardiographic signals," *Medical and Biological Engineering and Computing*, vol. 36, pp. 302-308, 1998.

[60] Selkurt E. E., *Physiology*. Boston: Little Brown & Company, 1971.

[61] Strang G. and Nguyen T., *Wavelets and Filter Banks*. Wellesley, MA: Wellesley-Cambridge Press, 1997.

[62] Tavel M. E. and Katz H., "Usefulness of a new sound spectral averaging technique to distinguish an innocent systolic murmur from that of aortic stenosis," *American Journal of Cardiology*, vol. 95, no. 7, pp. 902-904, 2005.

[63] Unser M. and Aldroubi A., "A review of wavelets in biomedical applications," in *Proceedings of the IEEE*, vol. 84, no. 4, pp. 626-638, 1996.

[64] Vepa J., Tolay P., and Jain A., "Segmentation of heart sounds using simplicity features and timing information," in *Proceedings of the IEEE International Conference on Acoustics Speech and Signal Processing*, 2008, pp. 469-472.

[65] Voss A., Herold J., Schroeder R., Nasticzky F., Mix A., Ullrich P., and Huebner T., "Diagnosis of aortic valve stenosis by correlation analysis of wavelet filtered

heart sounds," in *Proceedings of 25th Annual International Conference of the IEEE Engineering in Medicine and Biology Society*, 2003, pp. 2873-2876.

[66] Voss A., Mix A., and Hubner T., "Diagnosing aortic valve stenosis by parameter extraction of heart sound signals," *Annals of Biomedical Engineering*, vol. 33, no. 9, 2005.

[67] Walker H. K., Hall W. D., and Hurst J. W., Eds., *Clinical methods: the history, physical, and laboratory examinations*. Stoneham, MA: Butterworth, 1990. (3rd ed.) [Online] Available: http://www.ncbi.nlm.nih.gov/bookshelf/br.fcgi?book=cm

[68] Wang P., Kim Y., Ling L. H., and Soh C. B., "First heart sound detection for phonocardiogram segmentation," in *Proceedings of 27th Annual International Conference of the IEEE Engineering in Medicine and Biology Society*, 2005, pp. 5519-5522.

[69] Wang P., Lim C. S., Chauhan S., Foo J. Y., and Anantharaman V., "Phonocardiographic signal analysis method using a modified hidden Markov model," *Annals of Biomedical Engineering*, vol. 35, no. 3, pp. 367-374, 2007.

[70] Wang W., Guo Z., Yang J., Zhang Y., Durand L.-G., and Loew M., "Analysis of the first heart sound using the matching pursuit method," *Medical and Biological Engineering and Computing*, vol. 39, pp. 644-648, 2001.

[71] Zhang Y.-T., Chan G., Zhang X.-Y., and Yip L., "Heart sounds and stethoscopes," in *Wiley Encyclopedia of Biomedical Engineering*, Akay M., Ed. Wiley, 2006.